

THE SYNTHESIS AND NMR STUDY OF
N6',N9-OCTAMETHYLENEPURINE CYCLOPHANE

By

© HOWARD NEIL HUNTER, B.Sc.

A Thesis

Submitted to the School of Graduate Studies
in Partial Fulfilment of the Requirements

for the Degree
Doctor of Philosophy

McMaster University

May 1988

THE SYNTHESIS AND NMR STUDY OF
N6',N9'-OCTAMETHYLENEPURINE CYCLOPHANE

DOCTOR OF PHILOSOPHY (1988)

(Chemistry)

MCMASTER UNIVERSITY

Hamilton, Ontario

TITLE: The Synthesis and NMR Study of N6',N9-Octa-
methylenepurine Cyclophane

AUTHOR: Howard Neil Hunter, B.Sc. (McMaster University)

SUPERVISOR: Professor R.A. Bell

NUMBER OF PAGES: xiii, 177.

ABSTRACT

N6',N9-Octamethylenepurine cyclophane was synthesized to act as a ^1H NMR probe for the study of the diamagnetic anisotropy about the adenine system. The title compound was formed from 6-chloropurine and cyclooctanone using two variations of the same general approach. The ^1H NMR studies resulted in the assignment and identification of each proton resonance. As a method of confirming the assignments, nuclear Overhauser enhancement studies as well as conformational analysis using X-ray crystallography were completed. Upon correlation of the proton magnetic resonance spectrum with the structure of the title compound, an attempt was made to use a model calculation to determine the diamagnetic shielding anisotropy of adenine by comparison with the methylene proton chemical shifts. Finally, in an effort to further characterize the diamagnetic shielding anisotropy about adenine, a homolog to the title compound, N6',N9-Nonamethylenepurine cyclophane, was synthesized.

ACKNOWLEDGEMENTS

First and foremost, I wish to express my deepest appreciation to my family - especially my parents for their support and encouragement during the period of my studies.

For the thesis and the accompanying research, I am truly grateful for the guidance, patience and constant interest expressed by my research supervisor, Dr. Russell A. Bell. His enthusiasm and good cheer made this research project a refreshing challenge.

I am also grateful for the assistance given by Brian G. Sayer, Dr. Donald W. Hughes, J. Ian Thompson, Dr. James F. Britten, Dr. Richard Smith and F. Ramelan for the many technical aspects of the research.

I would like to thank Dr. Michael J. McGlinchey for his informative discussions pertaining to the ring current studies and for the assistance in the modification of the anisotropy calculation. The timely advice of Dr. Brian E. McCarry was greatly appreciated during the synthesis portion of this work.

Last, but not least, I wish to thank all of my friends for their companionship and assistance in maintaining a vigilance over my state of mental health and abundant physical activity.

SYMBOLS AND ABBREVIATIONS

Å	Angstrom
BMS	borane methylsulfide complex
BB	broadband
DEAD	diethylazo dicarboxylate
DMF	N,N-dimethylformamide
DMSO	dimethylsulphoxide
FID	Free Induction Decay
γ_H	proton magnetogyric ratio
h	Planck's constant / 2π
HMPT	hexamethylphosphorous triamide
HOMO	Highest Occupied Molecular Orbital
$^3J_{H-H}$	three bond proton coupling constant
LUMO	Lowest Unoccupied Molecular Orbital
NOE	nuclear Overhauser enhancement
τ_c^{eff}	effective correlation time
T_1	spin-lattice relaxation time
T_1^{DD}	dipole-dipole contribution to T_1
T_2	spin-spin relaxation time
THF	tetrahydrofuran
ϕ_3P	triphenylphosphine

TABLE OF CONTENTS

Chapter	Page
ABSTRACT	
ACKNOWLEDGEMENTS	
1. Introduction	1
1.1 Theory	1
1.2 Ring Current Effects in DNA and RNA	7
1.3 Application of Cyclophanes for Determining Diamagnetic Anisotropy	10
1.4 Syntheses of Cyclophane Molecules	11
1.5 Adenine Cyclophanes	14
1.6 Objectives of This Thesis	18
2. Synthesis of N6',N9-Octamethylenepurine Cyclophane	23
2.1 Introduction	23
2.2 Formation of the Aminoalcohol <u>4</u>	24
2.3 Initial N6' Alkylation	30
2.4 N9 Alkylation	34
2.5 A Improved Synthesis of the Cyclophane <u>1</u>	39
2.6 Substituted Purines	44
3. NMR Studies	47
3.1 Spectral Analysis Introduction	47
3.2 Experimental Methods for the ¹ H and ¹³ C Assignments	49

Chapter	Page
3.3 Results of the ^1H and ^{13}C Assignments	50
3.4 Discussion of ^1H and ^{13}C Assignments	59
3.5 Introduction to the Conformational Analysis	68
3.6 Experimental Methods for the Conformational Studies	69
3.7 Results of the Conformational Studies	70
3.8 Discussion of the Conformational Studies	79
4. Structural Determination	85
4.1 Introduction	85
4.2 Experimental Methods	86
Results and Discussion	87
4.3 X-Ray Analysis and Comparative Studies	87
4.4 Other Methods of Analysis	101
5. Diamagnetic Anisotropy	107
5.1 Introduction	107
5.2 Results and Discussion	110
5.3 Conclusions	122
6. Synthesis of N6',N9-Nonamethylenepurine Cyclophane	123
6.1 Introduction	123
6.2 Results and Discussion	126
EXPERIMENTAL METHODS	131
Preparation of Cyclooctanone Oxime <u>8</u>	133

Chapter	Page
Preparation of Cyclooctanone Isooxime <u>9</u>	134
Hydrolysis of 2-Azacyclononanone and Purification of the Amino Acid <u>10</u>	135
Preparation of Ethyl 8-Aminooctanoate <u>15</u>	136
Preparation of 8-Aminooctanol <u>4</u>	137
Synthesis of 6 ω -Hydroxyoctylaminopurine <u>5</u>	138
Preparation of Diphenyl Ketimine <u>18</u>	139
Protection of 8-Aminooctanol with Diphenyl Ketimine	141
Preparation of 6-Chloro,N ⁹ -(8-aminooctyl)- purine <u>6</u>	141
Attempted Preparation of the Cyclophane <u>1</u>	143
Preparation of the 8-Cyclophane <u>1</u>	144
Attempted Reduction of 8-Aminooctanoic Acid with Borane-Methyl Sulphide (BMS)	145
Attempted Reduction of Potassium 8-Amino- octanoate with BMS	146
Synthesis of Isopentyltrifluoroacetamide <u>17</u>	147
Formation of N-Methoxytrityl Ethyl 8-Aminooctanoate <u>22b</u>	148
Reduction of N-Tritylated Ethyl 8-Aminooctanoates	150
Hydrolysis of N-Trityl 8-Aminooctanol	151

Chapter	Page
Synthesis of 6-Chloro,N9-(8-N-methoxytrityl- aminoethyl)-purine <u>24</u>	152
Synthesis of 6-Chloro,N9-(8-aminoethyl)purine Hydrochloride <u>6a</u>	154
Modified Synthesis of N6',N9-Octamethylene- purine Cyclophane <u>1</u>	155
Synthesis of 6-Chloro,9-octylpurine <u>25</u>	155
Synthesis of 6-Aminoethylpurine <u>27</u> and 6-Aminoethyl,9-octylpurine <u>26</u>	156
Synthesis of 9-Azidononanol <u>30</u>	158
Synthesis of 6-Chloro,9-(9-azidononyl)purine <u>31</u>	159
Reduction of the Azide of 6-Chloro, 9-(9-azidononyl)-purine	160
Synthesis of N6',N9-Nonamethylenepurine Cyclophane <u>34</u>	161
Appendix A	163
References	169

LIST OF FIGURES

Figure		Page
1.1	A Diagram Showing the Induced Magnetic Field Generated by Ring Current.	5
1.2	Some Previously Studied Cyclophane Molecules.	6
1.3	Synthetic Approach to a Bridged Dihydro- benzimidazole.	13
1.4	Atom Numbering for Adenine.	15
1.5	Synthetic Approach to a Stacked Adenine-phane.	17
2.1	A poly(N-alkyliminoalane).	27
2.2	Borane Reduction Structures.	29
2.3	Ring Closure During Formation of Cyclophane.	35
3.1	¹ H NMR Spectra of N6',N9-Octamethylenepurine Cyclophane.	51
3.2	¹ H Homonuclear Correlated 2D Spectrum of the Aliphatic Region of <u>1</u> .	53
3.3	2D Carbon-Proton Shift Correlation of the Aliphatic Region of <u>1</u> .	55
3.4	Matrix for Determining Coupling Constants.	59
3.5	¹ H NMR Variable Temperature Spectra of <u>1</u> .	71
3.6a	Chemical Shift vs. Temperature for for the Two Protons of Carbon C5'.	76
3.6b	Chemical Shift vs. Temperature for Carbon C5'.	77
3.7	Relationship Between T_1^{TOTAL} , T_1^{DD} , and τ_c .	83

Figure	Page
4.1 Crystal Structure of N6',N9-Octamethylene purine Cyclophane With ¹ H NMR Assignments.	97-98
4.2 Aliphatic Portion of the ¹ H NMR Spectrum of N6',N9-Octamethylenepurine Cyclophane With Assignments.	99
5.1 The Shielding Caused by a Ring Current Effect Without Loop Separation vs. the Experimental Chemical Shift Obtained at Room Temperature.	115
5.2 The Shielding Caused by a Ring Current Effect Without Loop Separation vs. the Experimental Chemical Shift Obtained at -118°C.	116
5.3 The Geminal Proton Chemical Shift Differences for the Calculated Shielding Values Caused by a Ring Current Effect vs. the Experimental Values Obtained at Room Temperature.	119
5.4 The Geminal Proton Chemical Shift Differences for the Calculated Shielding Values Caused by a Ring Current Effect vs. the Experimental Values Obtained at -118°C.	120
5.5 Dimethyl [6]-paracyclophane-8,9-dicarboxylate.	121
6.1 ¹ H NMR Spectrum of N6',N9-Nonamethylenepurine Cyclophane <u>34</u> in CDCl ₃ .	131

LIST OF SCHEMES

Scheme	Page
1.1 Synthetic Strategy for the Formation of <u>1</u> .	20
2.1 Synthesis of the Amino Acid.	24
2.2 Proposed Route to Ester Formation.	25
2.3 Proposed Polymerization of the Methyl Ester.	26
2.4 Attempted Cyclization Via Path A.	31
2.5 Attempted Cyclization Using Mitsunobu Reaction .	32
2.6 Formation of Trifluoroacetamide.	36
2.7 Formation of Cyclophane <u>1</u> .	38
2.8 Modified Synthesis of the Cyclophane <u>1</u> .	41
2.9 Formation of Alkylated Products.	45
6.1 Synthetic Approach to the 9-Cyclophane.	125
6.2 Reaction of Diql.	126
6.3 Formation of Nonamethylene Cyclophane.	128

LIST OF TABLES

Table		Page
3.1	Chemical Shift Differences for Geminal Protons.	54
3.2	^{13}C Chemical Shifts for <u>1</u> , <u>25</u> and <u>27</u> .	57
3.3	PANIC Simulation of $^2J_{\text{HH}}$, $^3J_{\text{HH}}$ Couplings and Calculated Dihedral Angles.	64
3.4	Methylene Proton Chemical Shifts for Various Temperatures.	73
3.5	^{13}C Chemical Shifts for Variable Temperature Spectra.	75
3.6	Determination of ^{13}C Spin-Lattice Relaxation.	78
4.1	Atomic Positional Parameters and Temp. Factors.	88
4.2	Selected Interatomic Distances and Angles for <u>1</u> and Adenine.	90
4.3	Hydrogen Atom Positional Parameters and Temperature Factors.	92
4.4	Proton Dihedral Angle Comparison Between Values Extrapolated from the Crystal Structure, Computer Modelling and PANIC Spin Simulation.	94
4.5	^{13}C Chemical Shifts for the Purine Portion of Adenine and <u>1</u> in DMSO-d_6 .	105
5.1	Experimental Chemical Shift Values, Calculated Ring Current Increments and Differences in Geminal Proton Chemical Shifts.	111

Chapter 1
Introduction

1.1 Theory

The nuclear magnetic resonance (NMR) phenomenon arises from transitions between nuclear spin states of a nucleus placed in an external magnetic field. The electromagnetic radiation required to induce these transitions falls in the radiofrequency domain.

A nucleus under study in an NMR experiment will have a resonance frequency (or chemical shift) which is indicative of the chemical environment of that nucleus. The range of chemical shift values stems from variations in the screening of different nuclei from the external magnetic field (B_0) by the valence electrons. As a result, the effective magnetic field (B) experienced at the nucleus is represented by

$$B = B_0 (1 - \sigma_{TOT}).$$

The value of the screening factor (σ_{TOT}) for a nucleus may be assessed by accounting for the various contributions to the local electronic shielding effects as well as contributions from other more distant magnetic

effects. The expression for overall shielding may be written (Harris, 1983) as a sum of individual shielding terms:

$$\sigma_{\text{TOT}} = \sigma_{\text{d}} + \sigma_{\text{p}} + \sigma_{\text{m}} + \sigma_{\text{e}} + \sigma_{\text{s}} + \sigma_{\text{r}}.$$

The term σ_{d} is the local diamagnetic effect originating from the electron motion around an atom induced by the external magnetic field. The σ_{p} term, representing the local paramagnetic effect, is aptly named since this contribution opposes the diamagnetic effect and thus reinforces the applied field B_0 ; this term arises because of the mixing of the molecular excited electronic states into the ground state wave function in the presence of B_0 . Contributions to σ_{m} arise from long range anisotropy effects due to local magnetic fields generated by the bonds to neighbouring atoms. The σ_{e} term is the long range contribution influenced by the presence of an electric field which alters the electron density and therefore the local terms. Contributions due to solvent effects are contained in the σ_{s} term.

The relative contribution to σ_{TOT} from each shielding component differs for each nucleus within a molecule. For protons, these components may be qualitatively assessed. The contribution from σ_{d} may be lowered if the electron density about the proton is reduced

by the inductive effects of nearby electron withdrawing groups. Since σ_p is linked to the mixing of electronic excited states into the ground state wave functions, and since the energy difference between the 1s and 2p levels is large, the σ_p contribution for protons is minimal. The contribution from σ_m may be significant, depending upon the proximity of the ^1H nucleus to bonding electrons or lone electron pairs to neighbouring groups such as acetylenic, carbonyl, nitrosyl or carbon-carbon single and double bonds. Usually σ_e is not significant for protons; however, contributions to this term increase as the distance to strongly polar groups decreases. The effect of σ_s depends mainly upon the chemical environment of the individual protons. For example, polar solvents will generate an electric field effect which could result in an augmentation of the contribution by σ_e . Also, solvents like benzene will impart diamagnetic anisotropic shielding about the solute molecule. Similarly, other solvents may produce a weak complex with the solute molecules thus altering the electron density at the proton nucleus. While σ_d and σ_p may contribute the most to the total absolute screening factor, it is the net difference in screening factors between nuclei which is generally studied. The variations in chemical shift between chemically similar nuclei usually reflects contributions from the shielding terms such as σ_s ; therefore

differences in chemical shift can provide an estimate of the relative contribution of the minor shielding components.

The shielding component of interest in this thesis is σ_r , the shielding contribution caused by a "ring current" generated by an aromatic system (Memory and Wilson, 1982). From a classical perspective, an external magnetic field induces a ring current caused by the circulation of delocalized π -electrons in the aromatic system (Waugh and Fessenden, 1957 and Johnson and Bovey, 1957). When the external magnetic field is normal to the plane of the aromatic system, the electrons in the π system are induced to move around the ring and thereby produce a so-called "ring current". This current intrinsically generates its own local magnetic field as shown in Figure 1.1. This local field acts so as to oppose the applied magnetic field at the center of the ring and augment the external field at the periphery of the aromatic system.

The ring current effect is a major factor in the ^1H NMR spectra of many aromatic systems. For example, the σ_r contribution has been considered largely responsible for the excessive deshielding of aromatic protons in benzene ($\delta 7.15$) as compared to the vinylic protons of 1,3-cyclohexadiene ($\delta 5.86$). Conversely, the δ -methylene protons of [8]paracyclophane are forced to lie above the center of an aromatic system. Compared to typical methylene protons (eg. cyclo-

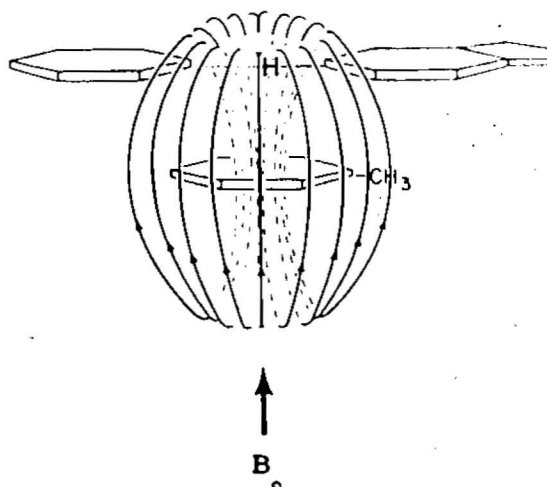
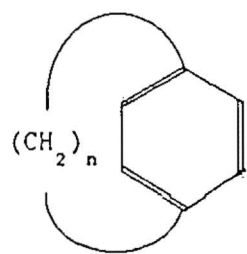
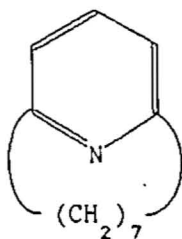


Figure 1.1 A Diagram Showing the Induced Magnetic Field Generated by Ring Current.

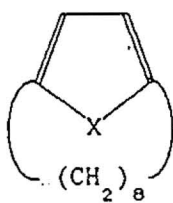
hexane, δ 1.38) these δ -methylene protons are substantially shielded and are observed at δ 0.19 (Kaneda et al., 1980); this observation has also been attributed to the ring current effect. It is important to note that ring current effects are observed in heteroaromatic systems as well. For example, [7](2,6)-pyridinophane (shown in Figure 1.2) contains protons displaying ^1H NMR shifts at δ 0.16 (Fujita and Nozaki, 1971) while Nozaki et al. (1969) reported resonances at δ 0.40, 0.70, and -0.40 for the compounds [8](2,5)-pyrrolophane, [8](2,5)-furanophane and [8](2,5)-thiophenophane, respectively. Even the system [10](3,5)-pyrazolophane (Parham and Dooley, 1967) indicates the range of compounds exhibiting the ring current effect by



[n]paracyclophane



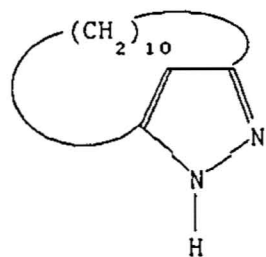
[7](2,6)-pyridinophane



X=NH; [8](2,5)-pyrrolophane

=O; [8](2,5)-furanophane

=S; [8](2,5)-thiophenophane



[10](3,5)-pyrazolophane

Figure 1.2 Some Previously Studied Cyclophane Molecules.

by displaying ^1H NMR shifts at 80.70.

1.2 Ring Current Effects in DNA and RNA

Ring current effects have been the subject of intense study with respect to the ^1H NMR spectra of ribo- and deoxyribonucleotides. For instance, the upfield chemical shifts of the aromatic heterobase protons (induced through vertical stacking) has been attributed to the diamagnetic susceptibility anisotropy of the neighbouring bases (Giessner-Prettre and Pullman, 1970). A detailed knowledge of the spatial distribution of the total diamagnetic shielding anisotropy about these aromatic systems could aid in the assignment of the heterobase protons in the ^1H NMR spectra of large oligomers and potentially lead to information about preferred orientations of the stacked molecules.

Much of the research in this area has been concentrated on using various methods of calculating the ring current contributions to the diamagnetic shielding anisotropy. Original semi-empirical calculations (Giessner-Prettre and Pullman, 1970) presumed that the majority of the shielding manifested by these systems was due to ring current effects. The "Free Electron Model", modified by Waugh and Fessenden (1957), was chosen as a suitable method

of simulating the ring current contribution to the shielding anisotropy. This model allowed the delocalized π -electrons in the presence of an external magnetic field to circulate freely in the molecular orbitals of the aromatic system (much like the circulation of electrons in a loop of wire). The magnitude of the magnetic field generated at any point in space by this loop would be a function of the electron current flowing in the loop, the distance from the loop and the radius of the loop. Furthermore, since the π molecular orbital is represented by not one but two separate doughnut-shaped clouds of electron density, a similar compensation was made in the model. These lobes were located apart from each other at a distance which accounted for the shielding difference between the vinylic protons of cyclohexadiene and the protons of benzene. The results of these calculations were expressed as isoshielding contour diagrams.

Further studies indicated that other local contributions to the total shielding anisotropy (atomic or local contributions and electric field effects) may play a significant role (Giessner-Prettre *et al.*, 1976, Ribas Prado and Giessner-Prettre, 1981, Giessner-Prettre and Pullman, 1976, Giessner-Prettre and Pullman, 1977). These studies resulted in a semi-empirical evaluation of the local atomic contribution using the dipolar contribution from the calculated diamagnetic susceptibility tensors by the method

of McConnell (1957) and Pople (1957). The combination of the local effects and the ring current effect were adjusted to account for the observed proton shifts of the aromatic heterobases associated through vertical stacking.

Using a similar empirical approach, Robillard and Reid (1979) used the crystal structure coordinates of a t-RNA sequence to relate proton chemical shifts to ring current shieldings. The ring current values for each heterobase were varied until the shift increments matched the chemical shift values obtained from the experimental spectrum. This procedure was repeated for various sets of crystallographic data and provided a thorough study of many t-RNA sequences.

Recent advances in computer technology have reduced the computational time required for quantum mechanical calculations, thereby increasing interest in their use. As a result, these methods have been applied to determining the shielding anisotropy with increasing levels of refinement. Giessner-Prettre (1984) has presented results obtained with the self consistent perturbation method developed by Ditchfield (1974) for Gauge Invariant Atomic Orbitals using a minimum basis set. Since this approach is a total shielding approximation, these calculations contain both ring current and local atomic contributions to the shielding. The limiting factor preventing extensive use of

this method is the size (i.e., number of atoms) of the system. Application of this method to account for ^{13}C and ^{15}N chemical shifts has demonstrated the potential utility of this method.

It can be seen that a great deal of research has been directed towards the calculation or semi-empirical determination of ring current to the overall shielding of heterobase protons using ^1H NMR methods. Investigations of the ring current contribution to the proton chemical shift of [n]paracyclophanes have previously been studied.

1.3 Application of Cyclophanes for Determining Diamagnetic Anisotropy

Attempts to account for the diamagnetic shielding anisotropy displayed by the methylene protons of [n]-paracyclophane molecules using semi-empirical and non-empirical methods have met with much success. Agarwal *et al.*, (1977) showed that both the classical "Free Electron" model (Wagh and Fessenden, 1957) and the quantum mechanical approach of Haigh and Mallion (1971) were very effective in accounting for the residual proton shift usually attributed to ring currents. In their study, local atomic contributions to the diamagnetic anisotropy were evaluated using ^{13}C chemical shielding tensors calculated by Barfield *et al.*,

(1975). Agarwal found that the electron ring (loop) separation used with the "Free Electron" model was not necessary and that the best correlation between the observed and calculated proton shielding values was obtained when the loop separation was zero.

The success of the ring current studies of [10]-paracyclophane provides inspiration for the investigation of the diamagnetic anisotropy of nitrogenous heterobases using a cyclophane approach. Firstly, a brief overview of cyclophane syntheses must be examined.

1.4 Syntheses of Cyclophane Molecules

The various types of reactions for generating cyclophanes may be categorized according to the synthetic route applied. Many of the reactions for synthesizing cyclophane molecules are discussed by excellent reviews (Rosenfeld and Cho, 1983, Ito *et al.* 1983, and Smith, 1964).

There are three basic methods of cyclophane ring formation: unimolecular or intramolecular cyclization, bimolecular or intermolecular cyclization, and aromatization after ring formation. The synthetic approach chosen for a particular problem depends upon both the reactivity of the aromatic system and the length of the bridging methylene chain - hence the strain introduced by

the formation of the cyclophane molecule often determines the synthetic approach.

Both the intra- and intermolecular methods have been applied successfully to the construction of molecules with minimal strain in the resulting cyclophane molecule. Typical reactions used in this type of approach are: the acyloin condensation, the Friedel-Crafts reaction; the pyrolysis of diacids; cyclization by amide formation; haloamine cyclizations; haloether cyclizations; Ziegler cyclizations; and the oxidative coupling of acetylenes and mercaptans. These methods have been used extensively for the formation of a wide variety of cyclophane molecules. The main shortcoming of these types of reactions are the poor yields obtained in the formation of bridged molecules with appreciable amounts of strain. For example, these methods fail to generate [n]paracyclophanes where n is less than nine. In some cases the problem of forming strained cyclophanes may be circumvented by generating an homologous (larger n) cyclophane and subsequently performing a ring contraction of the methylene bridge using the Wolff rearrangement (Allinger, et al., 1974).

Another synthetic strategy involves aromatization after formation of the cyclic system. This method is generally better suited to the preparation of more highly strained and (or) more reactive aromatic systems. For

example, Hayward and Meth-Cohn (1975) used aromatization after formation of the cyclic system for the generation of the imidazole portion of the bridged dihydrobenzimidazole (Figure 1.3).

Formation of the cyclic system before aromatization has also been applied to many systems including the strained [6]paracyclophane (Kammula et al., 1977) or the unstable [5]paracyclophane (Kostermans et al., 1987).

The overall strategy adopted for the formation of a specific cyclophane may be predetermined by the chemical properties of the aromatic system to be bridged. For

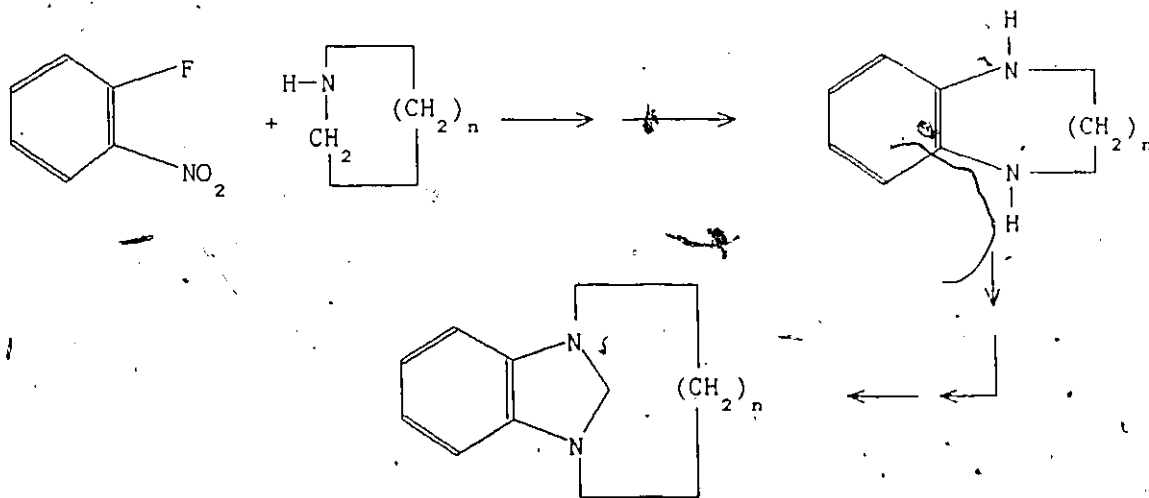


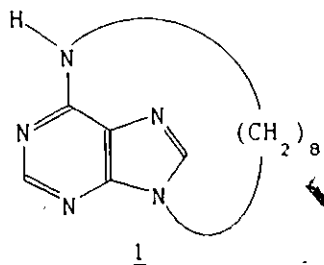
Figure 1.3 Synthetic Approach to a Bridged Dihydrobenzimidazole.

example, the ring formation followed by aromatization method is not readily applicable to a system where the ring is unusually difficult to form or for a fused aromatic system where adjacent aromatic rings are to be bridged. The latter two points are relevant to the aromatic heterobase adenine.

1.5 Adenine Cyclophanes

The synthesis of a bridged adenine cyclophane (e.g., 1) has not been previously reported in the literature. However, many reports of the formation of purine molecules connected by aliphatic chains exist (Hama *et al.*, 1981, Akahori *et al.*, 1984). Before a synthetic scheme for an adenine cyclophane can be created, a brief examination of the requirements of the cyclophane and the reactivity of purines must be undertaken.

Two important factors should be analyzed when designing a synthesis for the adenine cyclophane. The first factor to be considered should be the end use of the molecule. Since the cyclophane would be used to study the diamagnetic anisotropy of the aromatic system, the methylene chain should be fused to the purine so that it crosses as much of the plane of the aromatic system as possible. With this structural requirement in mind, the four possible sites



for substitution, C2, C6(N6'), C8 and N9, may be divided into two groups, C2-C8 and N9-C6(N6'), (see Figure 1.4 for the numbering pattern). Each group represents two possible sites for the fusion of an aliphatic chain to adenine and enables the maximum portion of the aromatic plane to be transversed.

The other factor which should be considered is the relative ease of formation of the required bonds at the desired sites. From the two possibilities (C2-C8 or N9-C6(N6')), a survey of the literature indicates that few examples exist for simple carbon-carbon bond formation at C2

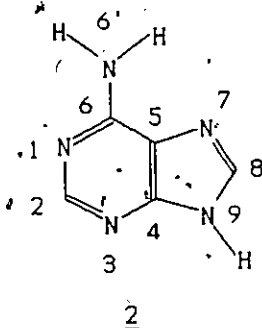


Figure 1.4 Atom Numbering for Adenine.

or C8 (Lister 1971⁹). Direct alkylation at C2 or C8 would require many steps and also require the method of ring formation followed by aromatization. A synthesis involving the N9-C6(N6') sites would appear to be more reasonable since N9 alkylation is well known. Although N6' alkylation does not readily occur, nucleophilic displacement of chloride at C6 using alkylamines is common.

A practical example of the relative reactivity of the different sites of purine can be illustrated using the synthesis of a stacked adenine-*phane* as outlined in Figure 1.5 (Akahori *et al.*, 1984). Since the C2-alkyl bond was the most difficult to form, it was made the initial synthetic target. Thus 1,4-di(2-adenyl)butane (Figure 1.5) was prepared in five steps from phenylazomalononitrile and adipodiamidine. The subsequent connection of C6 sites and N9 sites involved one step reactions and demonstrated the lability of each site. From this reaction scheme, it can be seen that C6 was the site of nucleophilic substitution while N9 was the site of alkylation.

The foregoing example indicates that C6 and N9 would be the most reactive purine sites, providing that C6 is properly substituted. Therefore, a plan for the synthesis of an adenine cyclophane may be formulated.

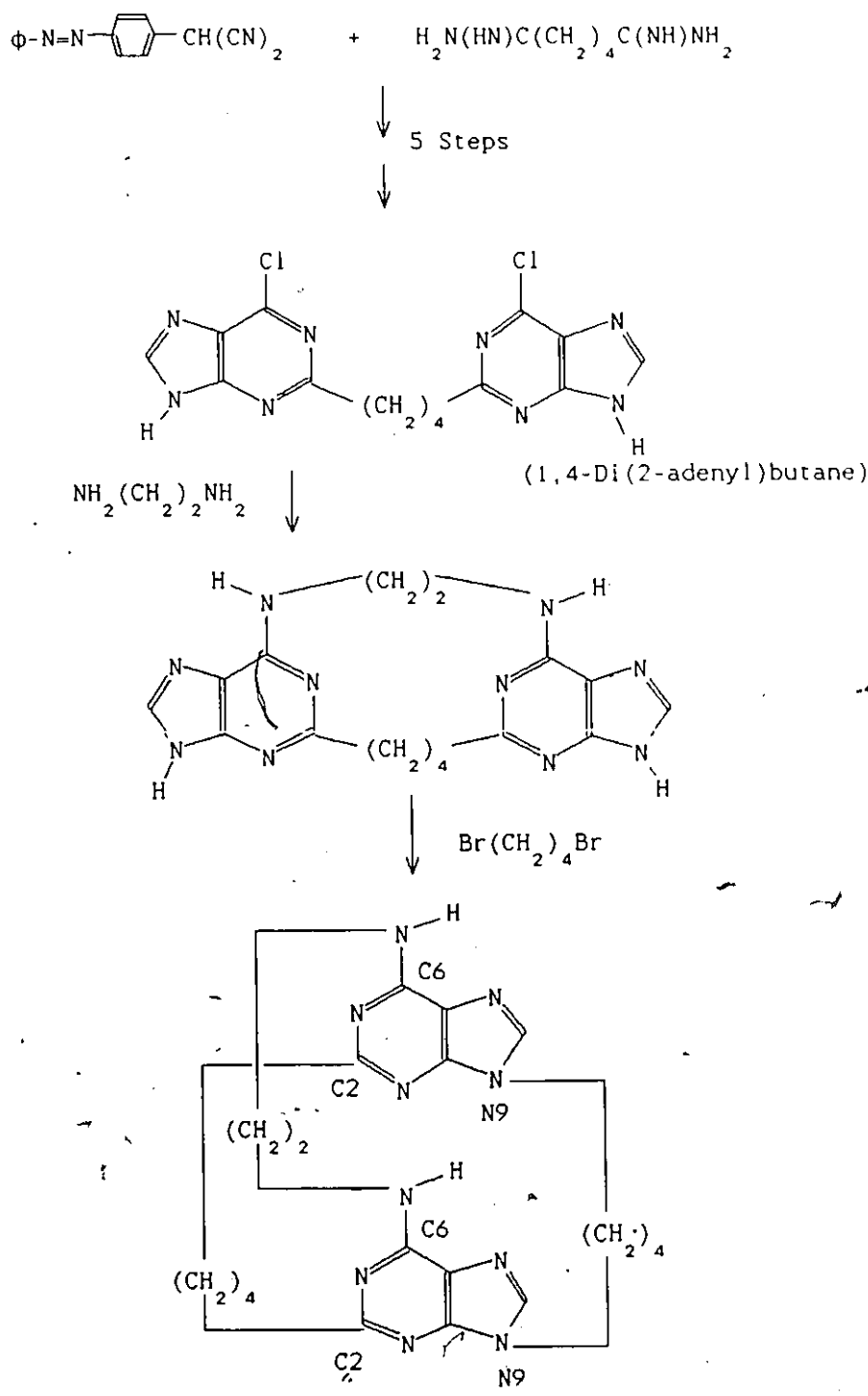


Figure 1.5 The Synthetic Approach to a Stacked Adenine-phenane.

1.6 Objectives of This Thesis

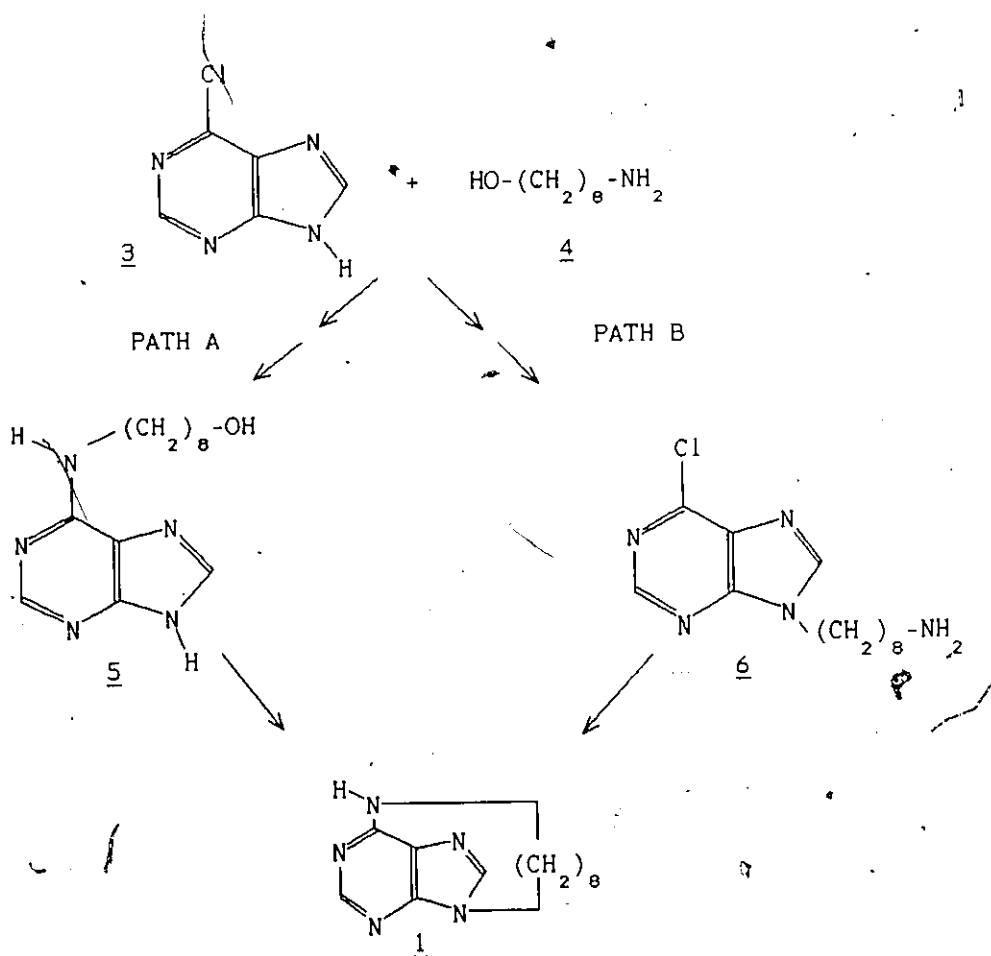
Every study of the diamagnetic shielding anisotropy of adenine has been concentrated on the calculation of the shielding constants or has tried to integrate these results with the proton chemical shifts of stacked ribo- or deoxyribonucleosides. However, apart from the study of short oligomer sequences using ^1H NMR, no effort has been made to experimentally determine the diamagnetic anisotropy of individual heterobases using a cyclophane approach. From the analysis of the variations in methylene proton chemical shifts (of a cyclophane), a means of assessing the diamagnetic shielding anisotropy of the heterobase would be provided. The main objective of this work is the synthesis of the adenine cyclophane 1 and the detailed NMR investigation of this compound in order to provide an experimental account of the shieldings of the adenine ring system.

Several special considerations must be taken into account when designing a cyclophane molecule derived from adenine such as the location of the fusion sites on adenine and the length of the methylene chain. The methylene chain should be linked at opposite sides of adenine, thus enabling a bridge to cross directly over the center of the aromatic plane. The resulting methylene proton chemical shifts should

provide a variety of shielding values representative of the different regions around the aromatic system. The analysis of the purine reactivity in Section 1.5 indicates that the favourable sites for fusion, from a synthetic viewpoint, would be N6' and N9.

The length of the methylene chain is also an important consideration for the design of a cyclophane molecule. The number of methylene units must be sufficient so that distortion of the aromatic plane as a result of strain imposed by the methylene bridge is minimized. On the other hand, the methylene chain should be relatively taut in order to restrict the movement of the methylene protons relative to the plane of the purine system. A minimum of chain flexibility allows for a more precise determination of the shielding anisotropies of the nuclei in a given region of space. Inspection of Drieding models reveals that an eight carbon chain would satisfy these requirements.

The synthetic approach to the adenine cyclophane is outlined in Scheme 1.1. Starting with the intact purine 3 and a bifunctional alkyl compound 4, two general strategies for the synthesis of the adenine cyclophane 1 are apparent (Path A and Path B). A flexible synthetic approach of this type increases the probability that a successful synthetic sequence will be found. Details of the synthetic work are described in Chapter 2.

Scheme 1.1 Synthetic Strategy for Formation of **1**.

Following the synthesis of 1, several NMR properties of this molecule will be studied. In Chapter 3, proton and carbon-13 chemical shift assignments will be pursued using several techniques:

- (i) one dimensional ^1H and ^{13}C NMR spectra,
- (ii) two dimensional NMR spectra derived from homonuclear correlated spectroscopy and $^1\text{H}/^{13}\text{C}$ shift correlated spectroscopy, and
- (iii) spin simulations.

Next, a set of studies designed to investigate the dynamic solution properties of 1 would include:

- (i) variable temperature ^1H spectra,
- (ii) variable temperature ^{13}C spectra,
- (iii) ^{13}C spin-lattice relaxation studies, and
- (iv) ^1H - ^1H nuclear Overhauser enhancement studies.

The complete proton assignments will be revealed in Chapter 4 through the study of crystallographic data. As well, an investigation of some of the other probes into the conformation of the methylene bridge and the aromatic portion of 1 will be discussed.

Chapter 5 will contain a study of an attempt to correlate the diamagnetic anisotropic effects displayed by the methylene protons of 1 to the "Free Electron" model of Waugh and Fessenden (1957). Following a similar approach as was taken by Agarwal *et al.*, (1977), the purinophane 1 is to

be used to provide an analysis of the diamagnetic susceptibility anisotropy through the study of the chemical shift values of the methylene protons.

The synthesis of a homolog of 1 will be discussed in Chapter 6. This molecule, containing a nine carbon methylene bridge, may be the subject of future diamagnetic anisotropy studies. For this thesis however, the compound N6',N9-octamethylenepurine cyclophane was chosen as the prime synthetic objective.

Chapter 2

Synthesis

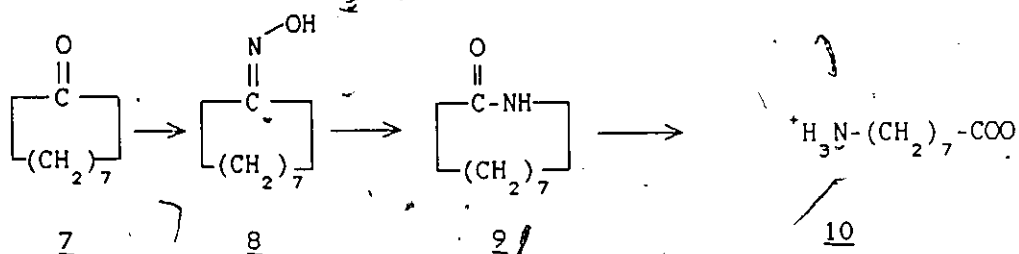
2.1 Introduction

The general approach to the formation of an adenine cyclophane 1 was indicated, in Scheme 1.1, to involve a bimolecular reaction to connect an alkyl chain to the purine moiety followed by a subsequent intramolecular cyclization. The bifunctional alkyl compound deemed most suitable for reaction with 6-chloropurine (3) was 8-aminoctanol (4). By using these two compounds, two possible approaches to connection of the aliphatic chain to 3 became available. In the first case, Path A, the amine group from 4 could replace the chlorine atom in 3, followed by cyclization at N9 of the substituted purine 5. Another possible pathway shown as Path B in Scheme 1.1, requires the alkylation of N9 first, followed by cyclization at C6 of 6.

This chapter will present a chronological account of: (a) the synthesis of 8-aminoctanol 4, (b) an attempt to form 1 by using the route called Path A in Scheme 1.1, (c) the synthesis of 1 using Path B, and then (d) a modified synthesis of 1.

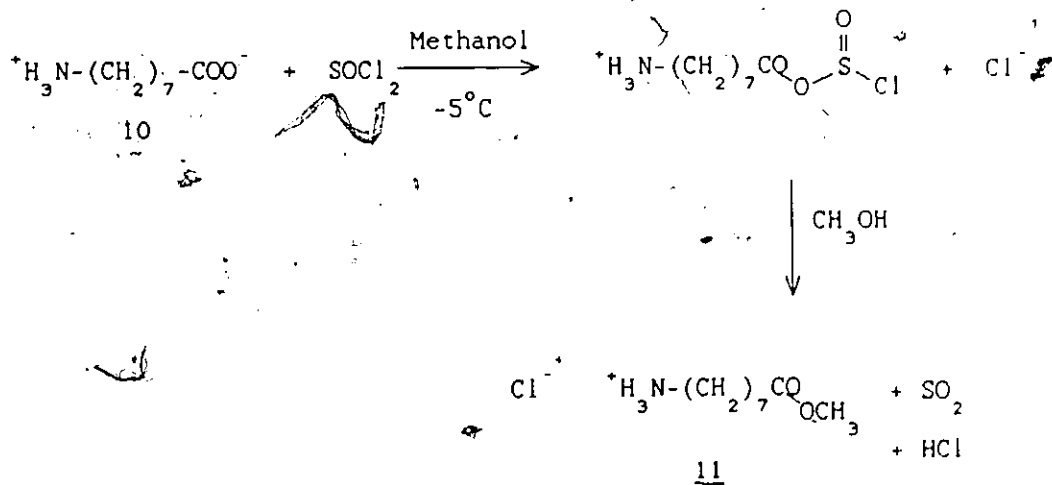
2.2 Formation of the Aminoalcohol 4

The initial work was directed towards devising a method of converting 8-aminooctanoic acid (10) into 8-amino-octanol 4. Although 8-aminooctanoic acid may be purchased, for this starting material it was more practical to generate this amino acid from cyclooctanone 7 (Scheme 2.1) via the Beckmann rearrangement and subsequent hydrolysis (Coffman *et al.*, 1948). The experimental ^{13}C NMR chemical shift values for cyclooctanone oxime 8 corresponded to those reported in the literature (Hawkes *et al.*, 1974). The isolation of the amino acid 10 from the hydrochloride salt was performed by a modified version of the method used by Takagi and Hayashi (1959). The ^1H NMR spectrum of the resulting amino acid 10 was found to be similar to that of an authentic sample.



Scheme 2.1 The Synthesis of the Amino Acid 10.

Initial attempts to reduce the amino acid 10 to the aminoalcohol 4 with lithium aluminum hydride proved fruitless because of the insolubility of the amino acid 10 in suitable aprotic solvents. In order to overcome the problem of solubility, the amino acid 10 was converted to the methyl ester 11 using thionyl chloride in methanol at -5°C (Huber and Brenner, 1953). The mechanism for this reaction was proposed to involve the zwitterionic form of the amino acid 10 (Scheme 2.2). The thionyl ester, upon heating, further reacted with the alcohol solvent to produce the amino ester 11 (Pizey, 1974).



Scheme 2.2 Proposed Route to Ester Formation

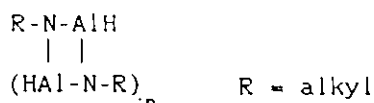


Figure 2.1. A poly(N-alkyliminoalane)

poly(N-alkyliminoalanes) as indicated in Figure 2.1. This family of compounds has been studied extensively by Cucinella *et al.*, (1974 and 1975) and ^1H NMR, mass spectral and X-ray methods of analyses have revealed a three dimensional cage-like structure. In the case of the amino acid methyl ester 11, there may have been a high degree of aluminum-oxygen bonding involved as well as aluminum-nitrogen bonding. The immense hydrophobic nature of these complex structures may result in the inability of water to hydrolyze the aluminate product in order to yield the amino-alcohol 4.

An alternate method was sought after to bring about reduction of the amino acid 10. Studies indicated that borane-methyl sulphide (BMS) was quite an effective method for reducing carboxylic acids (Pelter and Smith, 1979) since BMS in THF provides a much higher concentration of borane in solution than solutions of borane alone in THF. Also, compared to borane, BMS was reported to be much more stable and relatively unreactive to water. It was anticipated that the high concentration of reducing agent in solution would

permit reduction of the amino acid 10. Reaction of 10 with BMS in THF resulted in the formation of a white solid with ^{13}C NMR chemical shifts corresponding to values obtained from the appropriate segments of n-octylamine and n-octanol. However, ^1H NMR and low resolution mass spectral data did not support formation of the aminoalcohol 4. ^1H NMR indicated the appearance of a multiplet, with the expected chemical shift of $\delta 2.60$ but not the expected triplet multiplicity. A triplet would represent coupling to β protons (β with respect to the amine group). Low resolution mass spectra indicated peaks for masses ranging between 153 and 159 amu but not the values of 145 (M^+) or 144 (M^+-1) which would be expected for 4. Possible product structures which could explain the observed mass values are indicated in Figure 2.2. Coordination compounds of the type 12 and 13 have been studied by Mancilla *et al.*, (1982) and structure 14a had been examined by Letsinger and Skoog (1955). Study of the ^1H NMR spectra of compound 14b indicated that the N-CH_2 resonance was a multiplet. A similar observation was also reported by Meek and Springer (1966). For the literature system, the multiplet was attributed to spin-spin coupling with ^{11}B and $^{14}\text{N-}^1\text{H}$.

In addition, borane-amines have also been noted for their remarkable stability towards aqueous acid (Pelter and Smith, 1979), and in the work repeated here, it was found

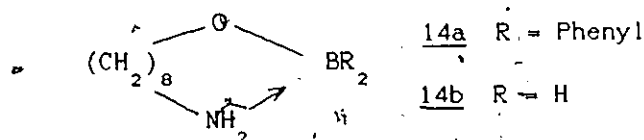
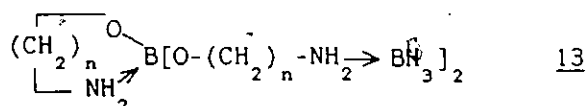
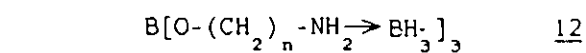


Figure 2.2 Borane Reduction Structures

that treatment of the borane-amine products, from reduction of 10 with BMS, with concentrated hydrochloric acid yielded the desired aminoalcohol 4 with extremely low returns.

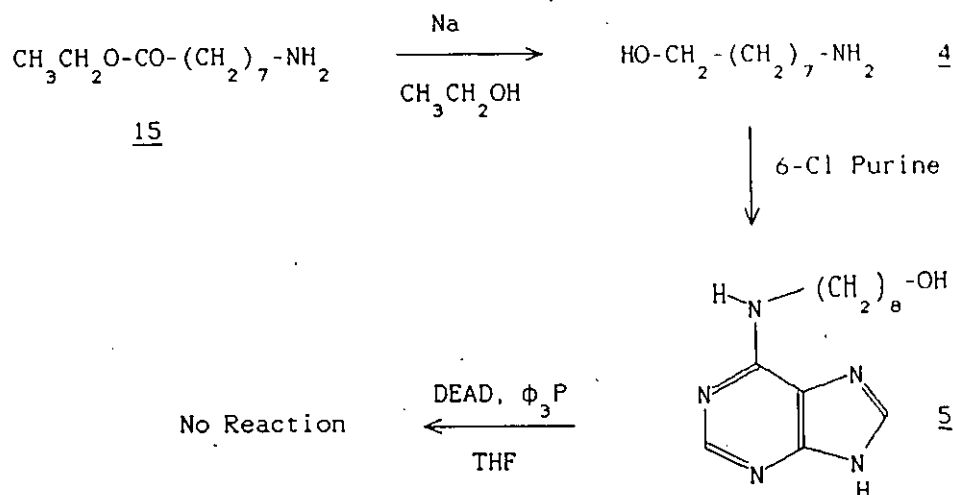
A variation of the borane reduction reaction, which was intended to increase the solubility of carboxylic acids, was studied by Yoon and Cho (1982). Using this method, the amino acid 10 was converted to the potassium salt and 18-crown-6 ether was added to enhance the solubility of the salt. Upon workup, the aminoalcohol 4 was obtained in extremely low yields. The identity of the product was based upon low resolution mass spectra which indicated a peak corresponding to a mass one unit less than the molecular ion. The ^{13}C NMR spectrum was consistent with chemical shift

data obtained from the appropriate portions of the spectra of n-octylamine and n-octanol. Also, the ^1H NMR spectrum revealed a triplet at δ 3.53 arising from the methylene protons adjacent to the hydroxyl group.

Satisfactory yields in the preparation of 4 were finally obtained from ester reduction using the Bouveault-Blanc reaction (Manske, 1943). In this case, the ethyl ester 15 was synthesized, by the method of Huber and Brenner (1953), in order to reduce the rate of polymerization of the aminoester 15. The ethyl group did prove to be of sufficient steric bulk to permit the isolation of the neat aminoethyl-ester 15 for brief periods at room temperature without subsequent polymerization. Evidence for the formation of 15 came from the ^{13}C NMR spectrum which was assigned using chemical shift values from ethyl octanoate and n-octylamine. Reduction of 15 by sodium in ethanol resulted in the formation of the aminoalcohol 4 in 30% yield with recovery of unreacted starting material.

2.3 Initial N-6' Alkylation

Intuitively, reaction Path A in Scheme 1.1 was the simplest route to the formation of the cyclophane 1. Therefore, the chlorine of 6-chloropurine 3 was displaced with the amine portion of the aminoalcohol 4 using the



Scheme 2.4 The Attempted Cyclization Via Path A.

method of Sutherland and Christensen (1957) yielding 85% of 5 (Scheme 2.4). N-6'Alkylation was confirmed by high resolution mass spectral data and by comparing methylene CH_2NH_2 chemical shift differences for the ^1H NMR spectra of the product 5 (δ 3.35) and the aminoalcohol 4 (δ 1.53) which showed the clear deshielding effect of the heteroaromatic ring of 5.

The final step of Path A required cyclization to occur at the N-9 atom of the substituted purine 5 using the Mitsunobu coupling conditions as shown in Scheme 2.5. Despite several attempts using a variety of reaction conditions, ring closure failed to occur. The inability to form 1 using this method may have originated from two

sources. Possibly the reaction conditions which required a dilute environment for the cyclization step (to prevent intermolecular reaction between substituted purine molecules) resulted in a reduced rate for several of the bimolecular steps involved in the Mitsunobu reaction. This reduction in the rate of the desired reaction may have caused other reaction pathways, which did not lead to 1, to predominate.

The other factor preventing the formation of 1 depended upon the distribution of electron density of the highest occupied molecular orbital (HOMO) on N9 of the intermediate 16. If the HOMO at N9 of 16 is perpendicular to the plane of the ring, the strain imposed upon the alkyl chain by attack of the $\text{CH}_2\text{OP}^+(\text{Ph})_3$ unit is minimized and an $\text{S}_{\text{N}}2$ transition state could conceivably be formed with a normal activation barrier. However, if the HOMO at N9 is in the plane of the purine system, increased strain would be imparted to the aliphatic chain, as well as to other parts of the molecule, if an $\text{S}_{\text{N}}2$ transition state were to be attained through reaction with the $\text{CH}_2\text{OP}^+(\text{Ph})_3$ unit. This increased strain is suggested by the use of molecular models which indicate torsional strain imparted to the aliphatic chain and bending of the purine ring to attain the second of the two possible transition states. Unfortunately, the results did not permit the investigation of the two factors

proposed to have prevented the formation of 1.

2.4 N9-Alkylation

The inability to form the cyclophane 1, by initial nucleophilic attack at the C6 site, led to the investigation of Path B (as shown in Scheme 1.1.) which requires cyclization by the formation of the N6'-C6 bond last. Unlike Path A, the approximate conformation of ring closure was easier to predict and did not impose as much steric strain upon the initially formed intermediates. Figure 2.3 indicates the probable steps involved in the conversion of the substituted 6-chloropurine 6 to the cyclophane 1. The tetrahedral, charge-separated intermediate arises from attack of the primary amine 6 at the p orbital on C6 which is perpendicular to the plane of the purine. This initial intermediate should not impose a large constraint upon the alkyl chain and thus arise from the passage through a reasonable activation energy barrier. The major portion of the strain would result from the following step involving the regeneration of the sp² hybridization at C6 through collapse of the tetrahedral intermediate by loss of chloride.

However, in order to pursue the other reaction (path B) outlined in Scheme 1.1, certain precautions had to be

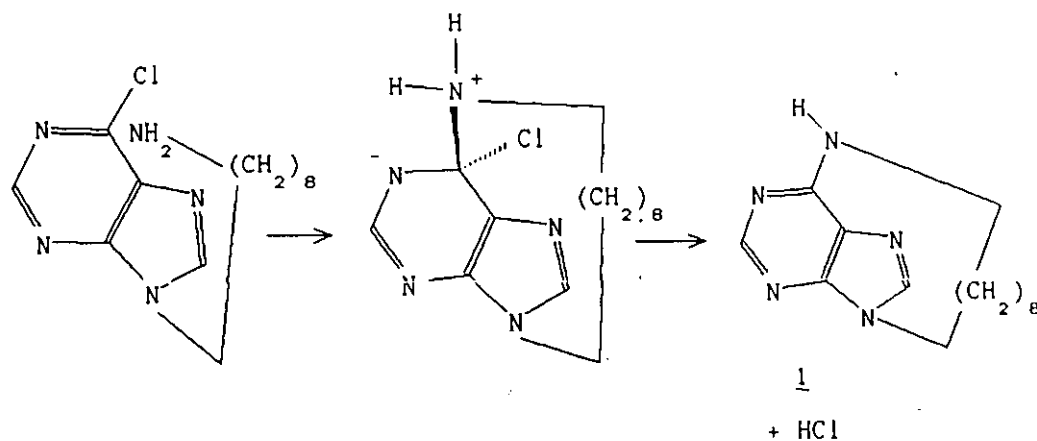
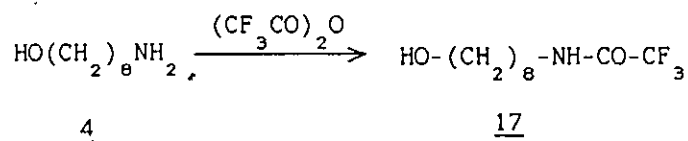


Figure 2.3 Ring Closure During Formation of Cyclophane

taken. A suitable protecting group was required for the amine portion of the aminoalcohol 4 since diethyl azodicarboxylate has been known to react with primary amines to give the appropriate mono and diamides (Barneis, Broeir and Bittner, 1976). The protecting group had to selectively protect the amine but not the hydroxyl group and in addition deprotection of the amine had to occur under mild conditions. The latter requirement was important because of the sensitivity of the C6 site to undergo acid catalysed nucleophilic displacement of chloride.

The first protecting group considered was the trifluoroacetyl moiety (Greene, 1981) shown in Scheme 2.6. Unfortunately, the mild conditions reported for the



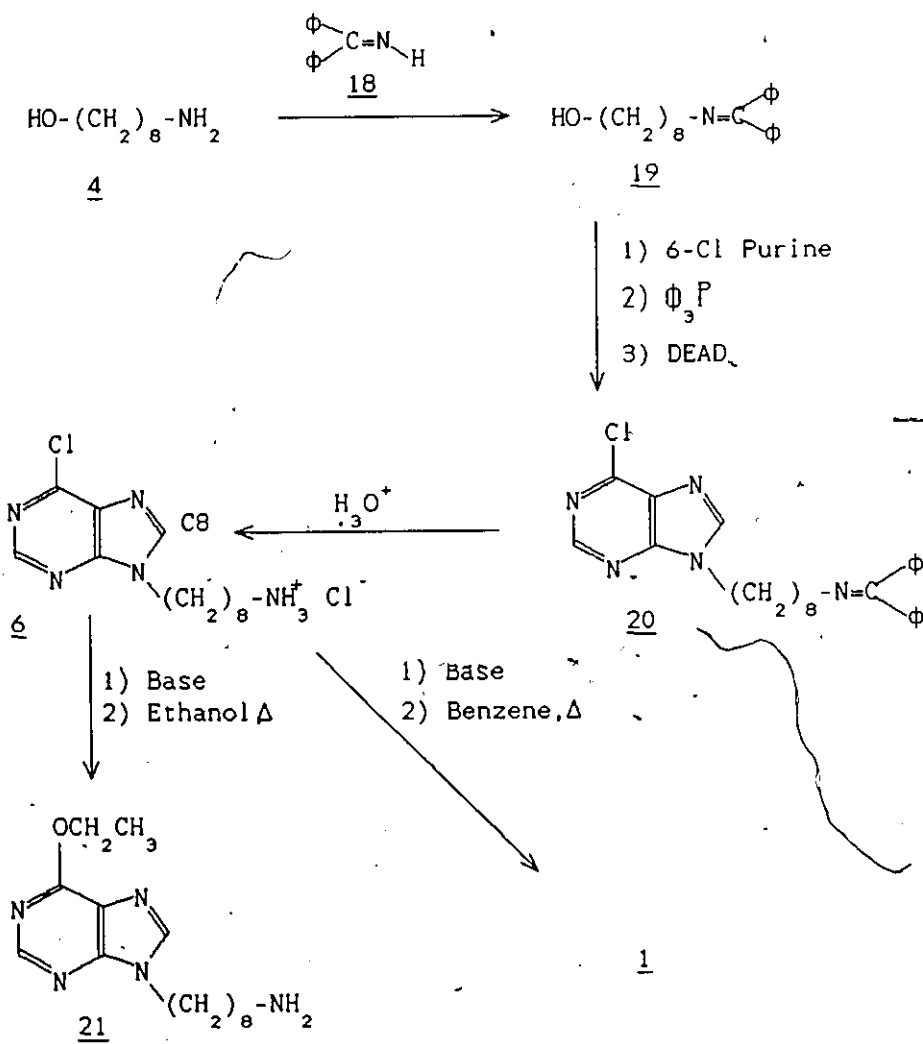
Scheme 2.6 Formation of Trifluoroacetamide

successful hydrolysis of the amide 17 proved ineffective. The acid conditions which lead to hydrolysis (Wolfrum and Bhat, 1967) also caused hydrolysis of the chlorine from the purine.

Literature precedent indicated that diphenyl ketimine 18 was a suitable protecting group for primary amines (O'Donnell, 1982) for two reasons. First of all, the driving force of the primary amine protection was loss of gaseous ammonia, and secondly, the protecting group was easily removed with aqueous acid. Diphenyl ketimine 18, prepared by the reaction of the Grignard reagent from bromobenzene with benzonitrile (Pickard and Tolbert, 1973), was reacted with the aminoalcohol 4 to give the protected amine 19 in quantitative yield (Scheme 2.7). Confirmation of imine formation was established by the disappearance of the ^1H NMR peak at δ 1.53 corresponding to the methylene protons adjacent to the primary amine.

The imine 19 underwent the Mitsunobu reaction with 6-chloropurine, however, attempts to isolate the pure purine-alkylketimine 20 from the crude reaction mixture proved unsuccessful. The difficulty in isolating 20 in a pure form may have been caused by the lability of the ketimine protecting group when subjected to silica gel or alumina column chromatography. Initial attempts to hydrolyze the ketimine 20 to the amine 6a under acidic conditions also resulted in hydrolysis of the chlorine at the C6 position of the purine. Successful aqueous hydrolyses of the Mitsunobu reaction product 20 gave the N9-alkylated purine 6a in only 30% yield.

Both the amine 6 and the hydrochloride salt 6a were examined by $^1\text{H NMR}$ spectroscopy; the spectra of 6 and 6a displayed signals for the methylene group adjacent to the amine function at δ 3.63 and δ 3.07 respectively. The failure to observe the C8 proton resonance of the hydrochloride salt 6a was attributed to deuterium exchange with the D_2O solvent catalyzed by the acid chemical shift reference (Elvidge and Jones, 1973). Confirmation of the amine 6 was provided by a low resolution mass spectroscopy which indicated a molecular ion at 281 amu (M^+). As a general rule, the amine was stored as the hydrochloride salt, 6a, in order to prevent intermolecular reaction between the primary amine and the 6-chloro group of the purine.

Scheme 2.7 Formation of Cyclophane 1.

The first attempt to form the cyclophane 1 involved the liberation of the amine 6 by alkaline extraction of the hydrochloride salt 6a followed by the addition of ethanol to give a dilute solution. Unfortunately, the solvent reacted with the purine to give 21 with the loss of chloride ion. Analysis of the ^1H NMR spectra of the reaction product showed proton resonances representing an ethoxy group; mass spectral evidence confirmed the ^1H NMR data. Therefore, an inert, non-nucleophilic solvent was needed for this cyclization reaction. When a 10^{-3} molar concentration of the amine 6 was heated in a benzene solution in a sealed tube at 100°C , a low yield of the cyclophane 1 was obtained. The formation of 1 was indicated by both the low and high resolution mass spectra; the proton NMR spectrum of the reaction product showed that the methylene protons at $\delta 1.35$ in the starting material 6a had been replaced by several multiplets between $\delta 1.58$ and $\delta -0.7$.

2.5 An Improved Synthesis of the Cyclophane 1

Some of the reactions leading to the cyclophane 1 described above proceeded in low yields or were difficult to reproduce. Thus an alternate amine protecting group to the diphenyl ketimine 18 and a better solvent for the key cyclization reaction were sought.

Szammer (1969) reported the conversion of α -amino acids to the corresponding aminoalcohol by reduction of N-triphenylmethyl (trityl) esters. This approach to the preparation of the aminoalcohol 4 was especially appealing to us since, with the nitrogen atom blocked, it would provide a method of reducing the ester in high yield while providing a protecting group for the Mitsunobu reaction. Therefore, starting with the amino acid ethyl ester 15, the trityl ester 22a was prepared as shown in Scheme 2.8. The structure of the ester 22a was confirmed by the change in chemical shift of the methylene protons adjacent to the amine from δ 1.53 to δ 2.15. Lithium aluminum hydride reduction of the N-trityl ester 22a resulted in the formation of the N-trityl aminoalcohol 23a in 87% yield. The ^1H NMR spectrum of this compound indicated the loss of the ester ethoxy group as well as the appearance of a triplet with the appropriate chemical shift for methylene protons adjacent to a hydroxyl group (δ 3.52).

Attempts to cleave the trityl group by hydrogenation using palladium on carbon in t-butanol and THF proved fruitless. However, the trityl group was successfully removed by acid hydrolysis using hydrochloric acid in methanol. Unfortunately, 6-chloropurine would not survive these conditions. A more labile protecting group had to be selected. Smith *et al.*, (1962) predicted that the lability

of the trityl group should increase as the number of p-methoxy substituents increased. Thus, the N-p-anisyldiphenylmethyl (methoxytrityl) ester 22b was prepared and reduced to the N-methoxytrityl aminoalcohol 23b under conditions similar to those used for 22a, to afford in a yield greater than 97% from the amino acid 10. The ^{13}C NMR spectra of both the methoxytrityl ester 22b and the methoxytrityl aminoalcohol 23b were assigned by comparison with ^{13}C shifts recorded for n-octanol, n-octylamine, ethyl octanoate, p-methoxybenzylamine, and triphenylcarbinol and were fully consistent with the assigned structures. Hydrolysis of the amine protecting group of 23b with trifluoroacetic acid in methylene chloride followed by methanol quench successfully cleaved a large portion of the methoxytrityl groups (Ogilvie and Kroeker, 1972). 6-Chloropurine when exposed to these hydrolysis conditions was recovered intact.

The next step was the coupling of 23a and 6-chloropurine. Reaction of the N-methoxytrityl aminoalcohol with 6-chloropurine, using the method of Mitsunobu, afforded the N-9-alkylated adduct 24. This product was partially purified by dissolution in chloroform followed by precipitation of triphenylphosphine oxide by the addition of hexane. The N-9-alkylated product was further purified by reverse phase chromatography using a Sep-Pak cartridge. This procedure removed most but not all of the impurities to give

approximately 50% yield as indicated by ^1H NMR. The ^1H NMR spectrum of 24 indicated purine protons at δ 8.74 and δ 8.08 and a triplet at δ 4.26 attributed to methylene protons adjacent to N9 of the purine. The ^{13}C NMR spectrum, assigned by comparison with chemical shift data recorded for 6-chloropurine, n-octylamine, triphenylcarbinol, and p-methoxybenzylamine, was consistent with the structure of 24.

Removal of the methoxytrityl group, using trifluoroacetic acid in methylene chloride, yielded the amine 6 isolated as the hydrochloride salt 6a. The ^1H NMR spectrum of this salt was shown to be identical to the spectrum of the previously prepared sample of 6a. Examination of amine 6 using mass spectroscopy indicated that the chlorine on the purine ring was still intact.

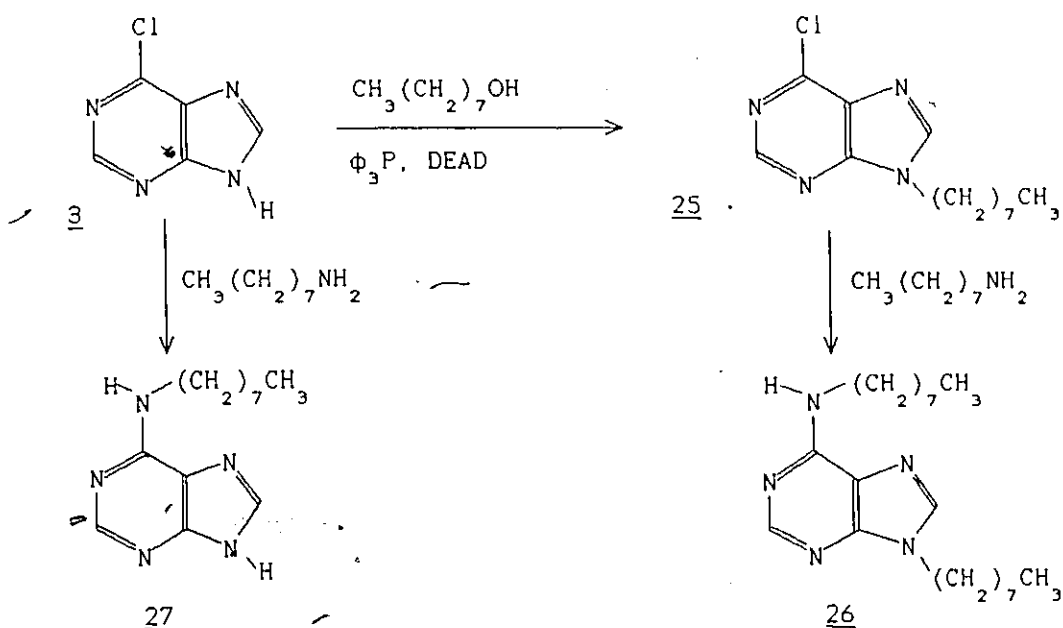
The final ring closure or cyclization reaction was accomplished by a modification of the procedure used in Section 2.4. Trial experiments had indicated that primary amines reacted quickly with 6-chloropurine in the aprotic solvent dimethylsulphoxide (DMSO). For example, approximately equimolar amounts of 6-chloropurine and n-butylamine reacted in deuterated DMSO at 25°C with a half-life of approximately 6 minutes. It was felt that DMSO was unsuitable as a solvent for this reaction since DMSO decomposes slowly at temperatures above 65°C and a boiling point of 150° would make it tedious to remove large volumes

of the solvent. Therefore acetonitrile was chosen as a solvent since it possesses similar solvent characteristics as dimethylsulphoxide (Karger *et al.*, 1973) yet was easier to remove upon completion of the reaction. The free amine 6 was generated from the hydrochloride salt *in situ* by reacting the hindered non-nucleophilic base N,N-diisopropylethylamine with the hydrochloride salt 6a at 0°C to reduce the probability of intermolecular reaction of the primary amine 6. The reaction mixture was diluted with acetonitrile to a concentration of 10^{-3} molar, then heated to reflux. A pure sample of 1 was isolated by column chromatography using silica gel and a methanol-chloroform solvent mixture in 30% yield.

2.6 Substituted Purines

A series of substituted purines was synthesized as model compounds for UV and NMR spectral studies. Their syntheses are outlined in Scheme 2.9.

6-Chloro-N9-octylpurine 25, synthesized by the Mitsunobu method using 6-chloropurine and n-octanol, was obtained in a 79% yield and purified by column chromatography using 5% methanol in chloroform. The preparation of 25 was confirmed by the change of the ^1H chemical shift of the alkyl methylene protons (adjacent to

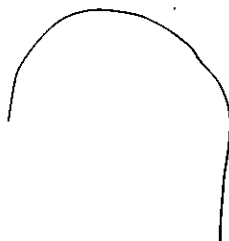


Scheme 2.9 The Formation of Alkylated Purines.

N9) to δ 4.27 from δ 3.65.

Both 25 and 6-chloropurine were converted to 6-aminoctyl, N9-octylpurine 26 and 6-aminooctylpurine 27 with n-octylamine. These compounds were purified by column chromatography using 5% methanol in chloroform. Compound 26 was obtained in a 50% and 27 in a 73% yield. The molecular formulae of these compounds were confirmed by high resolution mass spectrometry and by the appearance of methylene protons adjacent to N6' at δ 3.6 in their ^1H NMR spectra.

These compounds will be used for comparison of the ultraviolet spectral properties discussed in Chapter 4, and the ^{13}C NMR properties discussed in Chapters 3 and 4.



Chapter 3

NMR Studies

3.1 Spectral Analysis Introduction

The two objectives of using ^1H and ^{13}C NMR methods for the study of the purinophane were 1) to assign each proton of the methylene chain to a specific resonance, and 2) to gain insight into the molecular dynamic properties leading to the conformational analysis of the methylene chain in solution. The first section of this chapter will address the problem of assigning the ^1H and ^{13}C spectra. Following the acquisition of the ^1H and ^{13}C NMR spectra, the task of assigning the NMR resonances was tackled. The coupling information contained in the two and three bond proton-proton and one bond carbon-proton coupling can be exploited in several ways.

The proton-proton shift correlated two dimensional (COSY 2D) experiment (Aue *et al.*, 1976) presents a two dimensional contour diagram of the proton spectrum which provides an indication of protons that are mutually coupled through bonding interactions. This type of spectrum will indicate the presence of both geminal and vicinal couplings. The heteronuclear shift correlated experiment allows one to

determine which proton(s) are attached to each carbon nucleus.

Another experiment which presents geminal proton coupling information while concurrently assisting in the assignment of methylene carbon resonances is a modification of the heteronuclear shift correlated two dimensional experiment (Wilde and Bolton, 1984). In this experiment, J_{H-H} coupling between spins not attached to the same ^{13}C nucleus is removed from the F_1 domain. This technique is combined with a composite 180° decoupling ^{13}C pulse. As a result, the homonuclear COSY and the heteronuclear shift correlated experiments provide data required to assign the geminal protons for each carbon in the methylene chain.

In order to specifically assign each proton from the geminal pairs, the Karplus relationship (Karplus, 1959 and 1963) is used. The Karplus equation correlates the proton-proton vicinal coupling constants between the two vicinal protons with the dihedral angle. The coupling constant information may be obtained directly from spectra or through computer generation of a simulated multiplet for each resolvable proton resonance.

With these NMR data, the assignment of the 1H chemical shifts and final determination of the time-averaged solution conformation can be made by correlation with the crystallographic data presented in Chapter 4.

3.2 Experimental Methods for the ^1H and ^{13}C Assignments

The ^1H and ^{13}C NMR studies of the purinophane 1 were performed with a Bruker AM500 NMR spectrometer using either 40% methylene chloride in Freon (CFCl_3) or deuterated chloroform as the solvent. The methylene chloride-Freon solvent system was used to create a nonpolar environment where solvent interactions with 1 would be minimized. In order to create a constant concentration and remove dissolved oxygen, the sample was degassed and sealed *in vacuo*.

The homonuclear shift correlated two dimensional NMR spectrum was obtained at 27°C from a sample of 1 dissolved in deuteriochloroform. The basic pulse sequence was:

delay- 90° - t_1 - 90° -FID ($t_1=1$ sec.).

256 F_1 values were collected, each with 1024 points along F_2 . After Fourier transformation, the resulting digital resolution was 8.56 Hz/point in both dimensions.

The heteronuclear shift correlated, two dimensional spectrum, also obtained from a sample of 1 dissolved in deuteriochloroform, was acquired using the following pulse sequence:

^1H : $d_0 - 90^\circ - d_0 - 90^\circ - d_3 - 180^\circ - d_3 - 90^\circ - d_0 - d_3 - 90^\circ$ BB
 ^{13}C : d_1 ----- (180) ----- $90^\circ - d_4$ -FID.

The following delays were used: $d_0 = 3$ microseconds, $d_1 = 2$ seconds, $d_3 = 3.5$ milliseconds, and $d_4 = 1.8$ milliseconds. 128 F_1 values were collected, each with 256 points along F_2 . Zero filling was used to increase the time domain to 512 points in F_1 and 4096 points in F_2 before Fourier transformation. The resulting digital resolution was 9.21 Hz/point along F_1 and 7.18 Hz/point along F_2 .

The on-resonance homonuclear decoupled experiments required for the simulation studies were performed in the homodecouple mode using a decoupler power of less than 0.05 Watts. The simulation studies were performed using the Parameter Adjustment in NMR by Iterative Calculation (PANIC.81) spin simulation method distributed by Bruker Spectrospin. Comparisons with the experimental resonances were evaluated by assigning each peak from a multiplet to the corresponding calculated transition.

3.3 Results of the Proton and Carbon-13 Assignments

The ^1H NMR spectra of 1, shown in Figure 3.1, indicate the presence of: two purine proton singlets in the aromatic region (CH2 and CH8); the NH6' broad singlet; and fourteen complex multiplets representing sixteen methylene

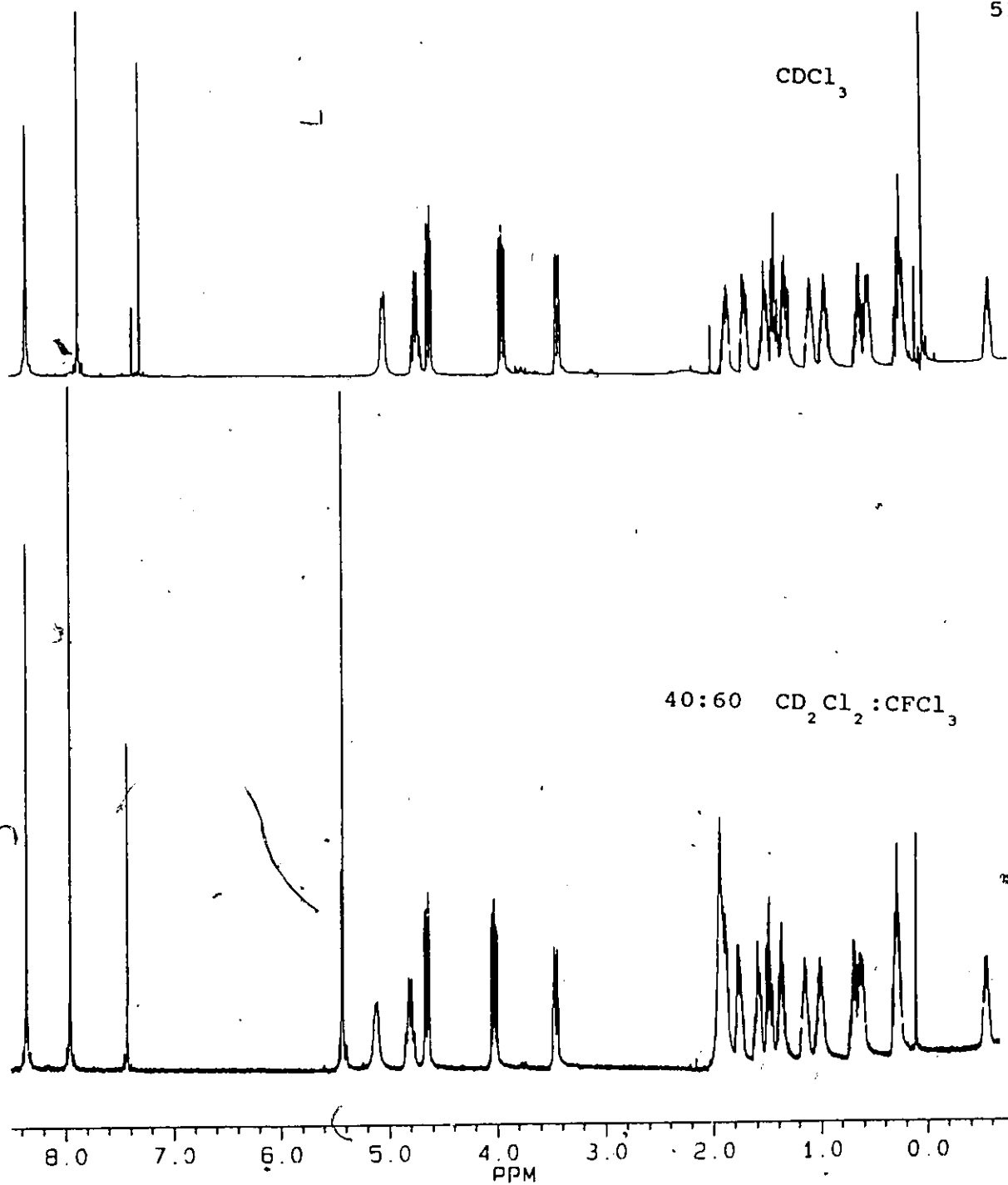


Figure 3.1 ^1H NMR Spectra of $\text{N}6',\text{N}9$ -Octamethylene-purine Cyclophane.

protons ($\delta 4.2$ to $\delta 0.7$).

The two spectra also provide an example of the different effects caused by changes of the solution environment of 1 upon going from chloroform to methylene chloride-Freon. The most notable change is the slight chemical shift difference between the protons at $\delta 0.5$ and $\delta 0.6$. The spectrum obtained in chloroform shows two distinct multiplets as opposed to the spectrum obtained in methylene chloride-Freon solvent which shows substantial overlap of the two proton resonances. As a result, studies requiring individual multiplets were done with the chloroform sample.

The proton-proton correlated (COSY) 2D spectrum (Figure 3.2) provides a great deal of information necessary for the assignment of the geminal and vicinal relationships. Chloroform was used as the solvent because of the enhanced resolution of the resonances at $\delta 0.5$ and $\delta 0.6$ (Figure 3.1). Emphasized with squares in this figure are the more intense off-diagonal contours indicating the geminal couplings. The other off-diagonal contours indicate the vicinal relationships. The sweep width and offset frequency for the COSY experiment were chosen so that only the methylene and NH6' protons were observed. This choice of sweep width resulted in a fold back of the C2H and C8H resonances (aliased) into the chosen region. Fortunately, these two folded resonances did not overlap with any other

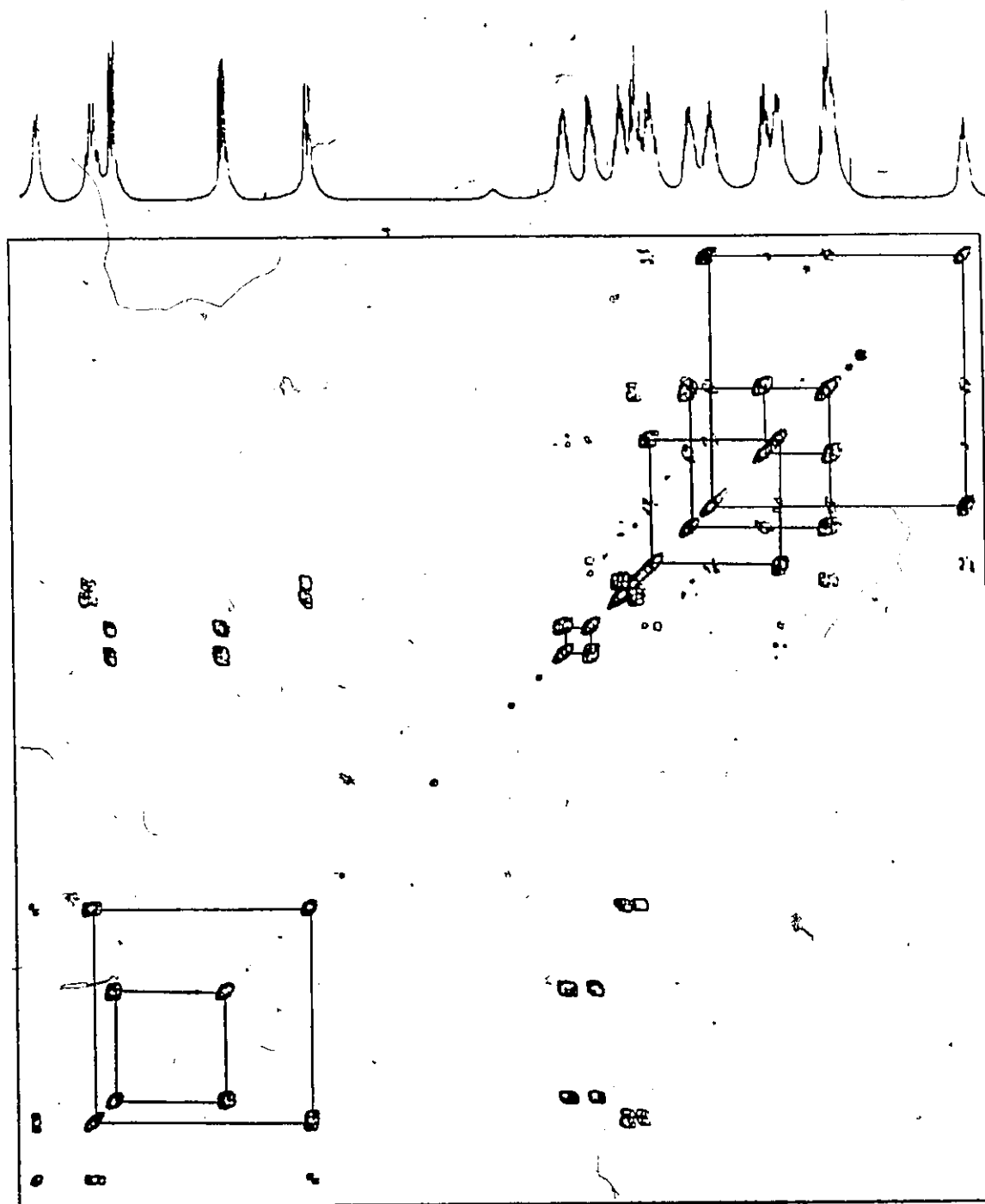


Figure 3.2 ¹H Homonuclear Correlated 2D Spectrum
of the Aliphatic Region of **1**.

Table 3.1 Chemical Shift Differences for Geminal Protons.

Carbon #	Chem. Shift Diff. (ppm) ^a
1'	1.34
2'	0.09
3'	0.85
4'	0.41
5'	1.53
6'	0.33
7'	0.16
8'	0.63

^a Values obtained for Methylene Chloride-Freon at 27°C.

proton signals; while the selection of a narrow sweep width for the COSY spectrum afforded higher resolution of the methylene proton resonances. By inspection of the off-diagonal contours, the chemical shift differences between geminal protons are determined and listed in Table 3.1.

The ¹H-¹³C shift correlated 2D-NMR spectrum of 1, also obtained in chloroform (shown in Figure 3.3), served two purposes. Since one axis represents the ¹³C chemical

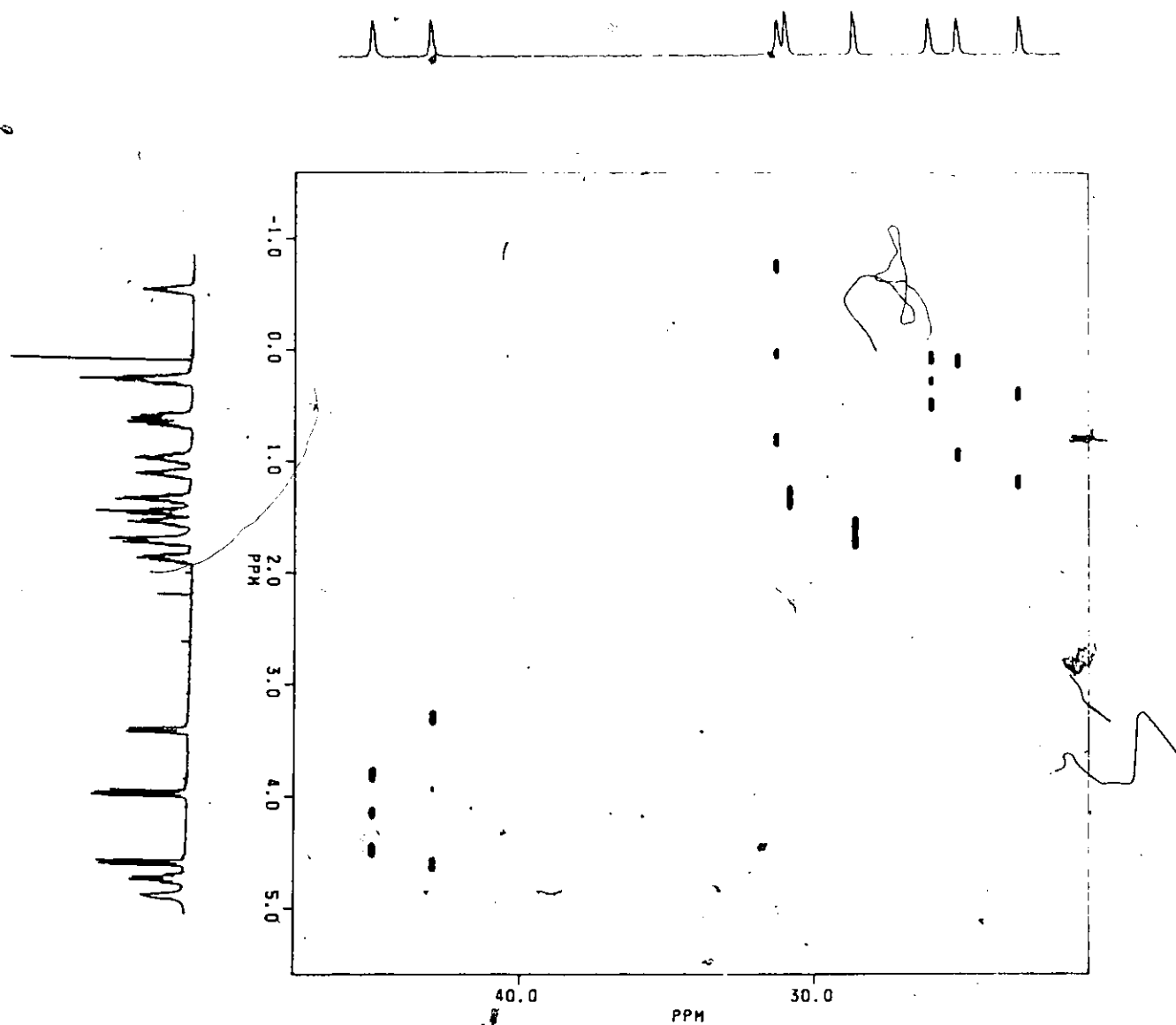


Figure 3.3 2D Carbon-Proton Shift Correlation of the Aliphatic Region of 1.

shifts and the other axis the ^1H shifts, off-diagonal contours represent correlations between protons which are directly bonded to ^{13}C atoms. Therefore, this spectrum verifies the geminal proton assignments made from Figure 3.2.

The second objective of the hetero-correlated experiment was the complete assignment of the ^{13}C chemical shifts for the cyclophane 1. Initial inspection of the ^{13}C chemical shifts for the methylene carbons of 1, shown in (Table 3.2) indicates a unique resonance for each of the eight carbons. The carbons at either end of the chain show large α -substituent effects causing them to be deshielded more than the other aliphatic carbons. Table 3.2 also provides a comparison of the ^{13}C chemical shifts of the alkyl carbons for 1 and the open chain compounds 25 and 27. The differences in chemical shifts range from $\delta 0.55$ for $\text{C}8'$ to $\delta 3.38$ for $\text{C}6'$ of 1.

Having completed the assignments of the methylene protons in the ^1H spectra and the methylene carbons in the ^{13}C spectra, the unambiguous assignment of each proton of each geminal pair remained. This problem was approached by examining the coupling pattern displayed by each proton resonance. In order to simplify each multiplet somewhat, a series of homodecoupled ^1H spectra were obtained. This procedure, in most cases, simplified the spin systems and

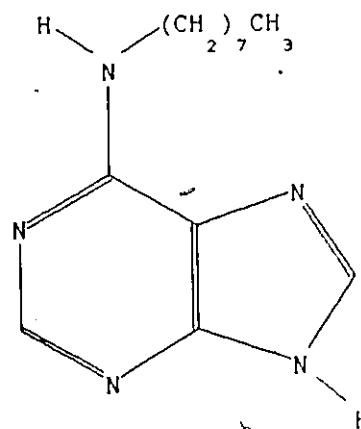
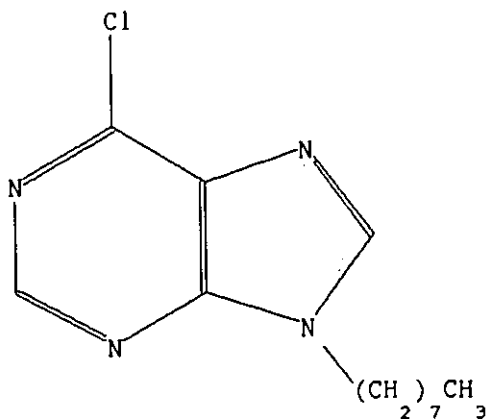
Table 3.2 ^{13}C Chemical Shifts for 1, 25^c and 27^c.

Methylene Carbon Number and Chemical Shift ^a								
Cmpd.	C1'	C2'	C3'	C4'	C5'	C6'	C7'	C8'
<u>1</u>	43.03	30.92	25.21	26.13	31.32	23.14	28.72	45.03
<u>25</u> ^b	14.13	22.47	29.77	28.83	28.92	26.52	31.57	44.48
<u>27</u> ^b	40.72	31.78	26.94	29.21	29.21	29.72	22.61	14.05

^a Chloroform was both solvent and internal reference.

^b Carbon numbering scheme is relative to compound 1.

^c Compounds 25 and 27 are shown below.



also aided in the assignment of vicinal couplings between protons.

A unique line-difference method was used to disentangle the individual couplings which composed each multiplet. The method involved the generation of a matrix formed from the frequency differences between observed transitions within a given multiplet. As shown in Figure 3.4, each row contained the differences between the frequency for a given transition with respect to the frequencies of the other transitions for that multiplet. For example, f_1 represents the frequency of the lowest field peak of the multiplet and likewise f_2 represents the frequency of the second lowest field peak, etc.. The values below the diagonal were not calculated since they are the negative of the upper set and are redundant. After construction of the matrix, the average value taken from each upper left to lower right diagonal represented a crude approximation for one possible coupling value for the multiplet. After accumulation of the approximate couplings, computer-assisted multiplet simulations could be done.

Upon accumulation of the coupling values, the Parameter Adjustment in NMR by Iteration Calculation (PANIC.81) spin simulation method was used to generate a calculated facsimile of each multiplet. This program allowed

and geminal spin-spin couplings. The large range of chemical shift differences for each pair of geminal protons implied that there were substantial differences in the diamagnetic shielding anisotropies experienced by each proton of a given methylene pair (Table 3.1). The unique chemical environments of these protons may be attributed in part to the low symmetry in this purinophane since systems of higher symmetry such as [10]paracyclophane (Agarwal *et al.*, 1977) display much simpler spectra. One of the more interesting resonances in the purinophane 1 was the signal at δ -0.6 indicating a proton in a shielded region, similar to those reported at δ -0.3 and δ -0.9 for [7]paracyclophane (Wolf *et al.*, 1973) and δ -0.7 for [8]naphthalenophane (Wiberg and O'Donnell, 1979).

The assignment of methylene proton pairs was greatly facilitated through the study of the proton-proton COSY 2D spectrum (Figure 3.2). Each terminus of the alkyl chain provided a starting point from which to follow the connectivities, since these protons were the most deshielded out of all the methylene protons. The protons on the carbon attached to N6' were easily assigned due to the off-diagonal contours correlating the NH6' proton with the C1' protons.

Some of the geminal protons displayed large chemical shift differences (see Table 3.1). The two largest differences (C1' and C5' protons) are greater than 1 ppm,

reflecting dramatic differences in the shielding anisotropies experienced at those methylene units. In the case of the C5' protons which reside over the purinophane ring, the higher field proton (δ -0.64) is probably more proximal to the center of the aromatic system while its lower field geminal partner (δ 0.89) is further removed from the shielding effects of the purine system. A similar large shift difference was also found for the two geminal protons (δ 0.77 and δ -1.59) located at the center of the [7]-tropolonophane methylene chain (Saito *et al.*, 1984).

Contrarily, the geminal protons of C2' and C7' had very similar chemical shifts, implying that any deshielding effects of the purine system were relatively small in the locality of these protons. The shift differences for the geminal protons on carbons C3', C4', C6' and C8' show intermediate effects.

The examination of the methylene carbon portion of the ^{13}C spectrum of 1 reveals a difference in shielding effects for the ^{13}C nuclei as compared to the proton nuclei. Inspection of the shift values from Table 3.2 indicates that the contribution to the ^{13}C shielding due to the diamagnetic anisotropy was not large. This conclusion was evident by comparing the chemical shifts of C5' in 1 (δ 31.32) with the corresponding carbon from the model compound 25 (δ 28.92). This carbon is bonded to the most shielded proton in the ^1H

NMR spectrum. The chemical shift of C5' of 1 was even more interesting in that it was more deshielded than could be accounted for by the usual substituent effects (Levy *et al.*, 1980). A similar anomalous chemical shift was reported for the δ -methylene carbons of [8]paracyclophane (Kaneda *et al.*, 1980).

Ring current effects were not expected to be dominant in the carbon spectrum since the ^{13}C shielding constant contains a major contribution from large paramagnetic effects and the shielding anisotropy contributions usually prove to be small in comparison (Trost and Herdle, 1976).

In the hetero-correlated spectrum (Figure 3.3), an artifact appears midway between practically every pair of geminal protons. These artifacts are believed to be caused by coherence transfer between the geminal protons of each pair (1) and (2) during the 2D pulse sequence. The final result is the appearance of an artifact at a frequency that is the average of the two geminal protons. More information about this phenomenon will be available after further study (Bain *et al.*, 1988).

The remaining assignments required identification of each proton of a geminal pair. Fortunately, the spin-spin coupling patterns of each single proton multiplet provided a method for investigating the identity of each proton. Also,

by studying the fine structure of each multiplet, a great deal of information pertaining to the time-averaged solution conformation of the bridging alkyl chain could be obtained. The well known Karplus relationship (Karplus, 1959 and 1963) correlates the ${}^3J_{\text{H-H}}$ vicinal coupling constant to the dihedral angle between two vicinally coupled protons. Thus, determination of the vicinal couplings of the methylene protons of 1 should provide insight into the time-averaged solution conformation of the methylene carbon chain.

The ${}^2J_{\text{H-H}}$ and ${}^3J_{\text{H-H}}$ couplings and dihedral angles derived from the Karplus equation used by Bothner-By (1965) are shown in Table 3.3. Also included in this table are the tentative proton numbers to which coupling occurs based upon simulation of the partially homodecoupled spectra. Although the coupling values for the two overlapping protons at $\delta 0.21$ could not be directly determined, they were extrapolated from the values from their vicinal neighbours. It should be noted that two dihedral angles satisfy each coupling value, yet only one can lead to a realistic structure.

The dihedral angles determined by use of the Karplus equation for protons on C1'-C2' and C7'-C8' could have been subject to a larger error factor than the other protons. This error factor would be attributed to the electronic inductive effects resulting from the nitrogen substituents N6' and N9. Although methods of modifying the Karplus

Table 3.3 PANIC Simulation of ${}^2J_{HH}$, ${}^3J_{HH}$ Couplings and
Calculated Dihedral Angles.

Carbon & (${}^1H^*$ Number)	δ (1H (ppm)	Coupling Constant (Hz)	RMS error ^a	Calculated Dihedral Angles (deg.) ^{b, c}
C1'	4.68	-14.8	0.079	-
(1)		11.5		158 ^d
		11.5		158 (3)
		3.5		64, 110 (4)
C1'	3.35	-14.7	0.187	-
(2)		2.6		72, 102 ^d
		2.6		72, 102 (4)
		4.9		54, 120 (3)
C2'	1.47	-14.4	0.010	-
(3)		11.8		160 (1)
		5.4		50, 123 (2)
		5.7		49, 124
		3.1		67, 106
C2'	1.38	-14.8	0.014	-
(4)		3.4		64, 109
		3.4		64, 109
		12.0		162
		3.4		64, 109

continued...

Table 3.3 continued

Carbon & (¹ H Number)	δ (¹ H (ppm))	Coupling Constant (Hz)	RMS ^a error	Calculated Dihedral Angles (deg) ^{b, c}
C3'	1.03	-15.0	0.113	-
(5)		6.0		47, 126
		12.0		162
		6.2		46, 127
		3.0		68, 106
C4'	0.57	-12.7	0.099	-
(6)		6.5		43, 129
		10.5		13, 151
		6.7		42, 130
		10.5		14, 151
C5'	-0.64	-14.1	0.042	-
(7)		10.7		11, 152 (9)
		4.6		56, 118
		7.6		37, 134
		3.2		66, 108 (10)
C5'	0.89	-13.8	0.57	-
(8)		6.9		41, 131 (10)
		10.2		16, 149
		10.2		16, 149
		7.1		40, 132 (9)

continued...

Table 3.3 continued

Carbon & (¹ H Number)	δ (¹ H (ppm))	Coupling Constant (Hz)	RMS ^a error	Calculated Dihedral Angles (deg) ^{b, c}
C6' (9)	1.26	-14.9	0.074	-
		2.6		72, 102 (11)
		7.7		36, 135 (12)
		10.0		18, 148 (7)
		7.7		36, 135 (8)
C6' (10)	0.52	-14.8	0.053	-
		8.7		29, 140 (11)
		2.9		69, 105 (12)
		7.5		37, 134 (8)
		3.1		67, 106 (7)
C7' (11)	1.80	-14.5	0.022	-
		5.5		50, 123 (13)
		10.5		13, 151 (14)
		2.9		69, 105 (9)
		8.8		29, 141 (10)
C7' (12)	1.64	-14.7	0.030	-
		3.8		61, 112 (13)
		5.3		51, 122 (14)
		8.2		33, 138 (9)
		2.9		69, 104 (10)

continued...

Table 3.3 continued

Carbon & (¹ H Number)	δ (¹ H (ppm))	Coupling Constant (Hz)	RMS ^a error	Calculated Dihedral Angles (deg) ^{b, c}
C8'	4.54	-14.0	0.010	-
(13)		5.3		51, 122 (11)
		4.0		60, 113 (12)
C8'	3.92	-14.0	0.003	-
(14)		10.3		16, 150 (11)
		5.3		51, 122 (12)

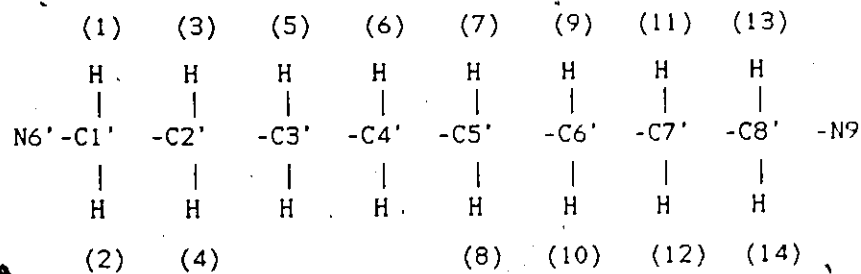
^a Comparison between PANIC and exptl. spectrum.

^b Karplus equation $^3J_{HH} = 7 - \cos\phi + 5\cos 2\phi$.

^c In brackets is shown the proton number, to which the coupling occurs.

^d Coupling to N6'H.

^e The numbers in brackets correspond to the following structure.



equation to account for substituents exist (Haasnoot *et al.*, 1980), the values for the C1'-C2' and C7'-C8' protons proved to be acceptably accurate.

The structural applications of these data will be discussed in Chapter 4.

3.5 Introduction to the Conformational Analysis

Although the results of the proton assignments ultimately lead to information about the time-averaged solution conformation, it was important to determine if the observed average solution conformation could be altered through temperature variation. Such a change could be accompanied by a shift in the resonance frequency of certain methylene protons which may lead to the determination of other solution conformations using the previously discussed spin simulation method. This method of analysis was accomplished using ^1H and ^{13}C spectra recorded at various temperatures.

Since the gradient of the shielding anisotropy may change for the region of space surrounding the various methylene protons of 1, it was advantageous to study the flexibility (conformational mobility) of the methylene chain. A study of the ^{13}C spin-lattice relaxation would lead to the detection of increased mobility for a given portion

of the methylene bridge and therefore indicate which protons were apt to undergo a significant spatial movement with the change of temperature. This information can be derived from measurement of the spin-lattice relaxation of the methylene carbons of 1.

Finally, nuclear Overhauser enhancement (NOE) studies were used as a method of determining relative proton-proton intramolecular distances.

3.6 Experimental Methods for the Conformational Studies

The methylene chloride solvent system proved to be suited for low temperature work by having a freezing point below the low temperature limit of the spectrometer.

In order to increase the accuracy of the temperature measurement, a thermocouple suspended into the probe was used to determine the internal temperature prior to data accumulation. A correction was made for the change of chemical shift of the internal reference with temperature. This correction was obtained from a plot of the change of spectral reference frequency with changing temperature.

The spin-lattice (T_1) measurements were made using the inversion recovery method using variable recovery delays. The pulse sequence used was as follows:

^1H : BB(S_1)----- S_2 -----
 ^{13}C : D_1 - 180° -VD- D_2 - 90° -FID

A 20 second time period was used to allow equilibrium to be reestablished. The dipolar contribution to the T_1 relaxation times were evaluated from two sets of spectra. One set was acquired using an inverse gated proton decoupled method and the other set was obtained using a simple broadband decoupling method. Both types of experiments used a 90° pulse and a 20 second recovery period.

The proton-proton NOE experiments were acquired by an automated process using a set of on-resonance offset frequencies including one off-resonance frequency. The off-resonance spectrum was subtracted from each of the on-resonance experiments revealing the NOE effects.

3.7 Results of the Conformational Studies

Examination of Figure 3.5 indicates that as the temperature was lowered, the fine structure of each multiplet was lost. Simultaneously, broadening of each resonance occurred which could be attributed to field inhomogeneity or more likely a T_2 exchange effect. It is not likely that this broadening was caused by solvent viscosity since the TMS reference peak remained relatively sharp

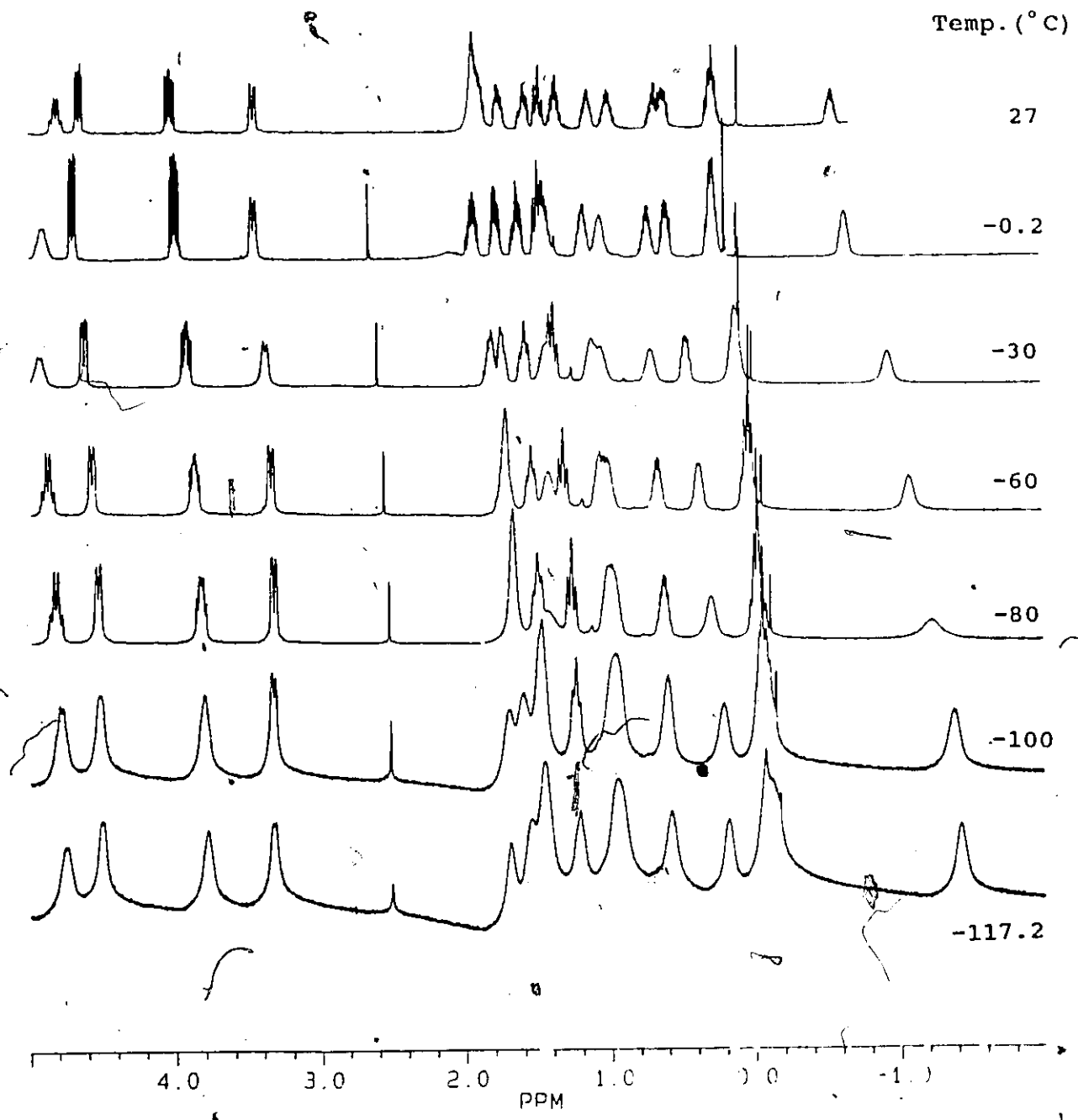


Figure 3.5 ¹H NMR Variable Temperature Spectra of 1.

despite the broadening of the other peaks. This loss of resolution of each multiplet precluded the ability to obtain any suitable data for spin simulation from the low temperature spectra, and therefore to apply the Karplus relationship to detect detailed conformational changes.

Moreover, the chemical shifts of individual protons could be followed from the ^1H spectra as listed in Table 3.4. These data indicate that as the temperature decreased, the most shielded proton (δ -0.69 at 27°C) decisively shifted further upfield to δ -1.26 at -117°C . During the change in temperature, some of the resonances became overlapped. For example, one of the signals from the proton on C6' overlapped a signal from a proton on C2' (δ 1.45 shown at -0.2°C) and upon further lowering of the temperature, the two protons became two separate resonances. The identity of the proton on C2' was revealed by the acquisition of a homonuclear COSY obtained at -90°C .

The variable temperature ^{13}C chemical shifts for the alkyl carbons are listed in Table 3.5. As was the case with the proton spectra, only single resonances were observed and the shifts moved upfield as the temperature was lowered (see Figure 3.6b).

The data collected from the measurement of the spin-lattice relaxation times of the proton bearing carbon atoms of **1** are included in Table 3.6. Included with the T_1 values

Table 3.4 Methylene Proton Chemical Shifts for
Various Temperatures^a.

Temp. (°C)	Protons According to Carbon Number						
	C1'	C1'	C2'	C2'	C3'	C3', C4'	C4'
27.0	4.78	3.29	1.58	1.41	1.09	0.17	0.57
-0.2	4.79	3.35	1.63	1.48	1.18	0.17	0.62
-13.0	4.82	3.36	1.61	1.45	1.16	0.16	0.65
-20.0	4.85	3.36	1.60	1.42	1.14	0.14	0.66
-30.0	4.89	3.37	1.58	1.40	1.13	0.12	0.68
-40.2	4.91	3.37	1.58	1.40	1.12	0.11	0.70
-52.4	4.92	3.38	1.56	1.35	1.08	0.10	0.72
-60.0	4.92	3.40	1.55	1.33	1.07	0.09	0.73
-70.0	4.92	3.42	1.53	-	1.01	0.09	0.73
-80.0	4.93	3.44	1.50	-	1.00	0.08	0.74
-90.0	4.93	3.46	1.48	1.25	0.97	0.08	0.74
-100.0	4.92	3.47	1.47	1.25	0.98	0.05	0.74
-111.0	4.92	3.49	1.46	1.21	0.96	0.05	0.75
-117.2	4.91	3.49	1.45	1.20	0.96	0.04	0.74

continued...

Table 3.4 continued

Temp. (°C)	Protons According to Carbon Number							
	C5'	C5'	C6'	C6'	C7'	C7'	C8'	C8'
27.0	-0.69	0.97	0.49	1.31	1.85	1.70	4.63	3.86
-0.2	-0.75	1.06	0.49	1.48	1.92	1.78	4.58	3.89
-13.0	-0.80	1.04	0.48	1.45	1.89	1.76	4.59	3.90
-20.0	-0.84	1.04	0.48	1.42	1.86	1.75	4.60	3.90
-30.0	-0.89	1.04	0.47	1.40	1.83	1.74	4.61	3.91
-40.2	-0.94	1.05	0.46	1.40	1.80	1.74	4.61	3.91
-52.4	-0.98	1.03	0.45	1.56	1.75	1.73	4.62	3.92
-60.0	-1.02	1.03	0.44	1.55	1.72	1.72	4.62	3.92
-70.0	-1.06	1.01	0.42	1.53	1.70	1.70	4.63	3.93
-80.0	-1.11	1.00	0.42	1.50	1.67	1.67	4.64	3.94
-90.0	-1.20	0.97	0.38	1.48	1.64	1.64	4.65	3.94
-100.0	-1.24	0.98	0.36	1.47	1.60	^b 1.69	4.66	3.94
-111.0	-1.25	0.96	0.35	1.46	1.56	^b 1.68	4.66	3.95
-117.2	-1.26	0.96	0.35	1.45	1.54	^b 1.68	4.66	3.94

^a Spectral reference vs Temp was used to correct shifts.

^b These values may be interchanged.

Table 3.5 ^{13}C Chemical Shifts for Variable Temperature Spectra.

Temp. ($^{\circ}\text{C}$)	Methylene ^{13}C Numbers and Chemical Shifts.							
	C1'	C2'	C3'	C4'	C5'	C6'	C7'	C8'
28	45.15	33.27	27.51	28.45	33.57	25.38	30.99	47.13
-32	42.60	31.08	25.50	26.00	32.18	23.29	28.35	45.12
-52	41.94	30.52	25.04	25.37	31.96	22.79	27.64	44.60
-77	41.13	29.67	24.34	24.62	31.46	22.10	26.64	43.94
-97	40.51	28.97	23.78	24.01	31.10	21.57	25.55	43.40

are the contributions made to the total spin-lattice values by the dipole-dipole relaxation mechanism.

The NOE experiments, carried out at 27°C , provided important information about the relative distances between certain geminal protons and protons in other parts of the molecule. Upon irradiation of the upfield resonance at $\delta=0.64$, an NOE was observed at $\delta 1.80$ and to H2 at $\delta 8.30$. In addition, irradiation of the resonance located at $\delta 3.92$ resulted in large NOE's for H8 ($\delta 7.79$) as well as for both of the protons bonded to C7'. These NOE's provided a means of verifying the proton assignments to be addressed in Chapter 4.

Figure 3.6a Chemical Shift vs. Temperature for the Two Protons of Carbon C5'

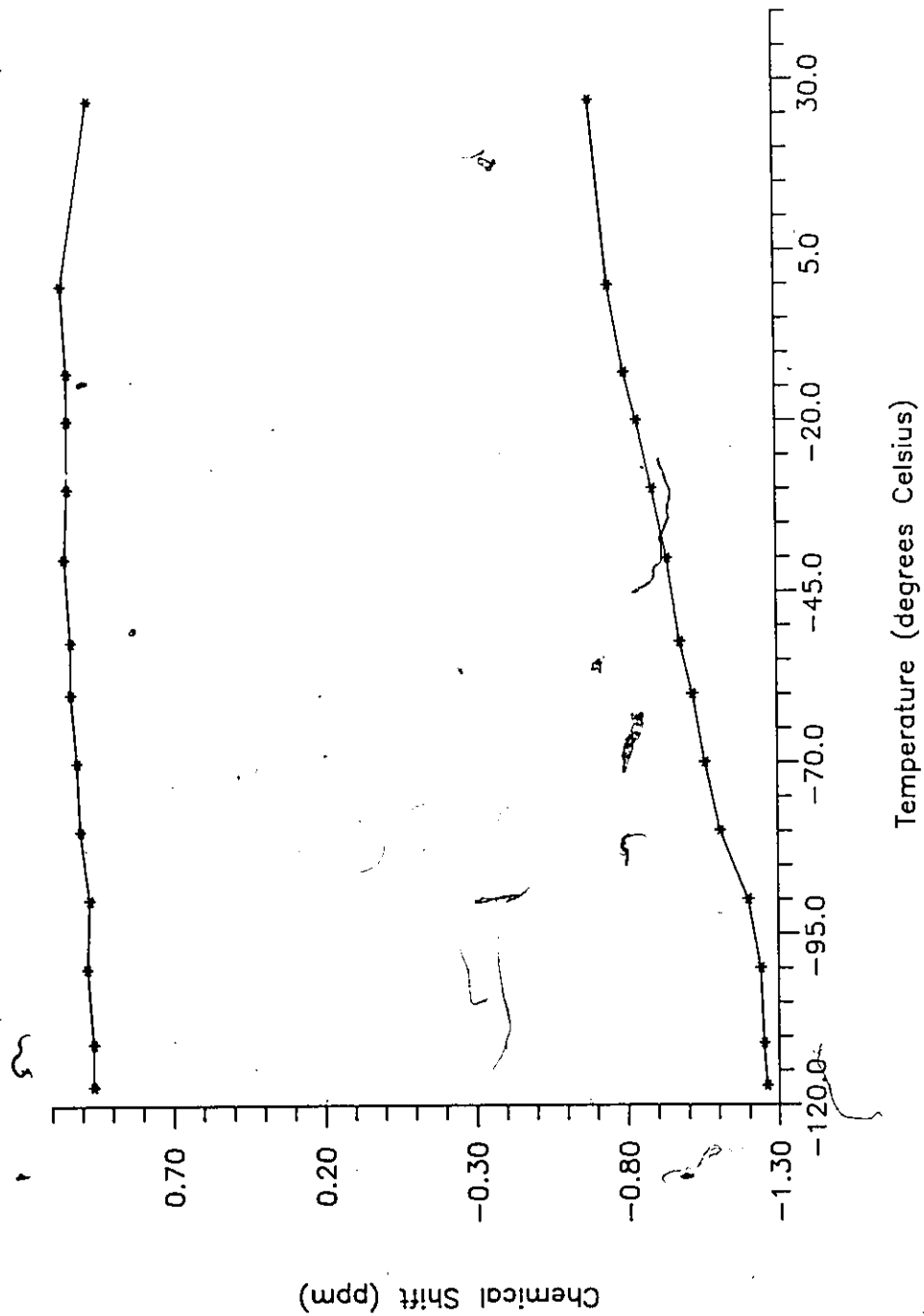


Figure 3.6b Chemical Shift vs. Temperature for Carbon C5'

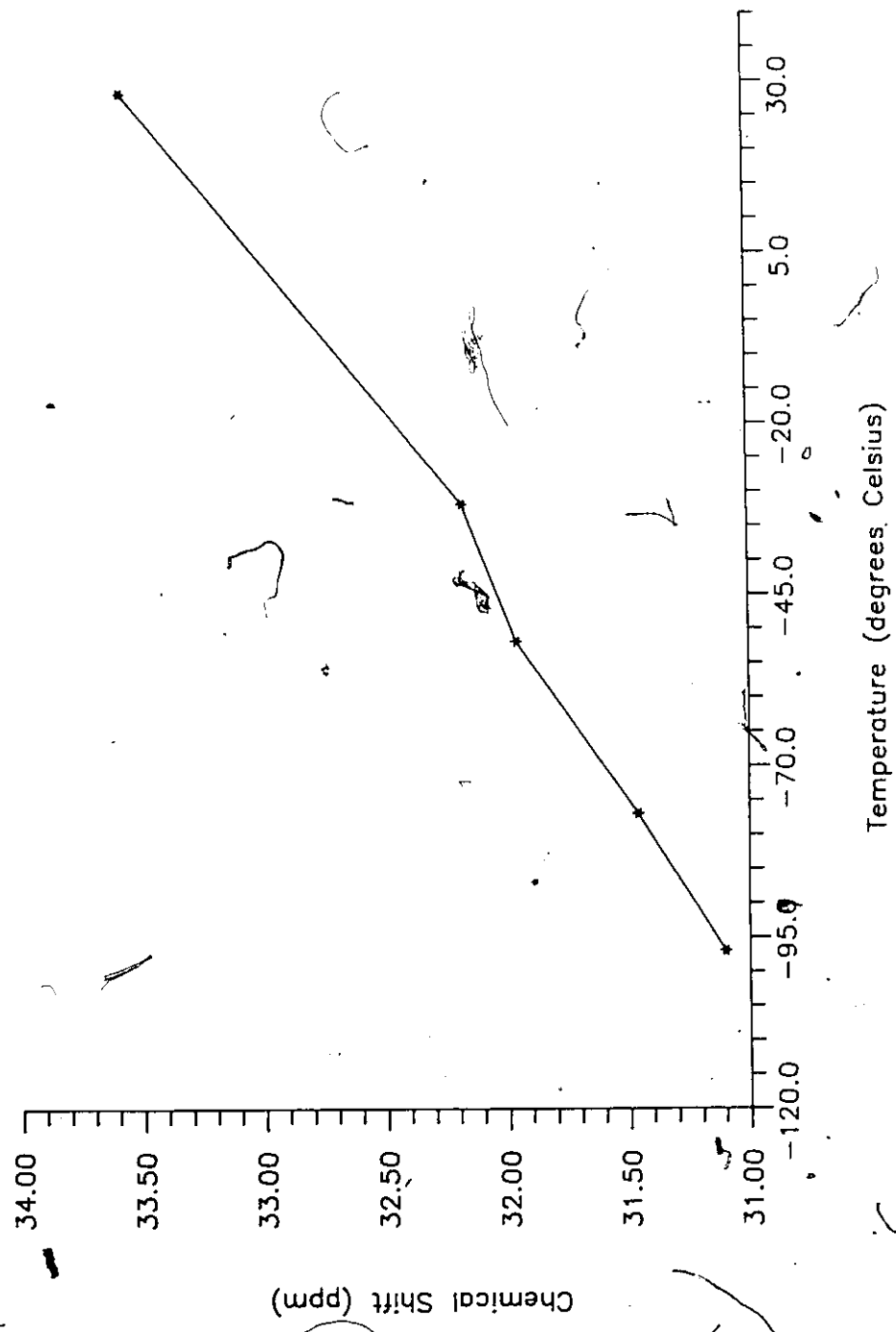


Table 3.6 Determination of ^{13}C Spin-Lattice Relaxation^a.

Carbon Number	Area without NOE	Area with NOE	NOE ^b	Dipole-Dipole Mech. (%)	T ₁ (sec)	T _{1DD} (sec)
C1'	9.88	26.92	1.72	87	1.5	1.8
C2'	11.76	31.28	1.66	83	1.8	2.2
C3'	9.99	28.65	1.87	94	2.0	2.2
C4'	10.63	29.70	1.79	90	2.2	2.4
C5'	10.62	29.64	1.79	90	2.1	2.4
C6'	9.54	29.12	2.05	103	2.2	2.2
C7'	11.12	32.32	1.91	96	1.9	1.9
C8'	9.45	27.94	1.96	98	1.8	1.8
C2	0.65	1.84	1.85	93	1.3	3.0
C8	0.82	2.09	1.54	78	1.1	3.9

^a Approximately 5% error in calculation.

^b $\text{NOE} = 1 + (\gamma_{\text{H}} / 2\gamma_{\text{C}}) (T_{1\text{DD}}^{-1} / T_1^{-1})$.

3.8 Discussion of the Conformational Studies

Part of the discussion of Section 3.4 focussed upon the ^1H NMR spectral analysis which reflected the shielding and coupling effects of the time-averaged conformation of the cyclophane 1. Since changing the temperature alters the relative populations of the various contributing conformations of the methylene chain, the acquisition of ^1H and ^{13}C spectra over a temperature range may give insight into the conformational mobility of 1. An alternate method of studying the flexibility of the alkyl chain would be to determine the correlation times of the methylene carbon atoms through the analysis of the ^{13}C T_1 values.

The spectra discussed in Section 3.5 were obtained at ambient temperature and because of this fact they reflected the time-averaged conformation of the methylene chain of 1. In order to investigate the conformational mobility of 1, a series of temperature dependent ^1H NMR spectra were collected over a range of 27° to -118°C .

The large range of chemical shift changes shown in Table 3.4 indicated that there was either a strong solvent induced temperature coefficient for individual proton signals or else more than one conformation was present. However, it is noteworthy to observe that some chemical

shifts change significantly (e.g., δ -0.69 to δ -1.26) while others show little change (e.g., δ 1.85 to δ 1.54). Since the change of chemical shifts with temperature for the aliphatic chain is not uniform, it is unlikely that the chemical shift changes are the result of a solvation effect. Therefore, a change in the conformation of the aliphatic chain accompanied by a change in the diamagnetic shielding of each proton would be the most likely cause of a change in chemical shift. The variation of the ^1H chemical shifts could probably be explained by a gradual change in the relative populations of the conformers which occurred as the solution cooled. The relative population change resulted in an alteration of the time averaged conformation as observed in the ^1H NMR spectra. However, at the lower temperatures separate signals representing the isolation of different conformers did not develop indicating that the rate of exchange between different conformers of \perp is fast on the NMR timescale. An example of the change of chemical shift with temperature for the protons of carbon C5' is illustrated in Figure 3.6a. The gradual change of the chemical shifts combined with the inability to resolve individual conformations indicated that the energy barrier between interconversion was relatively low and on the order of approximately 20kJ/mole (5kcal/mole) or less (Sutherland, 1971).

The ^1H spectra in Figure 3.5 illustrate the changes in several of the ^1H chemical shifts. The variability of the size of the chemical shift change could be caused by two factors. Either the protons undergo significant time-averaged spatial movement (with respect to the purine system) or else the methylene protons experience movement through a region with a large diamagnetic shielding gradient. Intuitively, it would be expected that protons closer to the atoms of the aromatic system would experience a larger change in ring current effects as compared to protons located further away from the aromatic plane. Each methylene proton distance to the aromatic plane could best be examined by studying the crystal structure data (Chapter 4).

The reason for performing the ^{13}C variable temperature experiment was to verify the findings of the proton studies which indicated that the energy barrier to conformational interconversion is relatively low. Carbon-13 spectra collected at different temperatures are usually better suited than ^1H spectra for observing conformational exchange since proton decoupling results in single lines for the ^{13}C resonances. Also, the methylene carbon chemical shift range is larger than for protons enabling the measurement of exchange rates which are not observable by proton methods (Mann, 1977). The advantage of using ^{13}C

spectra is lost if the difference in chemical shifts between different conformers is very small.

The data shown in Table 3.5 support the conclusion drawn from the proton low temperature spectra stating that no evidence exists for carbon resonances splitting into more than one signal at the lower temperatures. The gradual change in ^{13}C chemical shift is shown graphically in Figure 3.6b where the chemical shift of C5' is plotted as a function of temperature.

The variable temperature ^1H NMR studies (see above) indicated that certain protons either may have been located in a region of high shielding gradient or were experiencing significant spatial movement (or both). In order to further investigate the dynamic properties of the methylene chain of 1 in solution, the spin-lattice relaxation times of the proton bearing carbons were studied.

The spin-lattice relaxation time has been used to derive the rotational correlation time of ^{13}C nuclei (Breitmaier *et al.*, 1975). This correlation time may differ from the overall molecular correlation time depending upon the mobility of the observed carbon; that is, whether the carbon is rigid with respect to the molecule as a whole or whether the carbon undergoes additional intramolecular motion. The cause of the relaxation involves the interaction of the local magnetic fields of the carbon-hydrogen dipole

with respect to the overall magnetic field. Contributions made by this dipole-dipole (DD) relaxation mechanism may be evaluated from measurement of the nuclear Overhauser enhancement (NOE) of the carbon resonance by the directly bonded proton. The relationships between T_1 and T_1^{DD} as well as T_1^{DD} and the effective correlational time τ_c^{eff} are indicated in Figure 3.7. Since T_1^{DD} is inversely proportional to the number of attached protons, the carbons C2 and C8 should have approximately half of the dipolar contribution of the methylene carbons for an isotropically tumbling molecule; that is, a molecule which has no preferred axis of rotation.

$$(T_1^{TOTAL})^{-1} = (T_1^{DD})^{-1} + (T_1^{OTHERS})^{-1}$$

$$(T_1^{DD})^{-1} = h^2 \gamma_C^2 \gamma_H^2 \sum_{i,j} (r_{CHi})^{-6} \tau_c$$

Figure 3.7 Relationship between T_1^{TOTAL} , T_1^{DD} and τ_c .

The data displayed in Table 3.6 for C2 and C8 indicates that these values are not half of the average value found for the methylene carbons and implies that the cyclophane 1 may not tumble isotropically in solution but instead may have preferred axes of rotation. As a result,

the ability to derive quantitative results for comparing the T_1 values of the methylene carbons becomes restricted. Qualitative analysis of the data indicates that the central portion of the chain enjoys a larger degree of flexibility than either end of the bridging chain.

In summary, the conformational studies generally indicate that a solution of the cyclophane 1 consists of two or more conformations in dynamic equilibrium. The energy barriers which must be overcome to allow interconversion of the various conformations are too small to be accurately measured using ^1H or ^{13}C methods.

Chapter 4

Structural Determination

4.1 Introduction

The next step in the analysis of the compound N6',N9-octamethylenepurine cyclophane (1) required the detailed study of the structure using techniques in addition to the NMR methods discussed in Chapter 3. A method which could potentially yield the most information for the study of both the purine portion of the molecule and the aliphatic chain is X-ray crystallography. By studying the X-ray coordinates of the carbon and nitrogen nuclei, the proton coordinates and dihedral angles between methylene protons can be determined. Comparison of the dihedral angles reported in Table 3.3 with the values obtained by crystallography allows the unambiguous assignment of proton chemical shift values and provides insight into conformational changes of the methylene chain. Partial verification of the proton assignments can be provided by examining the NOE results.

Other methods of analysis used to study the more intricate molecular properties of 1 include molecular modelling, ultraviolet spectroscopy, and examination of the ¹³C NMR chemical shifts of the purine ring system in

comparison to other purine models.

4.2 Experimental Methods

The crystallographic structure determination was performed by Dr. C.J.L. Lock and R. Fagianni of McMaster University using crystals of 1 obtained by crystallization from benzene over a period of five days. The values of R and weighted R (R_w) were 0.0683 and 0.0493 while the error in observation of the unit weight (S) was 1.2448. The carbon and nitrogen atomic coordinates were used to calculate the accompanying proton coordinates and, subsequently, the dihedral angles between vicinal protons on the aliphatic chain. Also, from the carbon and nitrogen atomic coordinates of the purine system, the equation of the best fit plane through the pyrimidine and imidazole ring atoms was calculated using a least squares method of analysis.

Computer modelling studies of 1 were carried out independently of the X-ray crystallographic analysis and used the Macromodel computer program (Version 1.5, Still, 1987). The program operated in the following way. The molecular skeleton of 1 was drawn and subjected to an MM2 (85) Force Field minimization process (Allinger *et al.*, 1977) which enabled the bond lengths and bond angles to be systematically adjusted until the energy of the system

approached a local minimum. The program's algorithm generates slight atom movements which may or may not result in a structure with less overall strain. When a lower energy structure was obtained from certain atom movements, the resulting structure was stored. The program is very efficient in locating local energy minima but is poor in the location of a global energy minimum. The isolation of a local energy minimum implies that iterative atom movement was not sufficient to allow the structure to overcome the existing energy barrier(s) which may lead to a conformation with less strain. In order to make a thorough search for a global minimum, the dihedral angles along the C8 chain were systematically varied and each time the new structure subjected to an MM2 energy minimization. In this way, a total of seven low energy conformers were found.

Results and Discussion

4.3 X-ray Analysis and Comparative Studies

Analysis of the crystal data indicated the unit cell parameters were $a = 9.620(3)$, $b = 12.266(3)$, $c = 11.944(2)$, $\beta = 111.25^\circ (2)$ and that the unit cell volume was $1313.7(5) \text{ \AA}^3$. The space group $P2_1/n$ showed that indeed a racemic mixture of enantiomers of 1 existed within the unit cell.

Table 4.1 provides the carbon and nitrogen atomic

Table 4.1 Atomic Positional Parameters ($\times 10^4$) and
Temperature Factors ($\text{\AA}^2 \times 10^3$).

Atom	x	y	z	U_{eq}
N1	3392 (2)	9608 (2)	5456 (2)	42
C2	1952 (3)	9409 (2)	5270 (3)	43
N3	1398 (2)	8714 (2)	5825 (2)	39
C4	2446 (3)	8260 (2)	6763 (2)	32
C5	3953 (3)	8462 (2)	7146 (2)	33
C6	4438 (3)	9078 (2)	6369 (2)	37
N7	4719 (2)	7287 (2)	8193 (2)	39
C8	3677 (3)	7324 (2)	8376 (2)	40
N9	2271 (2)	7494 (2)	7539 (2)	37
N6'	5868 (2)	9157 (2)	6446 (2)	47
C1'	6930 (3)	8256 (3)	6913 (3)	50
C2'	6864 (3)	7408 (3)	5956 (2)	58
C3'	5335 (3)	6902 (3)	5276 (2)	51
C4'	4749 (3)	6144 (2)	6020 (3)	46
C5'	3067 (3)	6007 (3)	5498 (3)	45
C6'	2352 (3)	5436 (2)	6298 (3)	46
C7'	887 (3)	5956 (2)	6262 (3)	47
C8'	1012 (3)	6735 (4)	7285 (2)	46

$$U_{eq} = 1/3 (U_{11} + U_{22} + U_{33} + 2U_{13} \cos \beta)$$

positional parameters and is accompanied by selected interatomic distances and angles in Table 4.2 and hydrogen atom positional parameters in Table 4.3. Generally, the values for the carbon-carbon aliphatic bond lengths appear to be reasonably typical except for minor discrepancies such as the C2'-C3' and C4'-C5' bond lengths of 1.518 Å and 1.507 Å. These two bonds appear to deviate more than the other aliphatic carbon-carbon bonds from the expected value of 1.54 Å. The bond angles, shown in Table 4.2 for the purine portion of 1, correlate well with values reported for adenine (Taylor and Kennard, 1982). However, upon examination of certain dihedral angles in the aromatic plane, distortion of the purine system is evident. For example, the angles defined by C4-C5-C6-N1 and C2-N1-C6-N6' are 13.8° and 170.5° which deviate from the values of 0.2° and 180° respectively as reported for adenine.

Further distortion of the purine system is evident from the calculation of the best fit planes through the carbon and nitrogen atoms. Two such planes were calculated for the atoms of the pyrimidine and imidazole rings resulting in an angle of intersection of the planes of 167°. This value is distinctly different from the value of 180° determined for adenine (Taylor and Kennard, 1982) and implies that a noticeable amount of strain is imparted to the purine system by the eight carbon methylene bridge.

Table 4.2 Selected Interatomic Distances and Angles for 1
and Adenine.

Bond	Length (Å)		Bond	Length (Å)	
	<u>1</u>	Adenine		<u>1</u>	Adenine
N1-C2	1.339(4)	1.338	C6-N6'	1.349(4)	1.337
C2-N3	1.332(4)	1.332	N6'-C1'	1.471(4)	-
N3-C4	1.346(3)	1.342	C1'-C2'	1.530(5)	-
C4-C5	1.375(3)	1.382	C2'-C3'	1.531(4)	-
C5-C6	1.401(4)	1.409	C3'-C4'	1.528(5)	-
C6-N1	1.353(3)	1.349	C4'-C5'	1.518(4)	-
C5-N7	1.392(3)	1.385	C5'-C6'	1.534(5)	-
N7-C8	1.299(4)	1.312	C6'-C7'	1.533(5)	-
C8-N9	1.375(3)	1.367	C7'-C8'	1.522(4)	-
N9-C4	1.374(3)	1.376	C8'-N9	1.468(4)	-

Angle	Value (deg.)		Angle	Value (deg.)	
	<u>1</u>	Adenine		<u>1</u>	Adenine
C6-N1-C2	117.8(2)	118.8	C5-C6-N6'	124.7(2)	123.4
N1-C2-N3	129.8(2)	129.0	N1-C6-N6'	117.6(3)	119.0
C2-N3-C4	109.4(2)	110.8	C6-N6'-C1'	121.5(3)	-
N3-C4-C5	127.6(2)	126.9	N6'-C1'-C2'	113.1(2)	-
C4-C5-C6	116.1(2)	116.9	C1'-C2'-C3'	116.4(3)	-

Table 4.2 continued

Table 4.2

Angle	Value (deg.)		Angle	Value (deg.)	
	<u>1</u>	Adenine		<u>1</u>	Adenine
C5-C6-N1	117.7(2)	117.6	C2'-C3'-C4	115.1(3)	-
N3-C4-N9	126.6(2)	127.4	C3'-C4'-C5'	113.0(2)	-
C5-C4-N9	105.7(2)	105.7	C4'-C5'-C6'	116.5(2)	-
C4-N9-C8	105.3(2)	105.9	C5'-C6'-C7'	114.1(2)	-
N9-C8-N7	114.4(2)	113.8	C6'-C7'-C8'	115.7(2)	-
C8-N7-C5	103.4(2)	103.9	C7'-C8'-N9	112.5(3)	-
N7-C5-C6	132.3(2)	132.3	C8'-N9-C4	126.0(2)	-
N7-C5-C4	111.0(2)	110.7	C8'-N9-C8	125.2(2)	-
C4-C5-C6-N1	13.8	0.2	C2-N1-C6-N6'	170.5	180.0

Table 4.3 Atomic Positional Parameters and Temperature Factors (\AA^2) ($\times 10^3$) for Hydrogen Atoms.

Atom	x	y	z	U
H2	127(3)	982(2)	462(2)	52(8)
H8	384(2)	682(2)	904(2)	45(7)
H6	602(3)	951(2)	583(3)	72(10)
1'R	794(3)	859(2)	722(2)	66(8)
1'S	675(3)	789(2)	762(2)	54(8)
2'R	757(4)	677(3)	638(3)	105(12)
2'S	724(3)	775(2)	538(3)	71(9)
3'R	543(3)	649(3)	459(2)	76(9)
3'S	459(3)	755(2)	494(2)	62(8)
4'R	504(3)	641(2)	684(2)	54(8)
4'S	528(3)	542(2)	610(2)	67(8)
5'R	266(3)	677(2)	530(2)	48(7)
5'S	279(3)	566(2)	474(2)	50(8)
6'R	216(3)	465(2)	601(2)	61(8)
6'S	310(3)	542(2)	712(2)	48(7)
7'R	17(3)	537(2)	631(2)	50(7)
7'S	38(3)	634(2)	548(2)	46(7)
8'R	6(3)	722(2)	708(2)	62(8)
8'S	114(3)	637(2)	800(2)	47(7)

The data collected from the crystallography studies was also of major significance when correlating the spatial location of the methylene protons in the solid state to the relative positions of the solution state. With computer assistance, the proton coordinates were extrapolated from the carbon and nitrogen positions and used to generate the dihedral angles between the vicinal protons of the methylene chain. The methylene proton dihedral angles (shown in Table 4.4) are compared with the results of the PANIC simulation studies (Chapter 3) as well as values provided by computer modelling studies using the Macromodel computer modelling program. When comparing the X-ray derived data and the computer modelling data, it is important to note that the differences between these two sets is remarkably small and suggests that the computer modelling was successful in locating a minimum energy conformation of the methylene chain which was similar to the conformation found in the solid state.

By comparing the dihedral angles from the X-ray generated data and the PANIC data obtained from the ^1H NMR spectra, two important problems could be addressed. The first problem involved the assignment of each specific resonance in the ^1H spectrum to the corresponding prochiral methylene proton since the assignment of the protons described in Chapter 3 (using a 2D NMR approach) did not

Table 4.4 Proton Dihedral Angle Comparison Between
 Values Extrapolated From the Crystal Structure,
 Computer Modelling and PANIC Spin Simulation.

Proton Angle	X-ray	Modelling	PANIC
1'S 2'S	-51.2	-49.5	-64'
1'S 2'R	-168.7	-164.9	-159
1'R 2'S	68.3	65.2	68
1'R 2'R	-49.2	-50.1	-52
2'S 3'S	-70.6	-66.4	-64
2'S 3'R	-172.9	-179.9	-162
2'R 3'S	46.2	48.8	48
2'R 3'R	-70.3	-64.7	-67
3'S 4'S	155.9	152.8	-
3'S 4'R	41.1	37.2	13 ^a
3'R 4'S	-83.8	-93.0	-106 ^a
3'R 4'R	161.5	151.4	126 ^a
4'S 5'S	-171.9	-174.6	-149 ^a
4'S 5'R	76.7	71.8	56 ^a
4'R 5'S	-56.9	-59.2	-40 ^a
4'R 5'R	-168.3	-172.8	-152 ^a
5'S 6'S	139.7	144.0	133
5'S 6'R	25.1	30.0	38

Table 4.4 continued...

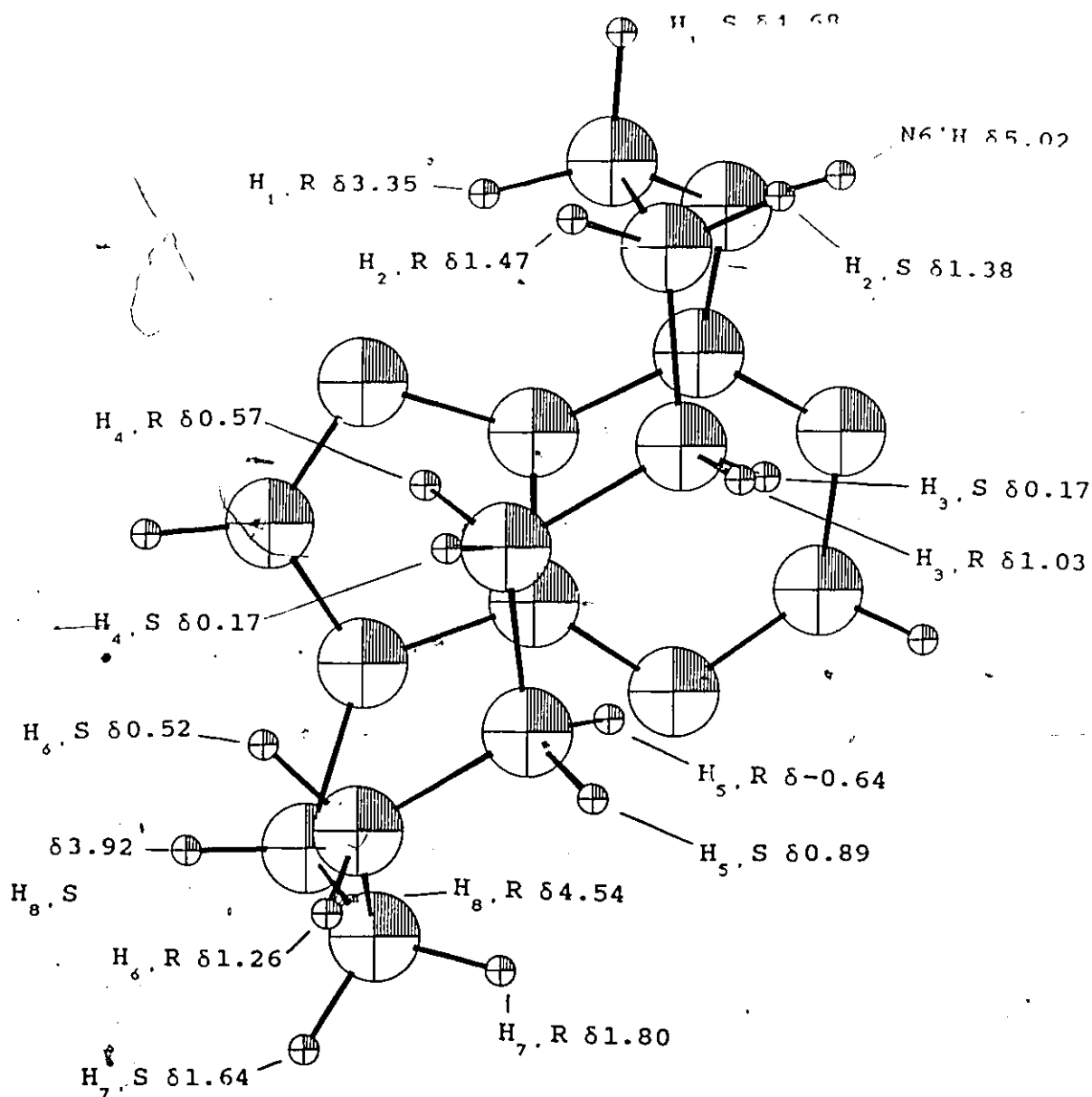
Table 4.4 continued

Proton Angle	X-ray	Modelling	PANIC
5'R 6'S	-104.9	-101.6	-107
5'R 6'R	-144.4	-144.4	-150
6'S 7'S	-93.8	-96.1	-104
6'S 7'R	148.6	149.4	141
6'R 7'S	23.9	18.1	35
6'R 7'R	-93.7	-96.3	-104
7'S 8'S	45.3	46.1	51
7'S 8'R	-75.1	-69.7	-61
7'R 8'S	159.2	159.8	151
7'R 8'R	38.3	<u>44.0</u>	51

* These values differ by more than 15° from the crystal structure values.

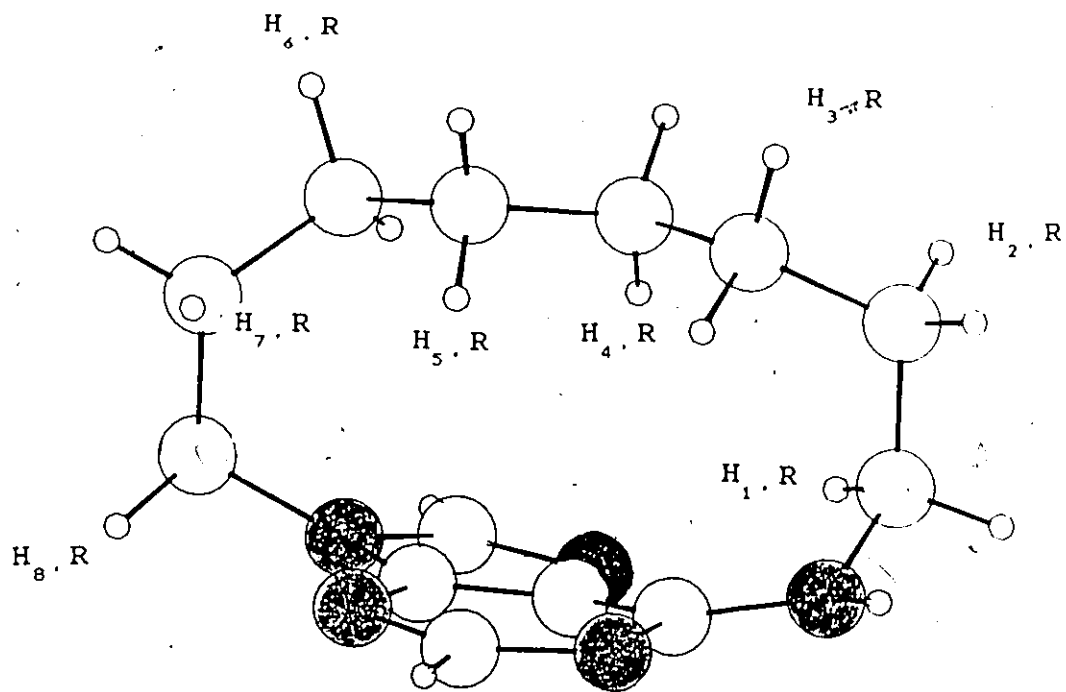
distinguish between the diastereotopic protons (H_R, H_S). The starting point for the assignment process involved the two protons of carbon C1' which were assigned according to the relative size of the vicinal coupling to N6'H and by inspection of the dihedral angle that each proton made with N6'H. Following the initial assignment of the C1' protons, each subsequent angle derived from the couplings fell into place, with internal verification being supplied by the assignment of H_S, R which was expected to be the proton closest to the aromatic plane of the two geminal C5' protons. The structure of the cyclophane 1 with the complete proton assignments is indicated in Figures 4.1 and 4.2.

The second problem clarified with the aid of the data in Table 4.4, involved accounting for the apparent difference in conformations between the structure obtained by X-ray analysis and the structure obtained using the coupling constants with the PANIC simulation-Karplus approach. By comparing these two sets of data, it became apparent that marked changes in the conformation of the methylene bridge occurred about the C3'-C4' and C4'-C5' bonds upon converting from the time-averaged solution state conformation to the solid state structure. Qualitatively, this observation implied that partial rotation occurred about these three carbon atoms as the temperature changed and as the molecular environment changed from a solution to



VIEW 1

Figure 4.1 Crystal Structure of N6',N9-Octamethylenepurine Cyclophane With 1H NMR Assignments.



VIEW 2

Figure 4.1 Crystal Structure of N6',N9-Octamethylenepurine Cyclophane

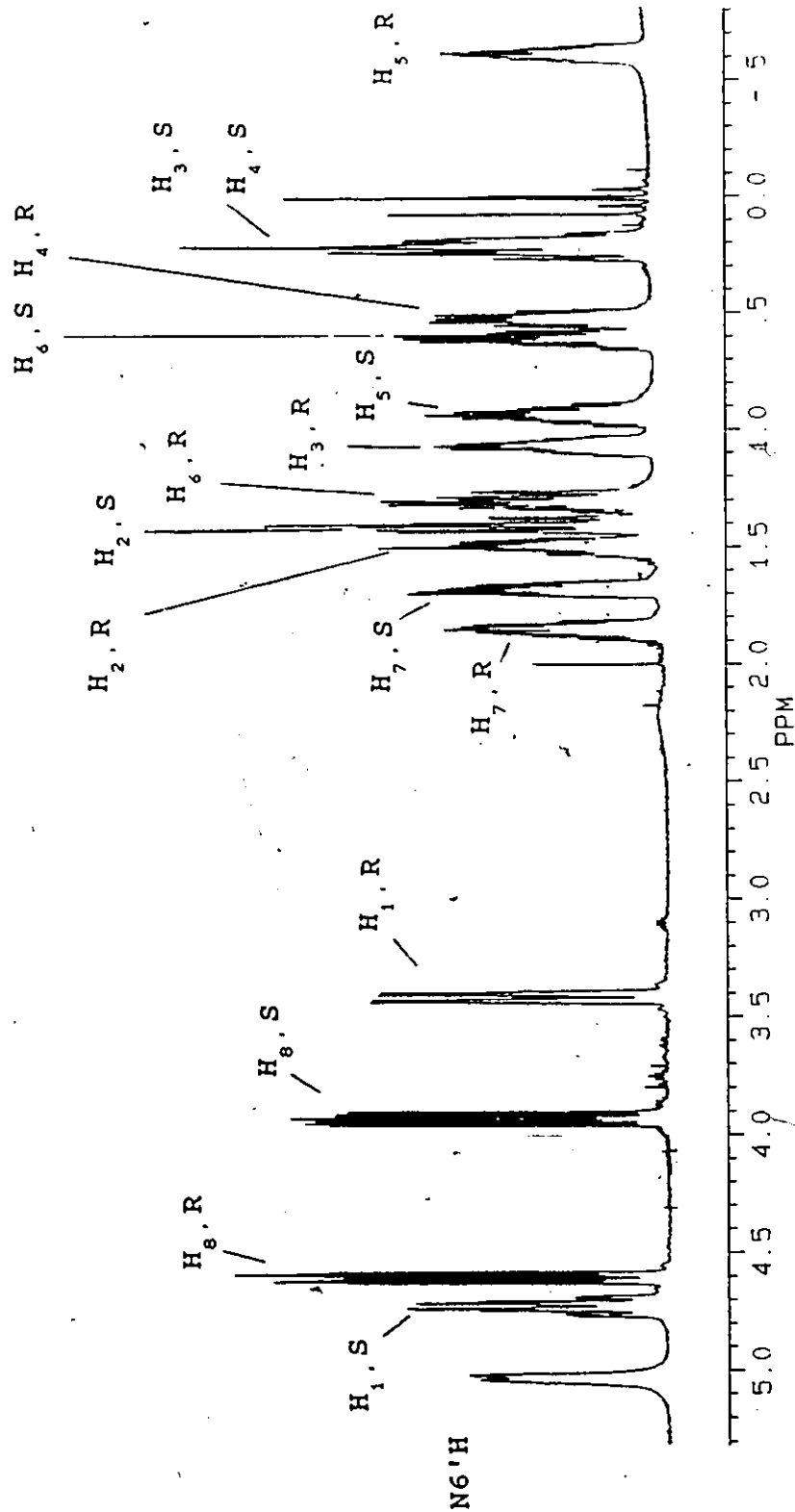


Figure 4.2 Aliphatic Portion of the ¹H NMR Spectrum of N6',N9-Octamethylenepurine Cyclophane With Assignments.

a crystal lattice. This conclusion assumed that lowering the temperature of the solution sample caused the time-averaged conformation of the molecule to approach that observed in the crystal structure; an idea which was in agreement with the computer modelling studies (see below).

The concept that 1 existed as a set of closely related and rapidly time-averaged conformers appeared to be consistent with the changes which occurred in the variable temperature ^1H NMR spectra of 1 (shown in Figure 3.5). By noting the total difference in chemical shift for each proton between the temperatures of 27°C and -118°C from Table 3.4, it is apparent that the protons which undergo the largest change in chemical shift are $\text{H}_{5,R}$ (0.57 ppm), $\text{H}_{7,R}$ (-0.31 ppm), $\text{H}_{2,S}$ (-0.21 ppm), and $\text{H}_{1,R}$ (0.20 ppm). However, of these values, $\text{H}_{5,R}$ is the only proton which appears to experience moderate spatial movement as a direct result of the bond rotation occurring about $\text{C}3'-\text{C}4'$ and $\text{C}4'-\text{C}5'$. Therefore it follows that the protons $\text{H}_{7,R}$, $\text{H}_{2,S}$ and $\text{H}_{1,R}$ are located in regions of high shielding gradient. Conversely, the protons $\text{H}_{5,S}$ (-0.01 ppm) and $\text{H}_{7,S}$ (-0.02 ppm) must be located in regions of relatively low shielding gradient in order to account for their very small chemical shift changes. It should be noted that an important premise of the above argument is that the chemical shift changes which occurred are not largely caused by solvation effects.

Such a premise is reasonable because the solvent used, methylene chloride-Freon, was of low polarity and many pairs of protons, for example $H_{7,S}$ and $H_{7,R}$ showed large shift change differences but were equally accessible to solvent molecules. Specific solvent effects are therefore considered very small.

Further comparison of the time-averaged solution conformation and the crystal structure was provided by a study of the intramolecular relationships obtained from the NOE studies briefly discussed in Section 3.4. The NOE difference spectra confirmed the proton assignments reported above; that the observed NOE's occur between protons which have been previously assigned as being proximal (see above). For example, irradiation of $H_{5,R}$ (δ -0.64) produced an NOE for $H_{7,R}$ (δ 1.80) and H_2 (δ 8.30), and upon irradiation of $H_{8,S}$ (δ 3.92), NOE's were observed for H_8 (δ 7.79) as well as for both of the $C7'$ protons. These values correlate well with the assignments shown in Views 1 and 2 of Figure 4.1 and thus provides partial confirmation the assignment of each prochiral methylene proton.

4.4 Other Methods of Analysis

Along with the study of the crystal structure, alternate methods were used to probe the properties of 1.

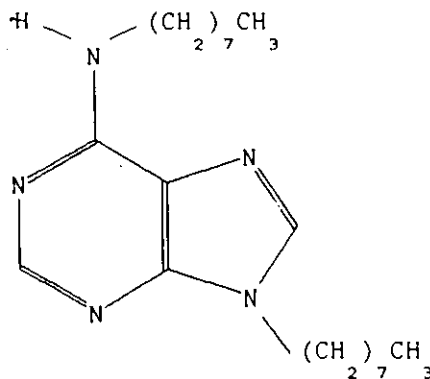
These methods involved the study of computer models, ultra-violet spectroscopy and the ^{13}C chemical shifts of the purine portion of the molecule.

As mentioned in Section 4.3, molecular modelling using the Macromodel computer modelling program was explored. During the energy minimization process, several local minima were detected and the conformation with the lowest total energy was designated as the global minimum on a potential energy surface. The relative energy of seven of the lowest total energy conformations, -3.11, 0.70, 4.07, 7.88, 8.73, 15.96 and 16.38 kJ/mole, showed that the difference in energy between the local minima and the global minimum at -3.11 kJ/mole was small. Although the modelling program used could not predict the energy barriers for the interconversion of different conformers, it was reasonable that several conformations can be in equilibrium in a room temperature solution of 1; for example, conformations with energies between -3.11 and 8.73 would be well populated.

The modelling program also allowed the creation of the time-averaged solution conformation by constraining the dihedral angles to the values obtained from the $^3J_{\text{H-H}}$ coupling constants of the methylene protons (using the PANIC values in Table 4.4). After removing the constraints and implementing an energy minimization calculation on the solution conformation, the resulting conformation

corresponded exactly to the global minimum. This result, obtained by computer methods, indicates that the conformation present in the crystal lattice may also represent the lowest energy conformation in solution. Much of the success of the application of the modelling program to 1 may dwell in the fact that there were no unusual inter- or intramolecular interactions present, such as hydrogen bonding interactions which are difficult to quantify energetically.

Another property of 1 which was investigated was the ultraviolet spectrum in absolute ethanol. The λ_{max} of 1 was determined to be 273 nm while the value for adenine was 261 nm and the dialkyl compound 26 was 268 nm. A similar increase in wavelength was reported in the [n]-paracyclophane series as the methylene bridge was shortened (Cram *et al.*, 1966). The change in wavelength may be attributed to either an increase in energy of the highest molecular orbital (HOMO) or a lowering in energy of the lowest unoccupied molecular orbital (LUMO) of the molecule but, since accurate determination of these molecular orbitals is difficult, a simpler phenomenological interpretation is preferred. Namely, as an aromatic ring is forced to bend, the ultraviolet wavelength increases, as was demonstrated by Cram *et al.*, (1966). Thus the increased λ_{max} observed for 1 was evidence for some bending of the purine



26

ring system in 1, although no quantitative value can be placed on the degree of bending. Ultimately, the result implied that there is strain on the aromatic portion which affects the electronic properties of the system.

The ^{13}C NMR spectrum of the purine portion of 1 also revealed distinct differences from those of adenine (Table 4.5). For example, there is a noticeable difference in the chemical shifts for C6 and C8 between adenine $\delta 155.1$, 139.2 and 1 $\delta 159.6$ and $\delta 143.7$. Although studies of the change in ^{13}C chemical shift have been reported for the [n]-paracyclophane series (Kaneda *et al.*, 1980), definite trends are not easily interpreted.

Table 4.5 ^{13}C Chemical Shifts for the Purine
Portions of Adenine and 1 in DMSO-d_6 .

Carbon #	Chemical Shifts (ppm)				
	2	4	5	6	8
Adenine	152.2	151.1	117.3	155.1	139.2
<u>1</u>	153.8	151.7	119.9	159.6	143.7

4.5 Conclusions

The elucidation of the crystal structure was of major importance for the study of 1. From the carbon and nitrogen atomic coordinates were obtained the proton coordinates which permitted the individual assignment of all proton chemical shifts. The solid state structure also enabled a comparison to be made with the PANIC NMR coupling data provided in Chapter 3.

All the methods used in this chapter generally indicated that a certain degree of strain is present in molecule 1. However, it could not be determined whether the strain significantly altered the diamagnetic anisotropy about the purine system of 1.

With knowledge of the proton coordinates, relative to the aromatic system, and the assignment of the proton

chemical shifts, it was possible to proceed with the study of a model to predict the ring current effect present in 1.

Chapter 5

Diamagnetic Anisotropy

5.1 Introduction

The studies undertaken in Chapters 3 and 4 resulted in the assignment of the methylene proton chemical shifts as well as their location in the region surrounding the aromatic portion of the molecule 1. Since the ultimate intention of studying the diamagnetic anisotropy of the heteroaromatic ring is to develop a method for predicting the magnetic shielding around adenine, a model is required to assist in these studies. A suitable model must be able to generate chemical shift increments for any point in space around the aromatic system. The resulting shift increments can then be compared with the experimental ^1H chemical shift values in order to evaluate the model.

A previous study of [10]paracyclophane (Agarwal *et al.*, 1977) employed a semi-empirical ring current model to generate shielding increments. The method used was based upon the "Free Electron Model" of Waugh and Fessenden (1957) in which the π -electrons were assumed to undergo circulation in a loop with diameter equivalent to that of the aromatic ring. The general relationship for the shift increment (Δ)

was

$$\Delta = (C/[(\alpha+\rho)^2+z^2]^{1/2} [K+(\alpha^2-\rho^2-z^2)/((\alpha-\rho)^2+z^2) E])$$

where :C = $ne^2/6\pi M_e c^2$, n was the number of circulating π -electrons, e was the charge of the electron, M_e was the mass of the electron, c was the velocity of light, ρ and z were the polar coordinates of a point in space relative to the center of the loop, α was the radius of the loop, and K and E were complete elliptical integrals of the first and second type with the argument

$$k^2 = 4\alpha\rho/((\alpha+\rho)^2+z^2).$$

The resulting integrals were:

$$K = \pi/2 \left[\left(1 + \sum_{N=0}^{\infty} \frac{(2N+1)!}{((N!)^2 (4^N) (2N+2))} k^{2N+2} \right) E + \pi/2 \times \left[1 - \sum_{N=0}^{\infty} \frac{((2N+1)! / ((N!)^2 (4^N) (2N+2)))^2 (k^{2N+2})}{(2N+2)} \right] \right].$$

The entire program used for the ring current model calculation is provided in Appendix A.

Several provisions were made so that the model could be applied to the cyclophane system 1. For example, the shift increments were recorded as the sum of the contributions of two loops of electron density; one above

and the other below the aromatic plane of each ring. This provision resulted from the fact that the π -electron density is not considered to be in the plane of the aromatic system but instead occupies a doughnut shaped molecular orbital located above and below the plane of the aromatic system. The actual ratio of π -electrons in each aromatic ring was derived from CNDO/2 and MNDO methods (Jordan and Sostman, 1972) but did not include the π -electron contribution from N6'. Also, the carbons occupying the ring fusion positions (C4 and C5) were treated as contributing half of the π -electron density to each ring.

Another provision incorporated into the model was that the plane of each aromatic ring was determined by calculating a least squares fit of the atoms forming the aromatic ring. Prior to the increment calculation, the origin was translated to the center of each aromatic ring so that two sets of increments were generated, one set for the pyrimidine and one set for the imidazole ring. Therefore, the calculated ring current increments represented the sum of the contributions of the five and six membered rings of the purine system. The methylene proton coordinates from Table 4.3 were translated to an orthogonal coordinate system before they were applied in the model (see Appendix A).

5.2 Results and Discussion

Table 5.1 presents the methylene proton chemical shift data for the cyclophane 1, obtained from experimental ¹H NMR data (Table 3.4) and the chemical shift increments generated for different π -molecular orbital loop separations. Included with both the experimental and calculated data are the chemical shift differences between protons within a pair of geminal protons in the methylene chain. Analysis of the data for various loop separations reveals that the correlation coefficients for the ring current increments, when compared to the experimental chemical shifts, do not change appreciably despite a significant change in the loop separation. Similarly, other investigations indicated that minor changes in the π -electron distribution between the six and the five membered aromatic rings results in minimal shielding changes. These observations would suggest that the inability to improve the correlation between the ring current model and the fit to the experimental data could be due to the neglect of the local atomic magnetic anisotropic contributions. The local contributions could be important for the unsymmetrical purine system since previous studies of benzenoid compounds have indicated that local atomic magnetic anisotropy can contribute as much as 40% to the calculated chemical shifts

Table 5.1 Experimental Chemical Shift Values,
 Calculated Ring Current Increments^a and Differences^b
 in Geminal Proton Chemical Shifts.

Proton #	Observed Chemical Shifts (δ)			
	27°C ^c	Geminal Differences	-118°C ^c	Geminal Differences
C1' 1S	4.63	1.34	4.91	1.42
2R	3.29		3.49	
C2' 1S	1.32	-0.09	1.38	-0.24
2R	1.41		1.62	
C3' 1R	0.97	0.85	1.11	1.07
2S	0.12		0.04	
C4' 1S	0.12	-0.41	0.04	-0.7
2R	0.53		0.74	
C5' 1S	0.84	1.53	1.11	2.37
2R	-0.69		-1.26	
C6' 1R	1.20	0.75	1.62	1.27
2S	0.45		0.35	
C7' 1R	1.74	0.16	1.71	-0.15
2S	1.58		1.86	
C8' 1S	3.86	-0.63	3.94	-0.72
2R	4.49		4.66	

continued...

Table 5.1 continued

Proton #	Calculated Ring					
	Current Increments					
	Loop ^f Sep.=0	Gem. Diff.	Loop Sep.=1	Gem. Diff.	Loop Sep.=2	Gem. Diff.
C1' 1S	0.36	-0.36	0.35	-0.36	0.31	-0.35
2R	0.72		0.71		0.66	
C2' 1S	0.06	-0.04	-0.04	0.04	0.01	0.04
2R	0.10		-0.08		-0.03	
C3' 1R	-0.46	0.75	-0.47	0.79	-0.50	0.91
2S	-1.21		-1.26		-1.41	
C4' 1S	-0.52	0.67	-0.54	0.68	-0.59	0.72
2R	-1.19		-1.22		-1.31	
C5' 1S	-0.76	1.36	-0.80	1.50	-0.93	1.97
2R	-2.12		-2.30		-2.90	
C6' 1R	-0.35	0.28	-0.35	0.27	-0.35	0.23
2S	-0.63		-0.62		-0.58	
C7' 1R	-0.10	0.15	-0.03	-0.10	0.18	0.06
2S	0.05		0.07		0.12	
C8' 1S	0.85	-0.14	0.76	-0.12	0.55	-0.05
2R	0.99		0.88		0.60	

continued...

Table 5.1 continued

	Loop ^f	Gem.	Loop	Gem.	Loop	Gem.
	Sep.=0	Diff.	Sep.=1	Diff.	Sep.=2	Diff.
r ^d (27°C)	0.90	0.37	0.90	0.37	0.90	0.41
y ^e (27°C)	^b -1.25	-	-1.33	-	-1.57	-
r(-118°C)	0.88	0.48	0.89	0.48	0.89	0.52
y(-118°C)	-1.13	-	-1.20	-	-1.41	-

^a No. of electrons in ring 6=5.275 and ring 5=4.881.

^b Differences calculated from ($\delta H_1 - \delta H_2$).

^c Negative values imply upfield shifts.

^d r=least squares analysis correlation coefficient
from comparison to experimental spectrum.

^e y=y-intercept from a comparison of calculated
versus experimental shift values.

^f Loop Separations are reported in Angstroms.

(Dailey, 1964).

In order to compare the shift increments to the experimental spectral data, Figures 5.1 and 5.2 graphically illustrate the correlation for experimental data collected at 27°C and -118°C with the calculated increments using zero π orbital loop separation. Not included with the data were the chemical shift values for the protons on C1' and C8' since it was expected that a large portion of the deshielding of these protons was due to the inductive effects of nitrogen atoms at N6' and N9.

The calculated ring current increments were compared with both extremes of the experimental chemical shift values (27°C and -118°C) for two reasons. Firstly, since the values obtained at room temperature were meticulously determined by use of the PANIC spin simulation program, they were expected to be the most precise experimental shift values for any of the temperatures at which spectra were recorded. Secondly, since the proton coordinates were determined from the cyclophane 1 in the crystalline state, the low temperature spectral data were expected to be a more realistic representation of the actual chemical shift values for the molecule. However, a least squares line fit analysis reveals that the correlation coefficient was improved when the calculated increments were compared to the room temperature spectral data (Figure 5.1) as opposed to a comparison using

Figure 5.1 The Shielding Caused by a Ring Current Effect Without Loop Separation vs. the Experimental Chemical Shifts Obtained at Room Temperature.

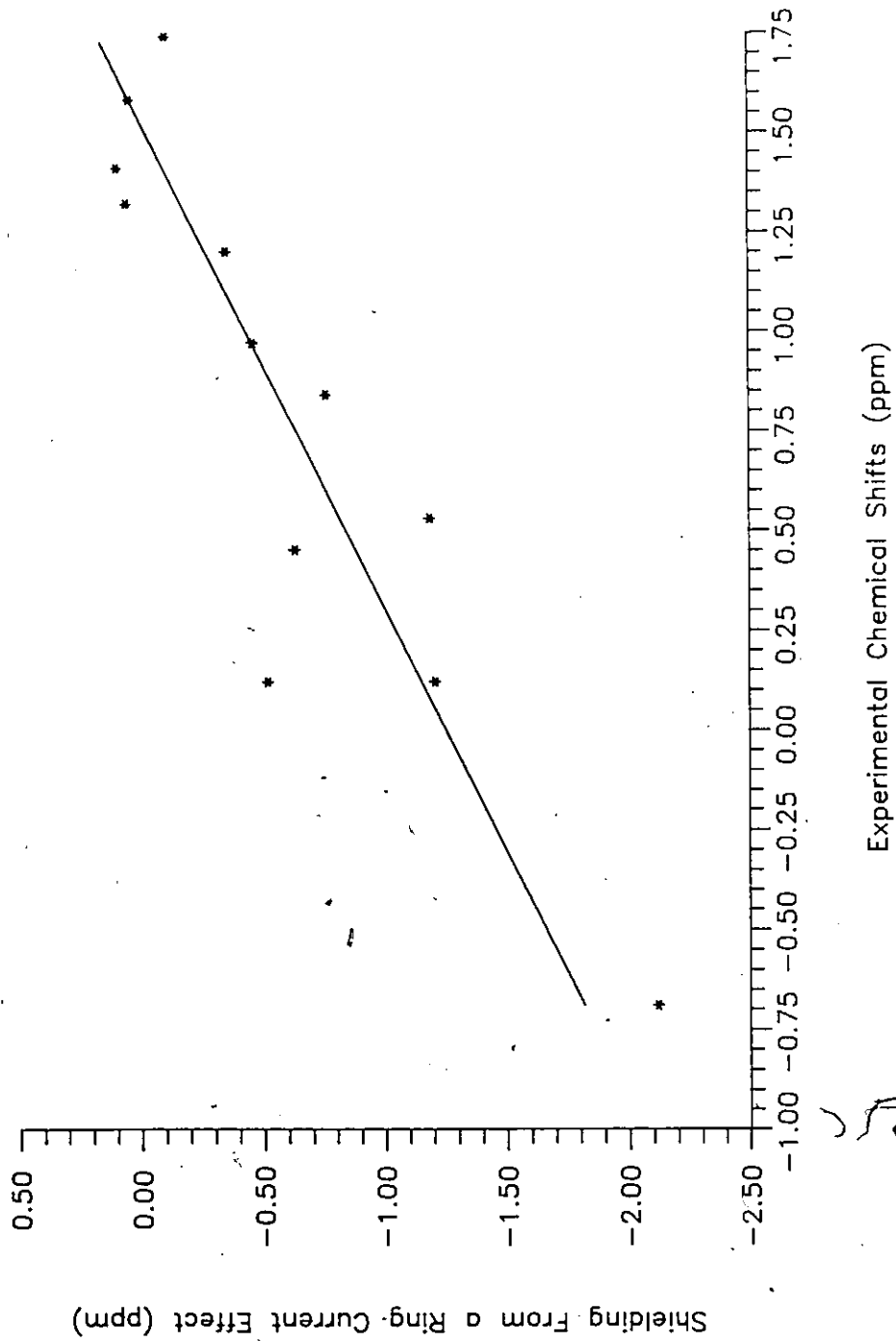
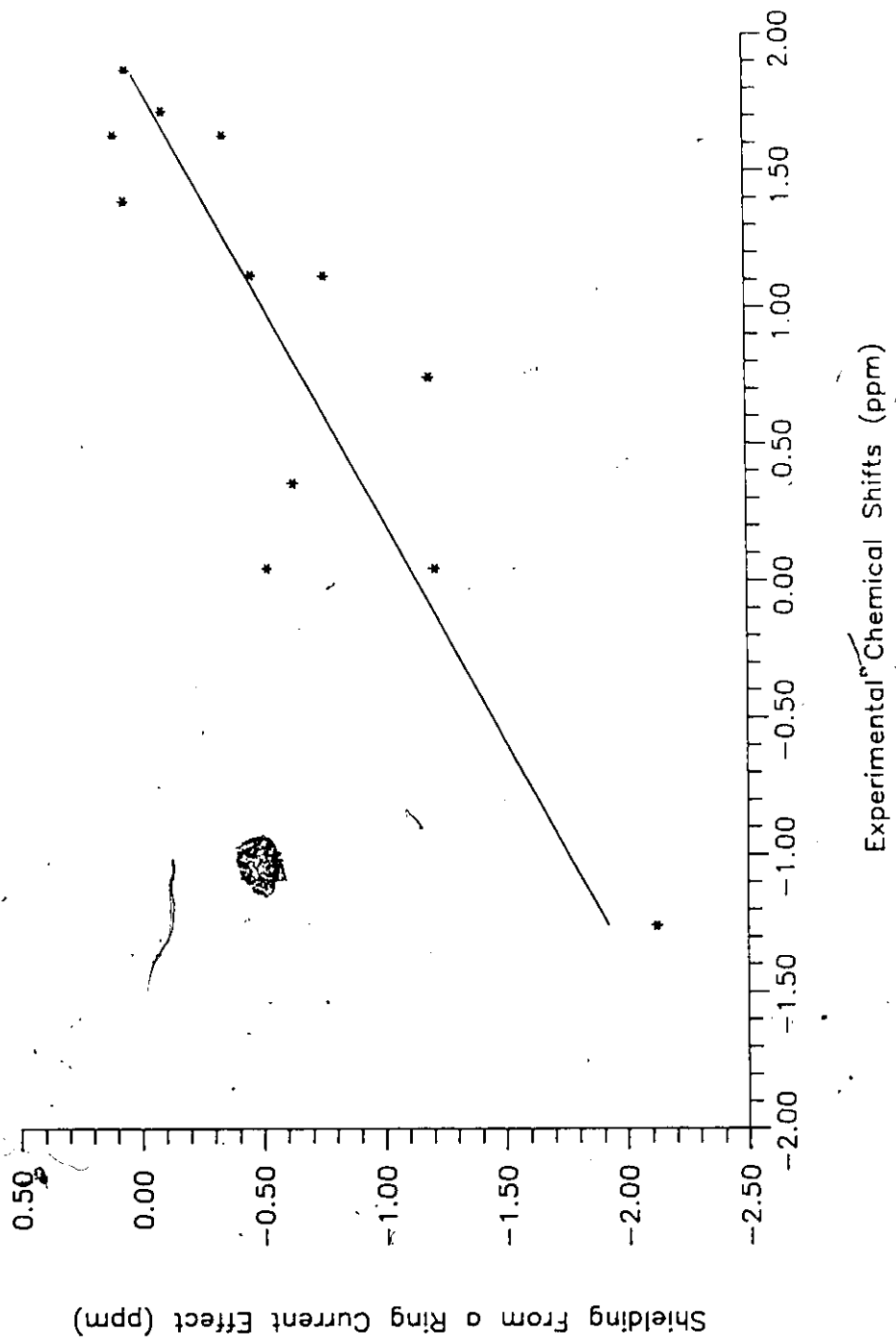


Figure 5.2 The Shielding Caused by A Ring Current Effect Without Loop Separation vs. the Experimental Chemical Shifts Obtained at -118 Celsius.



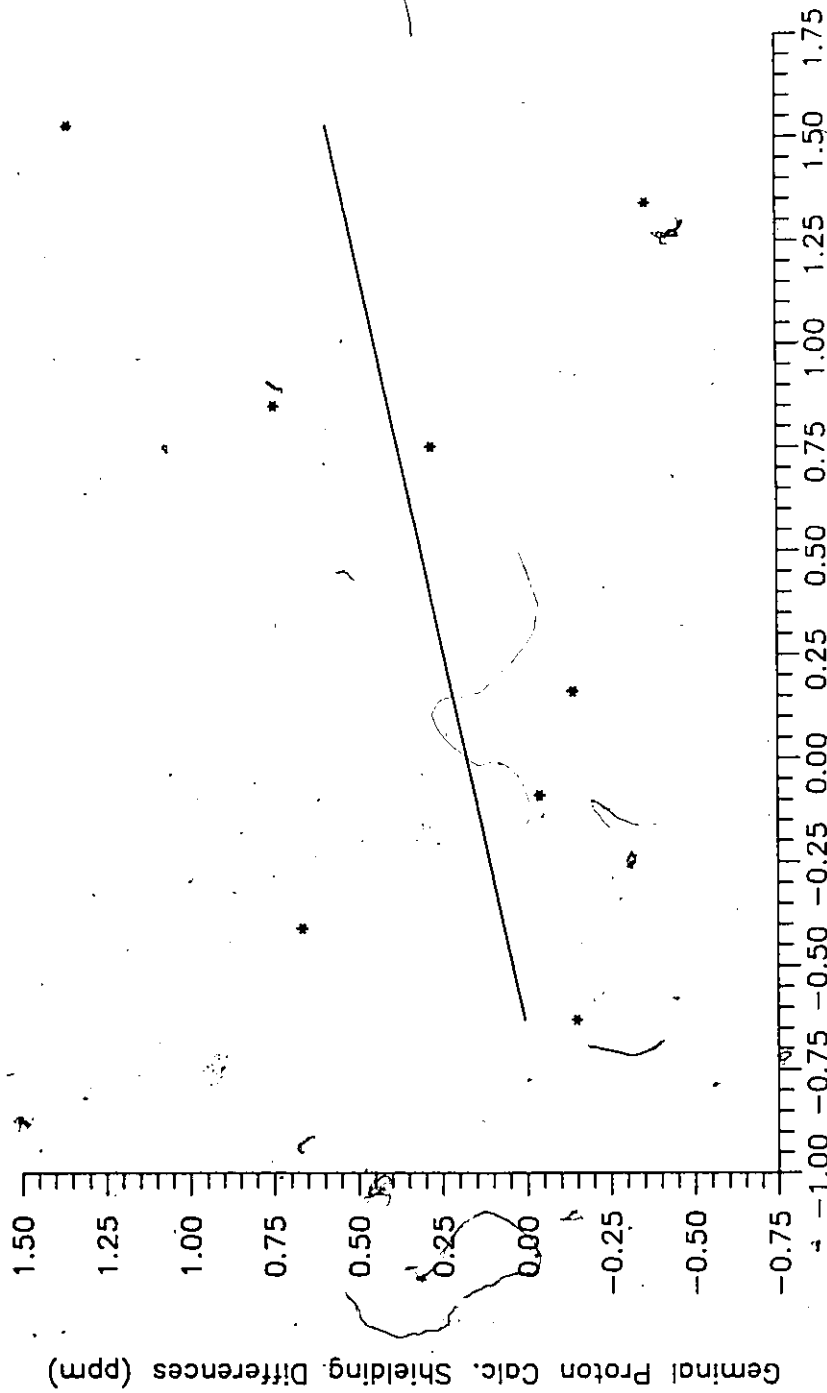
the low temperature spectral data (Figure 5.2). The poor correlation for the low temperature data may have been partially caused by the inability to accurately specify the low temperature chemical shifts since below -20°C the proton resonances broadened and lost their fine structure ($\nu_{1/2} \sim 15$ Hz). It is noteworthy to observe that the y-intercepts from the best fit lines for Figures 5.1 and 5.2 correspond to the approximate value for a "standard" methylene proton chemical shift.

Another possible reason for the poor correlation between the experimental chemical shifts and the increments obtained from the ring current model may have been caused by inductively transmitted substituent effects of the N6' and N9 nitrogen atoms. These effects are the major contributing factor for the observed deshielded resonances for the protons on C1' and C8' and for this reason, these protons were not included in Figures 5.1 and 5.2. Similarly, longer range inductive effects may have contributed to the deshielding of the protons on C2' and C7'. One method of reducing the contribution of inductive effects is to study the differences in chemical shifts for protons bonded to the same carbon. Presumably, the geminal shift differences only reflect dissimilarities in chemical shift caused by ring current effects and local anisotropy contributions. The relationships between the differences in the geminal proton

chemical shift values obtained from calculated increments and the two sets of experimental values are shown graphically in Figures 5.3 and 5.4. Assuming that the ring current model is valid, the poor correlation displayed by these two graphs indicates that local atomic contributions to the diamagnetic shielding anisotropy must change significantly within each pair of geminal protons. This reason for poor correlation is substantiated by literature precedent which led to the study of the atomic (or local) contributions to the proton chemical shifts about purines and pyrimidines (Giessner-Prettre and Pullman, 1976).

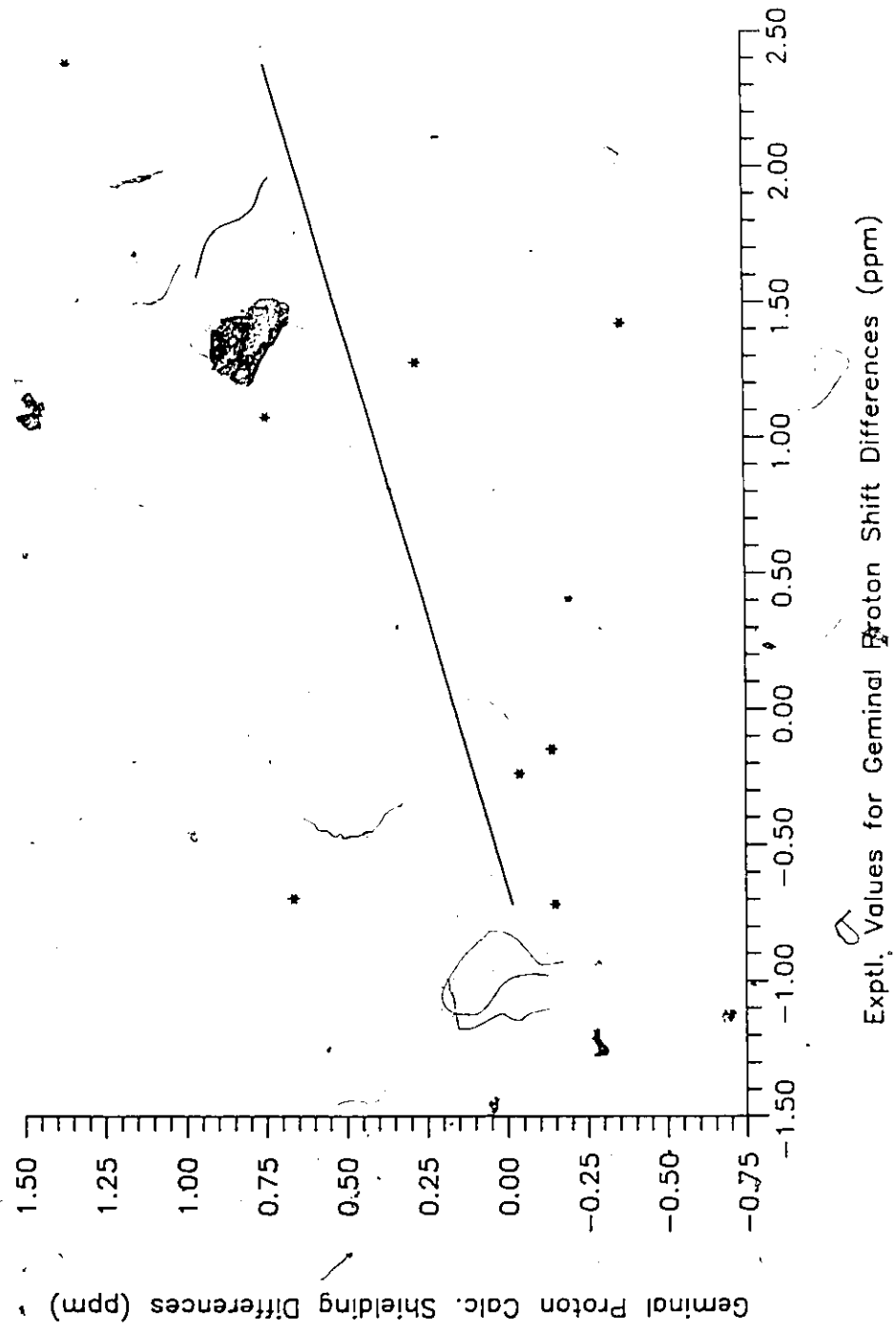
The shielding results from the study of 1 were comparable to the recent ring current and experimental chemical shift comparison for the molecule dimethyl [6]-paracyclophane-8,9-dicarboxylate which is shown in Figure 5.5 (Gunther *et al.*, 1985). This paracyclophane proved analogous to 1 in that the introduction of the carboxylate groups to a cyclophane system enhanced the diastereotopic nature of each of the methylene protons. The study of dimethyl [6]paracyclophane-8,9-dicarboxylate included a comparison between a ring current, shift increment model and the methylene proton chemical shifts. The results reported by these researchers indicated that the correlation between calculated shift increments and experimental data was similar to our study of the cyclophane 1.

Figure 5.3 The Geminal Proton Chemical Shift Differences for: the Calculated Shielding Values Caused by Ring Current Effects vs. Experimental Values Obtained at Room Temperature.



Exptl. Values for Geminal Proton Shift Differences (ppm)

Figure 5.4 The Geminal Proton Chemical Shift Differences for: the Calculated Shielding Values Caused by a Ring Current Effect vs. the Experimental Values Obtained at -118 Celsius.



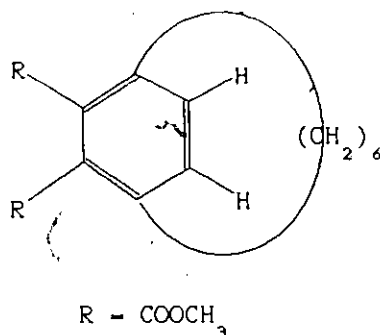


Figure 5.5 Dimethyl [6]paracyclophane-8,9-dicarboxylate

The study of [10]paracyclophane performed by Agarwal *et al.*, (1977) was more successful in correlating the chemical shift data for the calculated ring current as with the experimental chemical shift. However, the study of [10]paracyclophane involved the use local atomic contributions to the diamagnetic anisotropy provided from ^{13}C shielding tensors calculated for benzene (Barfield *et al.*, 1975).

The overall usefulness of the ring current model as applied to the calculation of the diamagnetic anisotropy of the cyclophane 1 may be regarded as surprising since the model itself does not take into account the difference in electronegativity between carbon and nitrogen in the heteronuclear aromatic system.

5.3 Conclusions

Generally, the results indicate that the extension of the free electron model to heteronuclear aromatic systems is applicable. The graphic results from Figures 5.1 and 5.2 indicate a correlation between the chemical shift increment values obtained using the ring current model calculation and the experimental chemical shift values. However, the necessity of a precise loop separation or π -electron distribution was not as essential as the need for a method for generating a reliable set local magnetic shielding values for the total diamagnetic anisotropy. Upon application of suitable methods of calculating the local atomic contributions to the total diamagnetic anisotropy, the semi-empirical method of calculating the ring current effect could prove to be an important tool for the determination of the diamagnetic anisotropy about adenine.

Chapter 6

Synthesis of N6',N9-Nonamethylenepurine Cyclophane

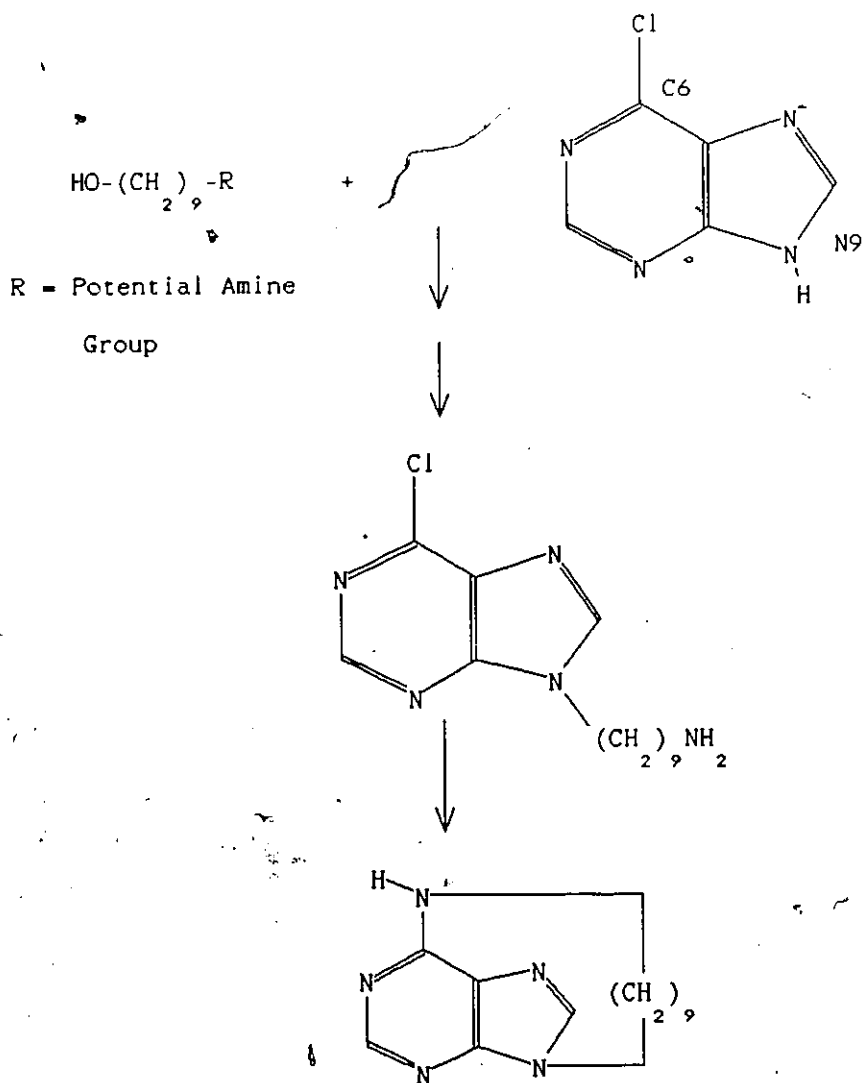
6.1 Introduction

Another cyclophane molecule was synthesized to assist in the determination of the diamagnetic anisotropy around adenine. A homolog of the cyclophane 1 containing a nine carbon methylene bridge attached to N6' and N9 of adenine would be advantageous for two reasons. Firstly, the methylene chain would undoubtedly assume different conformations from those of 1. As a result, the aliphatic protons would reside in different regions of space; thus providing different chemical shift values and more shielding values for adenine. Secondly, the strain imparted to the purine ring by an eight carbon methylene chain (see Sections 4.3 and 4.4) should be partially relieved by a nine carbon chain.

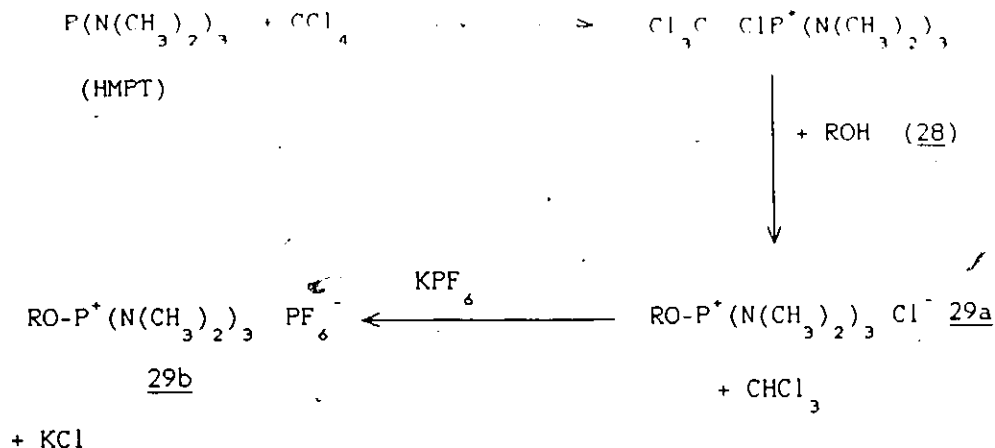
The approach taken towards the synthesis of the nine methylene cyclophane was essentially the same as was used for the eight methylene cyclophane as discussed in Chapter 2. Fortunately, the experience obtained from the synthesis of 1 proved quite beneficial since it was clear that the best synthetic pathway was the fusion of the bridging chain

at the N9 site of 6-chloropurine first followed by cyclization at the C6 site last as indicated in Scheme 6.1. Providing that a suitable bifunctional compound could be obtained, the synthetic goal was the compound 33 which would be cyclized to give 34 under the same type of conditions used to convert compound 6 to the cyclophane 1. The major difference from the synthesis used for 1 was that a totally different bifunctional compound had to be used as a precursor to 9-aminononanol since the nine carbon amino acid version of 10 was impractical to obtain.

One of the many possibilities available was to transform one hydroxyl group of 1,9-nonanediol 28 into a functional group which could be readily converted into an amine moiety when required. Most of the usual techniques for such a process are controlled by statistical factors. For example, if one equivalent of a given reagent was used, the result would be: 50% monofunctional alcohol; 25% di-substituted alcohol; and 25% unreacted alcohol. Literature precedent revealed that a method of circumventing the statistical yield had been developed by Boigegrain *et al.*, (1975). Under the conditions described by these workers, one terminus of the dialcohol 28 reacted with the hexamethylphosphorous triamide (HMPT) - carbon tetrachloride (CCl_4) adduct and immediately formed an insoluble salt. The salt precipitated out of solution before reaction could occur at



Scheme 6.1 Synthetic Approach to 9-Cyclophane



Scheme 6.2 Reaction of Diol

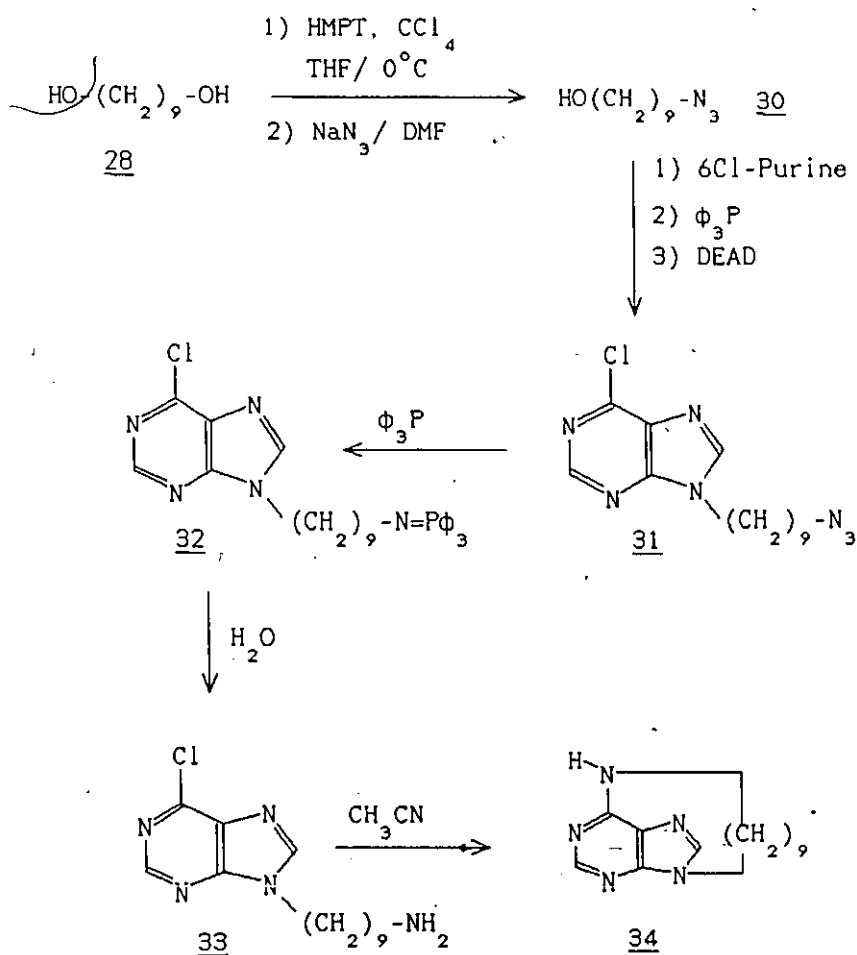
the other hydroxyl group. The mechanism of this reaction (see Scheme 6.2) is a modified version of the Mitsunobu reaction where diethyl azodicarboxylate was replaced by carbon tetrachloride and triphenylphosphine was replaced by HMPT. The phosphonium salt 29a could be isolated as 29b and readily converted to the azide or other appropriate functional group by $\text{S}_{\text{N}}2$ displacement. In this manner, monofunctional alcohol could be obtained in high yield.

6.2 Results and Discussion

Using the method of Boigegrain *et al.*, (1975) the combination of 1,9-nonanediol (28), HMPT and carbon tetrachloride resulted in the formation of an alkoxy-HMPT

salt (as shown by 29a in Scheme 6.2). For extraction purposes, the salt 29a was added to potassium hexafluorophosphate since the large diffuse alkoxy-HMPT cation and comparably bulky hexafluorophosphate anion are readily solubilized by methylene chloride. After isolation, the salt 29b was combined with sodium azide in DMF and converted to the azidoalcohol 30 (as shown in Scheme 6.3) in an overall yield of 70%. Confirmation of the formation of the azide 30 (Scheme 6.2) was obtained from the observed IR absorbance at 2095 cm^{-1} and the resonance at $\delta 3.16$ in the ^1H NMR spectrum indicating the methylene protons adjacent to the azide group.

The azidoalcohol 30 proved to be an advantageous synthon even though triphenylphosphine, as one of the important constituents of the Mitsunobu reaction, is known to react with azides to give triphenylphosphine imines (Vaultier *et al.*, 1983). Since it was possible that the azide would compete with the hydroxyl group for attack of triphenylphosphine, the order of addition of reagents was altered somewhat so that the azide alcohol 30 was added last. The structure of the alkylated purine 31 was confirmed by mass spectral data and also by ^1H NMR spectroscopy which showed the appearance of purine singlets at $\delta 8.19$ and $\delta 8.72$ and appearance of a triplet at $\delta 4.19$ from the pair of methylene protons next to N9 of the purine. The 6-chloro,9-



Scheme 6.3 Formation of Nonamethylene Cyclophane

(9-azidononyl)purine 31 proved to be much easier to purify than 6-chloro,9-(8-N-methoxytritylaminoctyl)purine (24) since column chromatography with silica gel readily afforded 31 in a high state of purity.

The next step of the synthesis was to convert the azide 31 into the corresponding amine 33 under conditions that would not interfere with the 6-chloro group. The reduction of the azide group using Lindlar catalyst has been reported by (Corey *et al.*, 1975), however, this procedure failed to convert 31 to 33. Conversion of the azide 31 to the amine 33 was found to be possible using triphenylphosphine (Vaultier *et al.*, 1983), the very same reagent which was considered to be a possible disadvantage to the Mitsunobu reaction. The phosphine imine 32 formed when 31 was treated with triphenylphosphine in THF at 60°C for 6 hours, underwent hydrolysis upon aqueous quench followed by stirring for 18 hours. The ¹H NMR spectrum of the hydrochloride salt 33 indicated the presence of methylene protons adjacent to the terminal primary amine at δ 3.00.

It was discovered that 6-chloro,9-(9-aminononyl)purine 33 could be isolated neat for brief periods of time without intermolecular reaction occurring. Therefore, formation of the cyclophane 34 could be completed in the following way. The neat compound was dissolved in chloroform and an aliquot of this solution was added periodically to

dimethylsulphoxide stirring at 70°C. By adding the reagent in this manner, the actual concentration of the reagent in DMSO could be maintained at the desired concentration (10^{-3} molar) while simultaneously using the least amount of DMSO possible. A small amount of DMSO was advantageous for reaction workup since removal of this solvent was difficult. Confirmation of the formation of N6',N9-nonamethylenepurine cyclophane 34 was obtained from mass spectroscopy which indicated a molecular ion corresponding to the parent compound with a mass of 259 amu and by ^1H NMR spectroscopy which indicated a wide range of proton resonances in the aliphatic region. The ^1H NMR spectrum of 34 is shown in Figure 6.1.

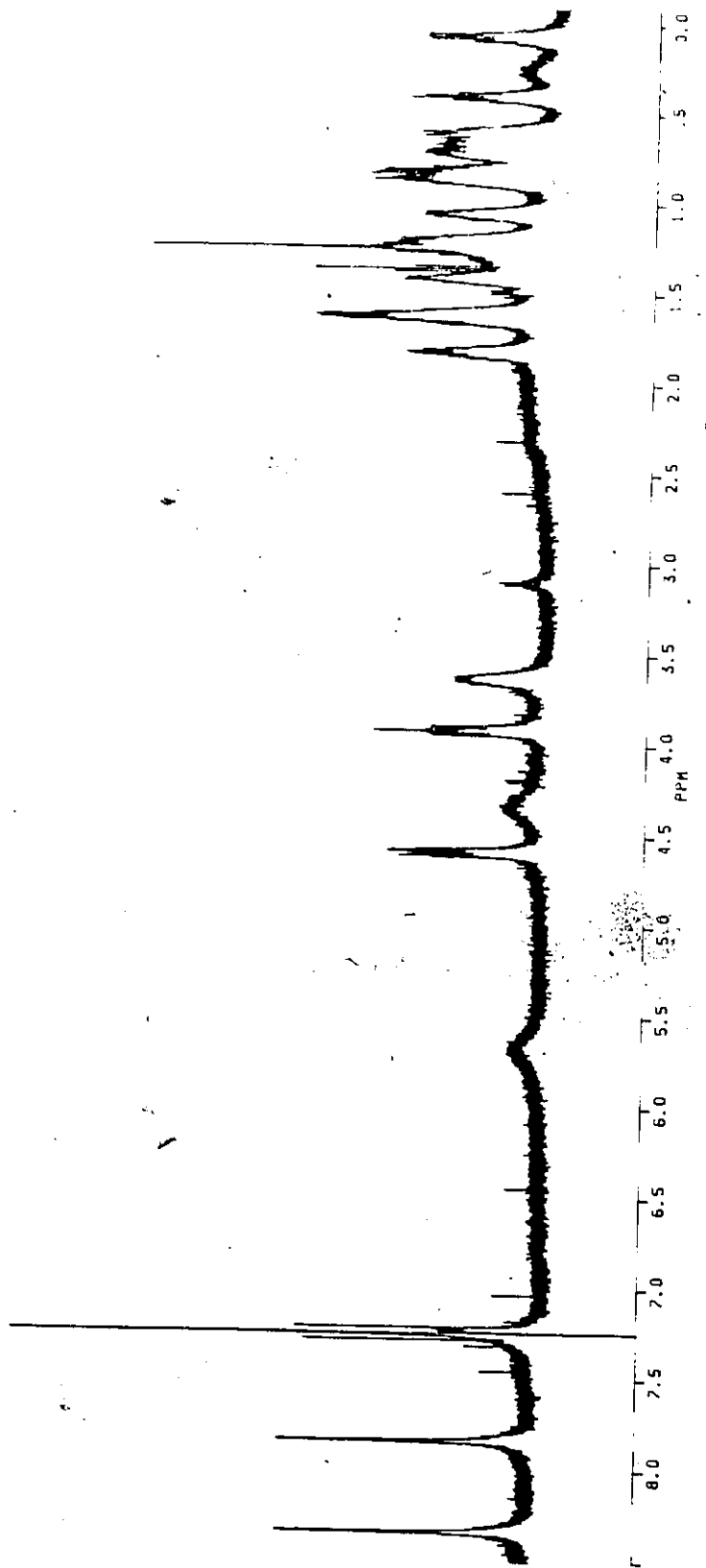


Figure 6.1 ¹H NMR Spectrum of N6',N9 Nonamethylenepurine Cyclophane in CDCl₃.

Experimental Methods

Melting points were recorded on a Gallenkamp capillary tube melting point apparatus and are uncorrected. Proton magnetic resonance ($^1\text{H-NMR}$) spectra were recorded on Varian EM-390, WM-250 and AM-500 spectrometers with chloroform-d as the common solvent unless otherwise noted. Unless specified, the usual internal references were tetramethylsilane (TMS) or chloroform. The abbreviations s=singlet, d=doublet, t=triplet, q=quartet and m=multipet are used in the description of the spin-spin splitting pattern present in the spectra. The natural abundance carbon-13 magnetic resonances ($^{13}\text{C-NMR}$) were recorded on Bruker WP-80 (at 20.115 MHz), WM-250 (at 62.896 MHz) and AM-500 (at 125.776 MHz) instruments using Chloroform-d as the solvent and internal reference unless otherwise noted. All ^{13}C spectra were broad band decoupled. Low resolution mass spectra (MS) and high resolution mass spectra (HRMS) were obtained at 70eV on a VG Micromass 7070F double focussing mass spectrometer with the samples introduced through a direct inlet system. Mass spectra acquired using the Fast Atom Bombardment (FAB) technique were accomplished using a VG ZAB-E mass spectrometer. Infrared spectra of neat

liquids were recorded on a Perkin Elmer 283 spectrometer. The symbols s=strong, m=medium, w=weak and sh=shoulder were used in the recording of the IR data to indicate the intensity of the recorded bands.

Dry ethanol was obtained by the method of Smith, (1927). N-butanol, triethylamine and pyridine were dried over calcium hydride and stored over 4Å molecular sieves and removed as needed. Tetrahydrofuran (THF) was dried by refluxing and distilling from sodium and benzophenone and was collected from the distillation apparatus as required. Methanol was dried by refluxing over magnesium followed by distillation and storage over molecular sieves. The NMR solvents chloroform-d, methylene chloride-d₂ and dimethylsulphoxide-d₆ were stored over molecular sieves prior to use.

Unless alternately specified, column chromatography was performed by the "flash" method of Still, Kahn and Mitra, (1978). The silica gel used for column chromatography was (5.0% of 100 up; 47.6% of 100-200 mesh and 47.4% of 200 mesh down) purchased from Terochem. Silica gel 60F254 (E.Merck Co.) plates of 0.2 mm thickness were used for analytical thin layer chromatography. Reversed phase Sep-Pak C18 cartridges were obtained from Waters Associates. Reversed phase KC18F glass-backed thin layer analytical plates (layer thickness 0.2mm) were purchased from the

Whatman Co.

Preparation of Cyclooctanone Oxime 8

The procedure used was similar to the method of Coffman *et al.*, (1948). To a stirred solution of cyclooctanone (10 g, 0.079 moles) in dry absolute ethanol (50 mL), was added hydroxylamine hydrochloride (8.81 g, 0.127 moles). An aqueous solution of 50 mL of 1.3M potassium carbonate was added dropwise and the solution was warmed to 50°C for 2 hours. The ethanol solvent was evaporated in a rotary evaporator and the remaining aqueous solution was extracted three times with 50 mL portions of chloroform. The chloroform extracts were combined, dried over anhydrous sodium sulphate and the chloroform evaporated under reduced pressure in a rotary evaporator. This yielded 9.4 g (84%) cyclooctanone oxime 8 (bp. 87-88°C at 2.5 mm Hg; lit. bp. 123-124°C at 14 mm Hg.)

Compound 8 showed:

HRMS: for C₈H₁₅NO; calcd. 141.1154; obs. 141.1130.

MS: m/z (RI%); 141 (21) [M⁺], 124 (12) [M⁺-OH], 113 (100), 98 (32) [M⁺-CHNO], 73 (82), 55 (50).

IR: ν_{max}; 1655 (m) [C=N] cm⁻¹.

¹H NMR: (EM 390) δ 1.47 (s, 6H, carbons 4, 5, 6 CH₂), 1.73 (s, 4H, carbons 3, 7 CH₂), 2.40 (m, 4H, carbons 2, 8

CH₂), 10.13 (s, 1H, OH).

¹³C NMR: (WP 80) δ 164.0 (s, 1C, C=NOH), 33.2, 27.3, 26.8,
25.5, 24.9, 24.5.

Preparation of Cyclooctanone Isooxime

(2-Azacyclononanone) 9

The procedure followed was similar to the method of Coffman *et al.*, (1948). To a stirred solution of sulphuric acid (4 mL of 96%) with distilled water (0.1 mL) at 110°C was added cyclooctanone oxime (951 mg, 6.74 mmoles) dropwise. The solution was cooled to room temperature, poured onto ice (90 g) and neutralized with small portions of solid sodium hydroxide. The solution was extracted with three times 100 mL portions of chloroform. The combined extracts were dried over sodium sulphate (anhydrous) and evaporated under reduced pressure in a rotary evaporator yielding 666 mg (70.0%) of a light brown solid (mp. 74.5-76.5°C, lit. mp. 77-79°C).

Compound 9 showed:

HRMS: for C₈H₁₃NO [M+1]⁺; calcd. 142.1232; obs. 142.1243.

MS: m/z (RI%); 141 (35) [M⁺], 124 (88) [M⁺-112 (24)], 98 (62) [M⁺-CHNO], 56 (100).

IR: ν_{max}; 3300 (s) [N-H], and 1650 (s) [CO] cm⁻¹.

¹H NMR: (EM 390) δ 1.6 (m, 10H, carbons 4, 5, 6, 7, 8 CH₂), 2.45

(t, J=6Hz, 2H, CH₂-CO), 3.35 (m, 2H, N-CH₂), 6.33 NH).

Hydrolysis of 2-Azacyclononanone and Purification of
the Amino Acid 10

The method used was similar to that of Eck, (1943) or Takagi and Hayashi, (1959). To a stirred solution of 2-azacyclononanone (0.54 g, 3.8 mmoles) dissolved in 5.2 mL of distilled water was added 1.5 mL of concentrated hydrochloric acid and the solution heated to reflux for 2 hours. Amberlite IR-120 resin (40 mL) was washed with three 20 mL portions of methanol and then washed with five times 20 mL portions of distilled water followed by 5 mL of 0.25M hydrochloric acid. After cooling to room temperature, the hydrolysis solution was added to the resin and the mixture was stirred for 12 hours. The solution was decanted and the resin was washed with distilled water until the washings were neutral. Distilled water (15 mL) and 1M ammonium hydroxide were added until the solution was pH 9 and this mixture was stirred for 1 hour. After decanting, more distilled water and ammonium hydroxide were added and the cycle repeated until four decantations were performed. These four solutions were combined and evaporated using a rotary evaporator under high vacuum. At the conclusion, benzene was used to form an azeotrope and remove any remaining traces of

water. A cream coloured solid (0.55 g, 98%) was isolated

Compound 10 showed:

¹H NMR: (EM 390) D₂O solvent (ref. 3-(trimethylsilyl) propionic acid, sodium salt) δ 1.37 (m, 10H, carbons 3, 4, 5, 6, 7 CH₂), 2.17 (t, J=6Hz, 2H, CH₂COO) and 2.97 (t, J=6Hz, 2H, CH₂NH₂).

Preparation of Ethyl 8-Aminooctanoate 15

The procedure described was similar to that of Huber and Brenner, (1953). To 10 mL of ethanol stirred under nitrogen atmosphere at -5°C (ice/acetone bath) were added thionyl chloride (0.50 mL, 6.9 mmoles) dropwise. After 5 minutes, 8-aminooctanoic acid 10 (1.0 g, 6.3 mmoles) was added and the solution stirred for 1 hour at -5°C followed by 2 hours at 40°C. The solvent was then evaporated under reduced pressure in a rotary evaporator and the residue was redissolved in 25 mL chloroform. Distilled water (25 mL) was added and the aqueous layer was adjusted to pH 8-9 with 1M sodium hydroxide. The chloroform layer was removed and the aqueous layer was extracted twice with 25 mL portions of chloroform. The chloroform extracts were combined, dried over anhydrous sodium sulphate and evaporated under reduced pressure in a rotary evaporator yielding 1.1 g (95%) ethyl 8-aminooctanoate 15.

Compound 15 showed:

HRMS: for $C_{10}H_{21}NO_2$ ($M+1$); calcd. 187.1572, obs.
187.1540.

MS: m/z (RI%); 188 (33) [$M+1$]⁺, 158 (2) [$M^+-CH_2CH_3$], 142
(63) [$M^+-OCH_2CH_3$], 114 (4) [$M^+-COOCH_2CH_3$] and 100
(100) [$M^+-CH_2COOCH_2CH_3$].

IR: ν_{max} ; 3400 (m) [NH_2] and 1735 (s) [$C=O$] cm^{-1} .

1H NMR: (EM 390) δ 1.23 (m, 15H, NH_2 and carbons 3,4,5,6,7 CH_2
and CH_3), 2.18 (t, $J=6Hz$, 2H, CH_2CO), 2.58 (t, $J=6Hz$,
2H, CH_2N) and 4.03 (q, $J=6Hz$, 2H, OCH_2).

^{13}C NMR: (WP 80) δ 173.6 (s, 1C, COO), 60.0 (s, 1C, OCH_2), 41.9
(s, 1C, NCH_2), 34.2 (s, 1C, CH_2CO), 33.2 (s, 1C, C7),
28.9 (s, 2C, C4 and C5), 26.5 (s, 1C, C6), 24.8
(s, 1C, C3) and 14.1 (s, 1C, CH_3). Assignments based
upon values for ethyl octanoate and n-octylamine
(Sadtler Standard ^{13}C NMR Spectra).

Preparation of 8-Aminooctanol 4

The procedure used was similar to that of Manske,
(1943). Ethyl 8-aminooctanoate 15 (97.5 mg, 0.518 mmoles)
was dissolved in anhydrous ethanol (5 mL). Without heating
or stirring, sodium metal (145 mg, 6.3 mmoles) was added as
one piece. After the reaction was complete, distilled water
(5 mL) was added dropwise. The ethanol was evaporated under

reduced pressure in a rotary evaporator and the remaining aqueous solution was extracted with three times 10 mL portions of chloroform. The chloroform was evaporated under reduced pressure leaving the aminoalcohol (4) 22 mg (30%) as a white solid. The aqueous extracts contained amino acid 10 and were recovered for reuse.

Compound 4 showed:

HRMS: for $C_8H_{19}NO$ ($M^+ - 1$); calcd. 144.1388; obs.!

✓ 144.1343.

MS: m/z (RI%); 144 (9) [$M^+ - 1$], 128 (8) [$M^+ - NH_2$], (40) [$M^+ - CH_2NH_2$] and 55 (100).

1H NMR: (EM 390) δ 1.27 (s, 12H, carbons 2, 3, 4, 5, 6, 7 CH_2), 1.53 (s, 3H, OH and NH_2), 2.60 (t, J=6Hz, 2H, CH_2N) and 3.53 (t, J=6Hz, 2H, CH_2O).

^{13}C NMR: (WP 80) δ 62.22 (s, 1C, $HOCH_2$), 42.0 (s, 1C, CH_2N), 33.5 (s, 1C, C7), 32.7 (s, 1C, C2), 29.2 (s, 2C, C4 and C5), 26.6 (s, 1C, C3) and 25.6 (s, 1C, C6). (Assignments based upon values for n-octanol and n-octylamine.)

Synthesis of 6-(ω -Hydroxyoctylamino)purine 5

The procedure used was similar to that of Sutherland and Christensen, (1957). 8-Aminooctanol, (4) (45 mg, 0.3098 mmoles) was dissolved in 2 mL of n-butanol. The solution was stirred at 80°C under nitrogen atmosphere and 6-chloropurine

(43.2 mg, 0.28 mmoles) was added. The solution was then heated to 110°C and stirred for 1.25 hours. Potassium carbonate (23 mg, 0.166 mmoles) was added and the solution stirred for 0.5 hours. The solution was then evaporated under reduced pressure in a rotary evaporator. The crude product was recrystallized from hot water yielding 62 mg (85%). Decomposition occurred at 164-166°C.

Compound 5 showed:

HRMS: for $C_{13}H_{21}N_5O$; calcd. 263.1745; obs. 263.1741.

MS: m/z (RI%); 263 (12) $[M^+]$, 246 (5) $[M^+ - OH]$, 232 (5) $[M^+ - CH_2OH]$, 218 (7) $[M^+ - (CH_2)_2OH]$, 204 (11) $[M^+ - (CH_2)_3OH]$, 190 (17) $[M^+ - (CH_2)_4OH]$, 176 (13) $[M^+ - (CH_2)_5OH]$, 162 (39) $[M^+ - (CH_2)_6OH]$ and 148 (100) $[M^+ - (CH_2)_7OH]$.

1H NMR: WM-250 DMSO- d_6 solvent; δ 1.256 (m, 10H, carbons 3', 4', 5', 6', 7' CH_2), 1.390 (m, 2H, CH_2), 3.355 (t, 2H, CH_2), 3.432 (t, 2H, CH_2), 7.495 (s, 1H, C8H) and 7.884 (s, 1H, C2H).

Preparation of Diphenyl Ketimine 18

The method of Pickard and Tolbert, (1973) was used. Magnesium turnings (1.34 g, 55 mmoles) were added to 30 mL anhydrous diethyl ether. To the stirred mixture was added 2 mL of a solution of bromobenzene (predistilled 8.6 g, 55

mmoles) in 10 mL anhydrous diethyl ether. The original ether solution was heated with a forced air heater until reaction was initiated. At this point, the rest of the bromobenzene solution was added dropwise and the mixture heated to reflux for 45 minutes. The solution was cooled and a solution of benzonitrile (predistilled 5.15 g, 55 mmoles) in 10 mL of anhydrous diethyl ether was added at a rate sufficient to maintain a gentle reflux. After the addition was complete, the solution was heated at reflux for 6 hours. The solution was cooled to 25°C and methanol (12 mL, 0.3 moles) was introduced. After the solution had stirred for 0.5 hours, the resulting mixture was filtered and the filtrate was evaporated under reduced pressure in a rotary evaporator. The crude product was distilled under vacuum (bp. 132.5-134°C at 4 mm Hg; lit. bp. 127-128°C at 3.5 mm Hg) to yield 5.62 g (62%) diphenyl ketimine.

Compound 18 showed:

HRMS: for $C_{13}H_{10}N$ (M^+); calcd. 180.0813; obs. 180.0804.

MS: m/z (RI%); 181 (41) [$M^+ + 1$], 180 (100) [M^+], and 104 (54) [$M^+ - C_6H_5$].

IR: ν_{max} ; 1600 (s) [CN] cm^{-1} .

1H NMR: (EM 390) δ 7.53 (m, 10H, $2C_6H_5$) and 9.73 (broad s, 1H, NH).

Protection of 8-Aminooctanol with Diphenyl Ketimine

The method followed was similar to that of O'Donnell and Polt, (1982). Diphenyl ketimine 18 (62.4 mg, 0.344 mmoles) was dissolved in methylene chloride (2 mL predried with anhydrous sodium sulphate). To this stirred solution, under nitrogen atmosphere, was added 8-aminooctanol 4 (50 mg, 0.34 mmoles). The solution was stirred for 12 hours and the solvent removed by rotary evaporation under reduced pressure. The yield was quantitative as indicated by ^1H NMR. Compound 19 showed:

HRMS: for $\text{C}_{21}\text{H}_{27}\text{N}$; calcd. 309.2092; obs. 309.2109.

MS: m/z (RI%); 309 (25) [M^+], 308 (75) [M^+-1], 292 (3) [M^+-OH], 278 (5) [$\text{M}^+-\text{CH}_2\text{OH}$], 264 (14) [$\text{M}^+-\text{(CH}_2)_2\text{OH}$], 250 (24) [$\text{M}^+-\text{(CH}_2)_3\text{OH}$], 236 (21) [$\text{M}^+-\text{(CH}_2)_4\text{OH}$], 222 (3) [$\text{M}^+-\text{(CH}_2)_5\text{OH}$], 208 (49) [$\text{M}^+-\text{(CH}_2)_6\text{OH}$] and 194 (100) [$\text{M}^+-\text{(CH}_2)_7\text{OH}$].

IR: ν_{max} ; 2930 (s), 2850 (sh), 1620 (m) cm^{-1} .

^1H NMR: (EM 390) solvent (CD_2Cl_2); δ 1.22 (m, 12H, carbons 2, 3, 4, 5, 6, 7 CH_2), 3.35 (t, 2H, CH_2N), 3.58 (t, 2H, CH_2O) and 7.38 (m, 10H, $2\text{C}_6\text{H}_5$).

Preparation of 6-Chloro,-N9-(8-aminooctyl)purine 6

Compound 19 (115 mg, 0.372 mmoles) was dissolved in

1 mL anhydrous tetrahydrofuran (THF). To this stirred solution, under nitrogen atmosphere was added a solution of triphenylphosphine (97.5 mg, 0.372 mmoles) dissolved in THF (2 mL). This was followed by the addition of 6-chloropurine (57.5 mg, 0.372 mmoles). Finally, a solution of diethyl azodicarboxylate (64.8 mg, 0.372 mmoles) in THF (0.5 mL) was added and the solution was stirred for 72 hours. The solvent was evaporated in a rotary evaporator and the residue was redissolved in 2 mL diethyl ether. Distilled water (3 mL) and 0.2 mL of 6M hydrochloric acid were added and the system stirred for 12 hours. The aqueous layer was separated and evaporated to dryness under vacuum. This yielded 35 mg (30%) of the hydrochloride salt 6a. For analysis, the free amine (6) was extracted from alkaline aqueous solution using chloroform.

Compound 6a showed:

¹H NMR: (EM 390) D₂O solvent and internal reference was 3-(trimethylsilylpropionic acid sodium salt δ 1.3 (m, 12H, carbons 2', 3', 4', 5', 6', 7' CH₂), 3.35 (t, 2H, CH₂N), 4.27 (t, 2H, N9CH₂), 7.43 (m, 10H, 2C₆H₅), 8.17 (s, 1H, C2H) and 8.8 (s, 1H, C8H).

Compound 6 showed:

MS: m/z (RF%) 281 (3) [M⁺], 279 (14), 167 (32) [M⁺ - C₇H₁₄NH₂], 149 (84) and 92 (100).

¹H NMR (EM 390) δ 1.33 (broad m, 12H, carbons 2', 3', 4', 5',

6',7'CH₂), 3.63 (t, J=6Hz, 2H, CH₂NH₂), 4.18 (m, 2H, CH₂N₉), 5.95 (s, 2H, NH₂), 7.77 (s, 1H, C8H) and 8.43 (s, 1H, C2H).

Attempted Preparation of the Cyclophane 1

(Preparation of 6-Ethoxy,-N9-(8-aminooctyl)purine)

6-Chloro,-N9-(8-aminooctyl)purine hydrochloride 6a (121.9 mg, 0.766 mmoles) was added to 400 mL of absolute ethanol. To this stirred solution was added sodium carbonate (81.2 mg, 0.766 mmoles). The solution was stirred at reflux for 8 days and evaporated to dryness using a rotary evaporator under reduced pressure. The recovered product was identified as 6-ethoxy,-N9-(8-aminooctyl)purine 21.

Compound 21 showed:

HRMS: for C₁₅H₂₅N₅O; calcd. 291.2059; obs. 291.2081.

MS: m/z (RI%); 291 (.2)[M⁺], 290 (10)[M⁺-1] and 163 (42)[M⁺-C₈H₁₆NH₂].

¹H NMR: (EM 390) δ 1.20 (m, 15H, carbons 2', 3', 4', 5', 6' and CH₃ and NH₂), 1.80 (m, 2H, carbon 7'CH₂), 2.57 (m, 2H, carbon 1'CH₂), 4.13 (t, 2H, NCH₂), 4.58 (q, J=6Hz, 2H, OCH₂), 7.82 (s, 1H, C8H) and 8.44 (s, 1H, C2H).

Preparation of the 8-Cyclophane 1

The hydrochloride salt 6a (52 mg, 0.16 mmol) was dissolved in 5 mL of distilled water. The solution was adjusted to pH 10 with 1M aqueous sodium hydroxide solution and extracted twice with 5 mL portions of chloroform and twice with 5 mL portions of diethyl ether. The combined organic extracts were dried over anhydrous sodium sulphate and added to distilled benzene (25 mL). The solution was concentrated to 25 mL in a rotary evaporator under reduced pressure and transferred to a tube. The tube was placed in liquid nitrogen until the solution was frozen and then evacuated. The solid solvent was allowed to melt while evacuated and this freeze-thaw cycle repeated twice. The tube was then sealed and heated to 250°C for 18 hours. The solution was evaporated under reduced pressure using a rotary yielding 3 mg crude product.

Compound 1 showed:

UV: $\lambda_{\text{max}}=277\text{nm}$; $\log \epsilon=3.67$ ethanol.

HRMS: for $\text{C}_{13}\text{H}_{19}\text{N}_5$; calcd. 245.1640; obs. 245.1669.

MS: m/z (RI%); 245 (79) [M^+], 216 (15) [M^+-NHCH_2], 202 (19) [$\text{M}^+-\text{NH}(\text{CH}_2)_2$], 188 (21) [$\text{M}^+-\text{NH}(\text{CH}_2)_3$], 174 (21) [$\text{M}^+-\text{NH}(\text{CH}_2)_4$], 160 (18) [$\text{M}^+-\text{NH}(\text{CH}_2)_5$], 134 (11) [M^+-CH_2], 148 (51), 83 (90) and 55 (100).

$^1\text{H NMR}$: (AM 500) (in CD_2Cl_2 -Freon) δ -0.64 (m, 1H, H5'R), 0.17

(m, 2H, H3'S and H4'S), 0.52 (m, 1H, H6'S), 0.57
 (m, 1H, H4'R), 0.89 (m, 1H, H5'S), 1.03 (m, 1H, H3'R),
 1.26 (m, 1H, H6'R), 1.38 (m, 1H, H2'S), 1.47
 (m, 1H, H2'R), 1.64 (m, 1H, H7'S), 1.80 (m, 1H, H7'R),
 3.35 (m, 1H, H1'R), 3.92 (m, 1H, H8'S), 4.54
 (m, 1H, H8'R), 4.68 (m, 1H, H1'S), 4.89 (br m, 1H, N6'H);
 7.79 (s, 1H, H8) and 8.30 (s, 1H, H2).

¹³C NMR: (AM 500) δ 23.146 (s, 1C, C6'), 25.213 (s, 1C, C4'),
 28.722 (s, 1C, C7'), 30.924 (s, 1C, C2'), 31.322
 (s, 1C, C5'), 43.030 (s, 1C, C1'), 45.032 (s, 1C, C8'),
 121.313 (s, 1C, C5), 143.106 (s, 1C, C8), 152.417
 (s, 1C, C4), 154.141 (s, 1C, C2) and 159.937 (s, 1C, C6).

Attempted Reduction of 8-Aminooctanoic Acid with
 Borane-methyl Sulphide (BMS)

8-Aminooctanoic acid 10 (542 mg, 3.40 mmoles) was
 added to 40 mL of THF and stirred under nitrogen atmosphere.
 To this mixture was added BMS in THF (5.1 mL of 2M in THF).
 After 36 hours, the mixture was quenched with 3.38 mL of 3M
 sodium hydroxide and 7 mL of distilled water. This solution
 was stirred for 12 hours and the THF was evaporated at
 reduced pressure. The aqueous residue was extracted three
 times with 40 mL portions of chloroform. The organic
 extracts were combined, dried over anhydrous sodium sulphate

and evaporated under reduced pressure in a rotary evaporator.

This compound showed:

HRMS: for $C_8H_{21}NOB$; calcd. 158.1716; obs. 158.1731.

MS: m/z (RI%); 159 (4), 158 (50), 157 (18), 156 (63), 155 (17), 154 (16), 153 (4), 138 (5), 128 (4), 115 (6), 95 (3), 82 (21), 69 (85) and 55 (100).

1H NMR: (EM 370) benzene- d_6 as solvent and ref. δ 1.38 (m, 17H, $(CH_2)_6$ and BH_2 and NH_2 and OH), 2.60 and 3.68 (t, 2H, CH_2O).

^{13}C NMR: (EM 390) benzene- d_6 as solvent and ref. δ 26.29 (s, 1C, C6), 27.10 (s, 1C, C3), 29.87 (s, 2C, C4 and C5), 33.43 (s, 1C, C2), 33.97 (s, 1C, C7), 42.38 (s, 1C, CH_2N) and 62.26 (s, 1C, CH_2O). (Assignments based upon values for n-octanol (Bruker ^{13}C Data Bank Vol.1) and n-octylamine (Sadtler Standard ^{13}C NMR Spectra)).

Attempted Reduction of Potassium 8-Aminooctanoate with Borane-methyl Sulphide (BMS)

The potassium salt of the amino acid 10 was prepared by titration of the amino acid with potassium hydroxide solution. 18-Crown-6 ether (328 mg, 1.25 mmoles) was dissolved in THF (5 mL). To this stirred solution was added

the amino acid salt (120 mg, 0.615 mmoles). Glass beads were added and the temperature was increased to reflux in order to effect dissolution of the amino acid salt. After 0.5 hours, the solution was cooled to 25°C and 0.31 mL of 2M BMS-THF complex was added dropwise. After 24 hours, saturated ammonium chloride (3 mL) was added and the solution heated to reflux for 2 hours. The solution was cooled to 25°C and the THF solvent was evaporated at reduced pressure on a rotary evaporator. The remaining aqueous solution was adjusted to pH 9-10 with solid sodium hydroxide. This solution was heated to reflux for 1 hour and cooled. The solution was extracted three times with 10 mL portions of chloroform. The organic extracts were combined, dried over anhydrous sodium sulphate and evaporated under reduced pressure in a rotary evaporator.

Synthesis of Isopentyltrifluoroacetamide 17

Isopentylamine (100 mg, 1.15 mmoles) was dissolved in 1 mL of methylene chloride. To this stirring solution were added pyridine (363 mg, 4.59 mmoles) and trifluoroacetic anhydride (602 mg, 2.87 mmoles). The solution was stirred for 0.5 hours. The solution was then diluted to a total of 10 mL with methylene chloride and washed twice with 10 mL portions of distilled water. The organic phase was dried

over anhydrous sodium sulphate, evaporated under reduced pressure in a rotary evaporator and kept under 3mm Hg vacuum for 3 hours. This yielded 186 mg (89%).

Compound 17 showed:

IR: ν_{\max} 1705 (s) [C=O] cm^{-1} .

^1H NMR: (EM 390) δ 0.88 (d, 6H, 2CH_3), 1.49 (m, 3H, CHCH_2), 3.33 (q, 2H, CH_2N) and 7.28 (broad s, 1H, NH).

Formation of N-Methoxytrityl Ethyl

8-Aminooctanoate 22b

The method used was a modified version of the method described by Zervas and Theodoropoulos, (1956). To a stirred solution of ethyl 8-aminooctanoate 15 (190.9 mg, 1.02 mmoles) dissolved in 5 mL of chloroform were added triethylamine (103.7 mg, 1.02 mmoles) and trityl chloride (1.05 eq). After 12 hours, the solution was washed three times with 25 mL portions of distilled water. The organic phase was dried over anhydrous sodium sulphate and then evaporated under reduced pressure in a rotary evaporator. The yield of the trityl derivative was 75%. The methoxy derivative was synthesized under the same conditions yielding 22b in 95%.

Compound 22a showed:

^1H NMR: (EM 390) δ 1.39 (m, 13H, $(\text{CH}_2)_5$ and CH_3), 2.15

(m, 4H, CH₂N and CH₂CO), 4.02 (m, 2H, CH₂ ethyl) and 7.25 (m, 15H, aromatic).

Compound 22b showed:

¹H NMR: (AM 500) δ 1.253 (m, 9H, (CH₂)₃ and CH₃), 1.455 (m, 2H, CH₂-C-N), 1.584 (m, 2H, CH₂-C-COO), 2.107 (t, 2H, CH₂N), 2.258 (t, 2H, CH₂COO), 3.766 (s, 3H, OCH₃), 4.109 (m, 2H, OCH₂) and 7.448 (m, 14H, aromatic).

¹³C NMR: (AM 500) δ 14.25 (s, 1C, ethoxy-CH₃), 24.92 (s, 1C, C3), 27.17 (s, 1C, C6), 29.07 (s, 1C, C4), 29.23 (s, 1C, C5), 30.81 (s, 1C, C7), 34.35 (s, 1C, C2), 43.73 (s, 1C, C8), 55.15 (s, 1C, CH₃O), 60.12 (s, 1C, CH₂O), 70.26 (s, 1C, MeOTr-C-N), 113.00 (s, 2C, meta anisyl), 126.04 (s, aromatic), 126.65 (s, aromatic), 127.29 (s, aromatic), 127.67 (s, aromatic), 127.84 (s, aromatic), 128.38 (s, aromatic), 128.56 (s, aromatic), 129.78 (s, aromatic), 146.74 (s, 2C, ipso-phenyl), 157.77 (s, 1C, para anisyl) and 174.04 (s, 1C, COO). Assignments based upon values for ethyl octanoate, p-methoxybenzylamine, n-octyl amine (Sadtler Standard ¹³C NMR Spectra) and triphenyl carbinol (Olah *et. al.*, 1974).

Reduction of N-Tritylated Ethyl 8-Aminooctanoates

The method used was similar to that used by Szammer, (1969). Lithium aluminum hydride (108 mg, 2.5 eq) was stirred anhydrous diethyl ether (8 mL) at 0°C under nitrogen atmosphere. To this solution was added an ethereal N-trityl ethyl 8-aminooctanoate (1.09 mmoles in 2 mL ether). The mixture was stirred at 0°C for 1 hour and at reflux for 2 hours. The reaction was quenched with 2 mL of methanol and 2 mL of distilled water. The mixture was filtered and the precipitate washed with 50 mL of ether and 25 mL of chloroform. The filtrate was concentrated (by rotary evaporation under reduced pressure) until only the water was remaining. This aqueous solution was extracted three times with 10 mL portions of chloroform. The combined extracts were dried over anhydrous sodium sulphate and evaporated under reduced pressure in a rotary evaporator. The yield of the trityl derivative 23a was 87%. The methoxytrityl compound was synthesized under the same conditions yielding 97% of the alcohol 23b.

Compound 23a showed:

¹H NMR: (EM 390) δ 1.22 (m, 12H, (CH₂)₆), 2.10 (t, 2H, CH₂N), 3.52 (t, 2H, CH₂O) and 7.30 (m, 15H, aromatic).

Compound 23b showed:

MS: m/z (B₂) 40 (5) [M⁺-C₆H₅], 318 (12), 288

(2) [M⁺-(CH₂)₈OH] and 273 (100) [M⁺-NH(CH₂)₈OH].

¹H NMR: (AM 500) 81.274 (m, 8H, (CH₂)₄), 1.459 (m, 2H, CH₂-C-N), 1.529 (m, 2H, CH₂COH), 2.109 (m, 2H, CH₂N), 3.603 (t, 2H, CH₂O), 3.760 (s, 3H, CH₃O) and 7.230 (m, 15H, aromatic).

¹³C NMR: (WP 80) 825.60 (s, 1C, C6), 27.19 (s, 1C, C3), 29.27 (s, 1C, C4), 29.42 (s, 1C, C5), 30.76 (s, 1C, C7), 32.66 (s, 1C, C2), 43.49 (s, 1C, C8), 55.05 (s, 1C, CH₃O), 62.82 (s, 1C, CH₂OH), 70.33 (s, 1C, MeOTr-C-N), 113.00 (s, 2C, meta-anisyl), 125.99 (s, 1C, s, aromatic), 127.63 (s, aromatic), 128.53 (s, aromatic), 129.75 (s, aromatic), 138.54 (s, 1C, ipso-anisyl), 146.60 (s, 2C, ipso-phenyl) and 157.76 (s, 1C, para-anisyl). Assignments based upon values for n-octylamine, p-methoxybenzylamine (Sadtler Standard ¹³C NMR Spectra), n-octanol (Bruker ¹³C Data Bank Vol.1) and triphenyl carbinol (Olah et al., 1974).

Hydrolysis of N-Trityl 8-Aminooctanol

N-trityl 8-aminooctanol 23a (3.076 g, 7.94 μmoles) was dissolved in 40 mL of absolute ethanol. Hydrogen chloride gas was bubbled through the solution for 0.5 hours. The solution was then stirred at 70°C for 3 hours and 25°C

for 12 hours. The solvent was removed under reduced pressure in a rotary evaporator and 30 mL of distilled water was added. The aqueous layer was washed three times with 30 mL portions of chloroform. The aqueous layer was adjusted to pH 9 with 1M sodium hydroxide and extracted three times with 30 mL portions of chloroform. These basic organic extracts were combined, dried over anhydrous sodium sulphate and evaporated under reduced pressure in a rotary evaporator. The yield was 430 mg (63%) of 4.

Synthesis of 6-Chloro,-N9-(8-N-methoxytritylamino-octyl)purine 24

The procedure used was similar to that of Mitsunobu, (1981) or Iwakawa *et al.*, (1978). N-methoxytrityl 8-amino-octanol 23b (500 mg, 1.197 mmoles) was dissolved in 5 mL of THF. To this stirred solution (under nitrogen atmosphere) was added a solution of triphenylphosphine (316 mg, 1.20 mmoles) dissolved in 3 mL of THF. 6-Chloropurine (185 mg, 1.197 mmoles) was added as well as a solution of diethyl azodicarboxylate (208.5 mg, 1.197 mmoles) dissolved in 2 mL of THF. The solution was stirred for 72 hours and then the solvent was evaporated under reduced pressure in a rotary evaporator. The residue was washed three times with 10 mL portions of a solution consisting of 20% chloroform in



hexanes. The combined washings were rotary evaporated reduced pressure and redissolved in a solution of 40% acetonitrile in distilled water sufficient to effect dissolution (30-40 mL). A 2 mL portion of this solution was applied to a reversed phase Sep-Pak. The Sep-Pak was washed with 5 mL of fresh acetonitrile water solution followed by elution with 10 mL of acetonitrile. The Sep-Pak was washed with 5 mL of methanol followed by 5 mL of distilled water and the separation procedure was repeated. The combined acetonitrile eluates were collected and evaporated under reduced pressure in a rotary evaporator. The yield of the partially purified product was 56% as indicated by ^1H NMR. TLC of 24 with Acetonitrile on RP KC18F TLC plates gave $R_f=0.51$.

Compound 24 showed:

^1H NMR: (WM 250) δ 1.283 (m, 8H, $(\text{CH}_2)_4$), 1.457 (m, 2H, NCCH_2), 1.921 (m, 2H, N^9CCH_2), 2.102 (t, 2H, CH_2NH), 3.771 (s, 3H, CH_3), 4.264 (t, 2H, N^9CH_2), 6.810 (m, 4H, ϕ), 7.252 (m, 10H, ϕ_2), 8.083 (s, 1H, H8) and 8.738 (s, 1H, H2).

^{13}C NMR: (WP 80) δ 26.49 (s, 1C, C6'), 27.12 (s, 1C, C3'), 28.82 (s, 1C, C2'), 29.74 (s, 1C, C5'), 30.70 (s, 1C, C7'), 43.44 (s, 1C, C8'), 44.42 (s, 1C, C1'), 55.09 (s, 1C, CH_3), 70.33 (s, 1C, MeOTr-C-N), 113.00 (s, 2C, meta-anisyl), 126.02 (s, aromatic), 127.64

(s,aromatic), 128.52 (s,aromatic), 129.75
 (s,aromatic), 138.51 (s,1C,ipso-anisyl), 145.02
 (s,1C,C8), 146.59 (s,2C,ipso-phenyl), 151.10
 (s,1C,C2), 151.86 (s,2C,C4 and C6) and 157.78
 (s,1C,para-anisyl). Assignments based upon values
 for n-octylamine, p-methoxybenzylamine (Sadler
 Standard ¹³C NMR Spectra), triphenyl carbinol (Olah
et.al., 1974), and 6-chloropurine (Szarek *et.al.*,
 1974).

Synthesis of 6-Chloro,-9-(-8-aminooctyl)purine
Hydrochloride 6a

6-Chloro-9-(8-N-methoxytritylaminoctyl)purine 24
 (46 mg, 0.083 mmoles) was dissolved in 2 mL of methylene
 chloride. To this stirred solution was added 12 µL of
 trifluoroacetic acid and 20 µL of methanol. After 0.5 hours
 more methanol (0.1 mL) and 8 mL of methylene chloride were
 added. The solution was extracted twice with 10 mL portions
 of 0.01M hydrochloric acid. The combined aqueous layers were
 evaporated under high vacuum in a rotary evaporator to
 dryness yielding 12 mg (50%) of a green solid.

Modified Synthesis of N⁶,N⁹-Octamethylenepurine
Cyclophane 1

6-Chloro,-9-(8-aminoctyl)purine hydrochloride 6a (12 mg, 0.0378 mmoles) was added to 1 mL of acetonitrile. The mixture was cooled to 0°C and N,N-diisopropylethylamine (10 mg, 0.080 mmoles) was added dropwise. After 0.5 hours, the mixture was added to 50 mL of acetonitrile. The solution was stirred at 60°C for 24 hours followed by evaporation under reduced pressure in a rotary evaporator. The residue was redissolved in 10 mL of chloroform and extracted three times with 10 mL portions of 0.01M hydrochloric acid. The organic layer was dried over anhydrous sodium sulphate and evaporated under reduced pressure in a rotary evaporator to dryness yielding 2 mg (0.01 mmoles, 30.2%) crude product. The product was purified by medium pressure chromatography on silica gel using a Lobar column. TLC of 1 with 5% methanol in chloroform gave R_f=0.198.

Synthesis of 6-Chloro,9-octylpurine 25

The same procedure was followed as for the synthesis of 6-chloro,-9-(8-N-methoxytritylaminoctyl)purine 24. The compound was purified by column chromatography yielding 79%. Compound 25 showed:

HRMS: for C₁₃H₁₉N₄Cl; calcd, 266.1298; obs, 266.1285.

MS: m/z (RI%); 266 (10) [M⁺], 237 (3) [M⁺-CH₂CH₃], 223
 (4) [M⁺-(CH₂)₂CH₃], 209 (10) [M⁺-(CH₂)₃CH₃], 195
 (7) [M⁺-(CH₂)₄CH₃], 181 (6) [M⁺-(CH₂)₅CH₃], 167
 (11) [M⁺-(CH₂)₆CH₃], 104 (82) and 59 (100).

¹H NMR: (EM 390) δ 0.80 (m, 3H, CH₃), 1.23 (m, 10H, (CH₂)₅),
 1.90 (m, 2H, CH₂-C-N), 4.27 (t, 2H, CH₂N), 8.10
 (s, 1H, C8H) and 8.77 (s, 1H, C2H).

¹³C NMR: (AM 500) (calculated by comparison with octylamine)
 δ 14.130 (s, 1C, CH₃), 22.466 (s, 1C, C7'), 26.520
 (s, 1C, C3'), 28.833 (s, 1C, C5'), 28.919 (s, 1C, C4'),
 29.774 (s, 1C, C6'), 31.574 (s, 1C, C2'), 44.477
 (s, 1C, C1'), 131.550 (s, 1C, C5), 145.114 (s, 1C, C8),
 150.934 (s, 1C, C2) and 151.815 (s, 2C, C4 and C6).

Synthesis of 6-Aminooctylpurine 27 and 6-Aminooctyl-
-9-octylpurine 26

6-Chloropurine or 6-chloro,9-octylpurine 25 was dissolved in 2.6 mL of acetonitrile. To this stirred solution were added octylamine (68 μl, 0.41 mmoles) and diisopropylethylamine (71 μl, 0.41 mmoles). After 24 hours at 65°C, the solution was evaporated to dryness under reduced pressure in a rotary evaporator. The crude product was purified by column chromatography. The yield of the

compound 27 was 73%. The yield of the compound 26 was 50%.

Compound 27 showed:

mp: 169-170°C; lit. 165-167°C.

HRMS: for $C_{13}H_{23}N_5$; calcd. 247.1797; obs. 247.1784.

MS: m/z (RI%); 247 (10) [M^+], 204 (8) [$M^+-(CH_2)_2CH_3$],
190 (14) [$M^+-(CH_2)_3CH_3$], 176 (6) [$M^+-(CH_2)_4CH_3$],
162 (25) [$M^+-(CH_2)_5CH_3$], 148 (100) [$M^+-(CH_2)_6CH_3$] and
119 (71) [$M^+-NH(CH_2)_7CH_3$].

1H NMR: (AM500) δ 0.855 (t, 3H, CH_3), 1.25 (m, 8H, $(CH_2)_4$),
1.416 (m, 2H, N-C-C- CH_2), 1.693 (m, 2H, N-C- CH_2), 3.600
(m, 2H, CH_2N), 6.068 (broad s, 1H, NH), 7.240
(s, 1H, C2H) and 7.962 (s, 1H, C2H).

^{13}C NMR: (AM 500 Calculated by comparison with octylamine)
 δ 14.052 (s, 1C, CH_3), 22.614 (s, 1C, C7'), 26.937
(s, 1C, C3'), 29.208 (s, 1C, C5'), 29.321 (s, 1C, C4'),
29.723 (s, 1C, C6'), 31.779 (s, 1C, C2') and 40.719
(s, 1C, C1').

Compound 26 showed:

UV: λ_{max} 268nm; log ϵ =4.071 ethanol.

HRMS: for $C_{21}H_{37}N_5$; calcd. 359.3049; obs. 359.3036.

MS: m/z (RI%); 359 (41) [M^+], 343 (37), 330 (23) [M^+-
 CH_2CH_3], 302 (57) [$M^+-(CH_2)_3CH_3$], 288 (23) [M^+-
 $(CH_2)_4CH_3$], 260 (92) [$M^+-(CH_2)_6CH_3$], 247 (37) [M^+-
 $CH(CH_2)_7CH_3$], 204 (23) [$M^+-(CH_2)_8CH_3$], 176 (34) [M^+-
 $(CH_2)_{10}CH_3$], 148 (100) [$M^+-(CH_2)_{12}CH_3$], 104 (73) and

59 (80).
¹H NMR: (EM 390) 80.88 (m, 6H, 2CH₃), 1.28 (m, 20H, 2(CH₂)₅),
 1.70 (m, 4H, 2CH₂-C-N), 3.68 (m, 2H, CH₂N6'), 4.17
 (t, 2H, CH₂N9), 5.91 (broad s, 1H, NH), 7.74 (s, 1H, C2H)
 and 8.45 (s, 1H, C2H).

Synthesis of 9-Azidononanol 30

The procedure used was that of Boige grain, Castro and Selve, (1975). 1,9-Nonanediol 28 (0.5 g, 3.12 mmoles) was dissolved in 10 mL of THF and the solution cooled to 0°C. Hexamethylphosphorotriamide (0.560 g, 3.43 mmoles) and carbon tetrachloride (1.920 g, 12.48 mmoles) were added. After 5 minutes, 20 mL of distilled water were added and the solution was washed once with 20 mL of diethyl ether. Potassium hexafluorophosphate (860 mg, 4.67* mmoles) was added to the aqueous solution which was then extracted three times with 20 mL portions of methylene chloride. The combined organic solutions were dried over anhydrous sodium sulphate and evaporated under reduced pressure in a rotary evaporator. The residue was dissolved in 10 mL of N,N-dimethylformamide. Sodium azide (1.01 g, 15.6 mmoles) was added and the stirred solution was heated to 80°C for 3 hours. The solvent was evaporated under reduced pressure on a rotary evaporator and the crude product was purified by column

chromatography on silica gel. TLC of 30 with 5% methanol in chloroform gave $R_f=0.49$. The yield was 75%.

Compound 30 showed:

IR: ν_{\max} 2095 [N_3] cm^{-1} .

1H NMR: (EM 390) δ 1.22 (m, 14H, $(CH_2)_7$), 3.16 (t, 2H, CH_2N) and 3.50 (t, 2H, CH_2O).

Synthesis of 6-Chloro,-9-(9-azidononyl)purine 31

Triphenylphosphine (135 mg, 0.514 mmoles), diethyl azodicarboxylate (89 mg, 0.514 mmoles) and 6-chloropurine (79 mg, 0.514 mmoles) were dissolved in 15 mL of THF. To this stirred solution was added a solution of 9-azidononanol (100 mg, 0.540 mmoles) dissolved in 3 mL of THF. After 48 hours, the solution was evaporated under reduced pressure in a rotary evaporator and the residue washed three times with 10 mL portions of a solution of 20% chloroform in hexanes. The washings were combined and cooled to $-5^\circ C$ to allow precipitation of triphenylphosphine oxide. After filtration, the filtrate was evaporated under reduced pressure in a rotary evaporator. The crude product was purified by column chromatography on silica gel. TLC of 31 with 3% methanol in chloroform gave $R_f=0.52$. The yield was 37 mg (0.115 mmoles, 22%).

Compound 31 showed:

HRMS: for $C_{14}H_{20}N_7Cl$; calcd. 321.1468; obs. 321.1470.
 MS: m/z (RI%); 321 (3) $[M^+]$, 265 (41) $[M^+ - CH_2N_3]$, 209
 (56) $[M^+ - (CH_2)_5N_3]$ and 155 (100) $[M^+ - C(CH_2)_5N_3]$.
 1H NMR: (EM 390) δ 1.22 (m, 12H, $(CH_2)_6$), 1.88 (m, 2H, CH_2CN_9),
 3.18 (t, 2H, CH_2N_3), 4.19 (t, 2H, CH_2N_9), 8.19
 (s, 1H, C2H or C8H) and 8.72 (s, 1H, C2H or C8H).

Reduction of the Azide of 6-Chloro,9-(9-azido-
nonyl)purine

The procedure used was similar to that of Vaultier, Knouzi and Carrie, (1983). 6-Chloro,9-(9-azidononyl)purine 31 (327 mg, 0.452 mmoles) was dissolved in stirred THF (5 mL). To this solution, under nitrogen atmosphere, was added triphenylphosphine (266 mg, 0.452 mmoles). After the solution had been heated at 60°C for 6 hours, 200 μ L of distilled water were added and this solution stirred at 25°C for 18 hours. This solution was concentrated, under reduced pressure on a rotary evaporator, to 1 mL and redissolved in 20 mL of chloroform. This solution was extracted three times with 10 mL portions of 0.01M hydrochloric acid. The combined aqueous solutions were adjusted to pH 8 with 1M sodium hydroxide and extracted three times with 30 mL chloroform. These combined organic solutions were dried over anhydrous sodium sulphate and evaporated, under reduced in a rotary

evaporator. The crude product 33 was not isolated but immediately subjected to cyclization conditions. The approximate yield was 51 mg (38%).

Compound 33 showed:

¹H NMR: hydrochloride salt in D₂O solvent ref. 3-(trimethylsilyl)propionic acid sodium salt (EM 390) δ1.30 (m, 14H, (CH₂)₇), 3.00 (t, 2H, (CH₂)NH₃⁺), 4.38 (t, 2H, CH₂N9) and 8.37 (s, 1H, C2H or C8H).

Synthesis of N6',N9-Nonamethylenepurine

Cyclophane 34

6-Chloro,-9-(9-aminononyl)purine 33 (25 mg, 0.085 mmoles) was dissolved in 1 mL of chloroform. Aliquots of 0.1 mL of this solution were added, at 0.5 hour intervals, to 1 mL of dimethylsulphoxide stirred at 70°C. Three hours after the addition of the last portion, the solvent was removed by vacuum distillation. The residue was redissolved in 20 mL of chloroform and washed three times with 10 mL portions of distilled water. The organic layer was dried over anhydrous sodium sulphate and evaporated under reduced pressure in a rotary evaporator. This yielded 5 mg of crude product 34.

Compound 34 showed:

MS: m/z (RI%); 259 (100) [M⁺], 216 (30) [M⁺-NH(CH₂)₂], (21) [M⁺-NH(CH₂)₃], 188 (25) [M⁺-NH(CH₂)₄], 175

(28) $[M^+ - (CH_2)_6]$, 162 (22) $[M^+ - (CH_2)_6 CH]$ and 148
(55) $[M^+ - (CH_2)_7 CH]$.

1H NMR: (AM 500) δ 0.07 (m, 1H), 0.40 (m, 1H), 0.65 (br m,
3H), 0.82 (m, 2H), 1.05 (m, 1H), 1.23 (m, 2H), 1.41
(s, 1H), 1.61 (m, 2H), 1.80 (m, 1H), 3.63 (m, 1H), 3.91
(m, 1H), 4.33 (m, 1H), 4.59 (m, 1H), 5.65 (br s,
1H, N6'H), 7.83 (s, 1H, H8) and 8.33 (s, 1H, H2).

^{13}C NMR: (AM 500) δ 24.06 (s, 1C), 24.13 (s, 1C), 26.47 (s, 1C),
27.01 (s, 1C), 27.47 (s, 1C), 29.92 (m, 2C), 42.72
(s, 1C, C1'), 45.06 (s, 1C, C9'), 142.49 (s, 1C, C8),
151.77 (s, 1C) and 158.25 (s, 1C, C6).

Appendix A

Ring Current Calculation Suitable for BASICA

```
10  REM program to calculate ring current shifts for fused
    five and six-membered rings.

20  DIM MF(60)
30  DIM NH$(20)
40  DIM X(20),Y(20),Z(20)
60  DIM P(3):DIM PZ(3)
70  DIM B(3):DIM SIG(3)
80  DIM FA(60):DIM FB(60)
90  EC=1*EXP(-38):PI=3.14159265#
140 PRINT "Would You like to choose a colour for the text?"
150 PRINT
160 PRINT " cyan=3; red=4; magenta=5; brown=6; white=7;"
170 PRINT " light blue=9; light green=10; light red=12;"
180 PRINT " light magenta=13; yellow=14"
190 INPUT CC:IF CC=0 then CC=7:
200 COLOR CC,0
210 PRINT "Do you want to have a loop separation for the
    ring current?"
220 PRINT "Press return for zero loop separation, otherwise
    input the value"
230 INPUT LL
```

```
240 PRINT "Unless otherwise requested, a 6-electron PI
      current is assumed for both rings: Hit RETURN or input
      the desired number of electrons"
250 PRINT
260 PRINT "HOW MANY PI ELECTRONS ARE IN THE SIX-MEMBERED
      RING ?":INPUT CA
270 IF CA=0 THEN CA=6
280 PRINT "HOW MANY PI ELECTRONS ARE IN THE FIVE-MEMBERED
      RING ?":INPUT CB
290 LPRINT "LOOP SEPARATION IS";LL
300 LPRINT "PI ELECTRONS IN THE SIX-MEMBERED RING=";CA
310 IF CB=0 THEN CB=6
320 LPRINT "PI ELECTRONS IN THE 5-MEMBERED RING=";CB
330 AA=1:BB=1
340 FOR MF=1 TO 57 STEP 2
350 AA=MF/(MF+1)
360 BB=BB*AA
370 FA(MF)=BB^2
380 FB(MF)=BB^2/MF
390 NEXT MF
400 FOR I=1 TO 16
410 READ I,NH$(I),X(I),Y(I),Z(I)
420 FOR QQQ = 1 TO 2
430 IF QQQ=1 THEN X=X(I)-1.95936:Y=Y(I)+10.93229:Z=Z(I)-
      3.45958
```

```
440 IF QQQ=2 THEN X=X(I) 1.95936:V=V(I)+10 93229:Z=Z(I)-
    1.3912
450 COLOR (CC-1),0
460 PRINT NH$(I),X,Y,Z
470 LPRINT
480 LPRINT NH$,X,Y,Z
490 IF QQQ=1 THEN A=1.349:CONST=8.97:ZZZ=0
500 IF QQQ=2 THEN A=1.154:CONST=8.97:ZZZ=0
510 Y=Y+(LL/2)
520 PRINT "LOOP SEPARATION IS ";LL
530 COLOR CC,0
540 FOR PP=1 TO 2
550 PRINT "Y IS ";Y
560 P=SQR(X^2+Z^2):PZ=ABS(Y)
570 W=(A+P)^2+PZ^2
580 R=4*A*P/W
590 G=1:EA=1:V=1
600 FOR MF=1 TO 57 STEP 2
610 G=G+(FA(MF)*(R^V))
620 EB=FB(MF)*(R^V)
630 V=V+1
640 IF EB<EC THEN 670
650 EA=EA-EB
660 NEXT MF
670 C=PI*G/2
```

```

680 E=PI*EA/2
690 S=A^2-P^2-PZ^2
700 T=(A-P)^2+PZ^2
710 IF QQQ=1 THEN B(LL)=(CA*CONST)/(6*SQR(W))*(C+S*E/T)
720 IF QQQ=2 THEN B(LL)=(CB*CONST)/(6*SQR(W))*(C+S*E/T)
730 PRINT "B(LL)= ";B(LL)
740 ZZZ=ZZZ+B(LL)
750 IF QQQ=1 THEN RCSIX=ZZZ
760 IF QQQ=2 THEN RCFIVE=ZZZ
770 Y=Y-LL
780 NEXT PP
790 COLOR (CC+1),0
800 IF QQQ=1 THEN PRINT "THE [6] RING CURRENT IS";(RCSIX)/2
810 IF QQQ=1 THEN LPRINT "THE [6] RING CURRENT
IS";(RCSIX)/2
820 IF QQQ=2 THEN PRINT "THE [5] RING CURRENT
IS";(RCFIVE)/2
830 IF QQQ=2 THEN LPRINT "THE [5] RING CURRENT
IS";(RCFIVE)/2
840 COLOR (CC),0
850 PRINT "*****"
860 NEXT QQQ
870 COLOR (CC-2),0
880 PRINT
890 PRINT "*****"

```

```
900 LPRINT
910 PRINT "TOTAL RING CURRENT SHIFT FOR"; NH$(I); "IS";
      (RCFIVE+RCSIX)/2
920 LPRINT "TOTAL RING CURRENT SHIFT FOR"; NH$(I); "IS";
      (RCFIVE+RCSIX)/2
930 PRINT "*****"
940 LPRINT
950 PRINT
960 LPRINT
970 PRINT
980 COLOR CC,0
990 NEXT I
1000 END
1010 DATA 1,H11-1,6.29942,-9.93378,2.68179
1020 DATA 2,H11-2,4.99320,-9.94065,1.68252
1030 DATA 3,H12-1,5.70493,-7.95101,3.64466
1040 DATA 4,H12-2,5.63755,-7.10001,2.03703
1050 DATA 5,H13-1,3.87428,-6.70883,3.25607
1060 DATA 6,H13-2,3.30935,-8.23241,3.66749
1070 DATA 7,H14-1,3.27455,-6.90338,1.06697
1080 DATA 8,H14-2,3.18861,-8.47665,1.11355
1090 DATA 9,H15-1,1.25490,-6.84107,2.25085
1100 DATA 10,H15-2,1.32226,-8.34969,2.57492
1110 DATA 11,H16-1,0.27069,-7.06061,0.29048
1120 DATA 12,H16-2,1.15359,-8.34454,-0.06297
```

1130 DATA 13,H17-1,-0.87201,-8.77519,1.88269

1140 DATA 14,H17-2,-1.40701,-8.56083,0.37694

1150 DATA 15,H18-1,-0.51876,-10.49113,-0.31306

1160 DATA 16,H18-2,-1.17943,-10.91684,1.06789

Note: The coordinates in lines 1010 to 1160 are based upon
an orthogonal system and are derived from Table 4.3.

References

- Agarwal, A., Barnes, J.A., Fletcher, J.L., McGlinchey, M.J.
and Sayer, B.G. (1977) Can. J. Chem. 55, 2575-2581.
- Akahori, K., Hama, F., Sakata, Y. and Misumi, S. (1984)
Tet. Lett. 25, 2379-2382.
- Allinger, N.L., Walter, T.J. and Newton, M.G. (1974) J.
Amer. Chem. Soc. 96, 4588-4597.
- Allinger, N.L. (1977) J. Amer. Chem. Soc. 99, 8127-8134.
- Aue, W.P., Bartholdi, E. and Ernst, R.R. (1976) J. Chem.
Phys. 64, 2229-2246.
- Bain, A.D., Hughes, D.W. and Hunter, H.N. (1988) Magn.
Reson. in Chem. (in press).
- Barfield, M., Grant, D.M. and Ikenberry, D. (1975) J.
Amer. Chem. Soc. 97, 6956.
- Barneis, Z., Broeir, Y. and Bittner, S. (1976) Chem. and
Ind. 19, 526-527.
- Boigegrain, R., Castro, B. and Selve, C. (1975) Tet. Lett.
2529-2530.
- Bothner-By, A.A. (1965) Adv. Magn. Res. 1, 195.
- Breitmaier, E., Spohn, K. and Berger, S. (1975) Angew.
Chem. Int. Ed. Engl., 14, 144-159.
- Bruker ¹³C Data Bank Vol.1 (1976) Karlsruhe, Bruker Physik.

- Coffman, D.D., Cox, N.L., Martin, E.L., Mochel, W.E. and
Van Natta, F.J. (1948) *J. Polymer Sci.* 3, No.1, 85-94.
- Corey, E.J., Nicolaou, R.D., Balanson, R.D. and Machida,
Y. (1975) *Synthesis*, 590-591.
- Cram, D.J., Montgomery, C.S. and Knox, G.R. (1966) *J. Amer.
Chem. Soc.* 88, 515-525.
- Cucinella, S., Salvatori, T., Bussetto, C., Perego, G. and
Mazzei, A. (1974) *J. Organometallic Chem.* 78, 185-201.
- Cucinella, S., Dozzi, G., Mazzei, A. and Salvatori, T.
(1975) *J. Organomet. Chem.* 90, 257-267.
- Dailey, B.P. (1964) *J. Chem. Phys.* 41, 2304-2310.
- Del Piero, G., Cucinella, S. and Cesari, M. (1979) *J.
Organometallic Chem.* 173, 263-268.
- Ditchfield, R. (1974) *Mol. Phys.* 27, 789-807.
- Eck, J.C. (1943) *Org. Synth. Vol. 2*, 28-29.
- Elvidge, J.A., Jones, J.R., O'Brien, C., Evans, E.A. and
Sheppard, H.C. (1973) *J. Chem. Soc. Perk. II*, 1889-1893.
- Fujita, S. and Nozaki, H. (1971) *Bull. Chem. Soc. Jpn.* 44,
2827-2833.
- Giessner-Prettre, C. and Pullman, B. (1970) *J. Theor. Biol.*
27, 87-95.
- Giessner-Prettre, C., Pullman, B., Borer, P.N., Kan, L.S.
and Ts'o, P.O.P. (1976) *Biopolymers*, 15, 2277-2286.
- Giessner-Prettre, C. and Pullman, B. (1976) *Biochem.
Biophys. Res. Commun.* 70, 578-581.

- Giessner-Prettre, C. and Pullman, B. (1977) *J. Theor. Biol.* 65, 189-201.
- Giessner-Prettre, C. (1984) *J. Biomol. Str. Dyn.* 2, 233-248.
- Greene, T.W. (1981) in "Protective Groups in Organic Synthesis". Wiley, N.Y., 254-255.
- Gunther, H., Schmitt, P., Fisher, H., Tocher mann, W., Lieber, J. and Wolff, C. (1985) *Helv. Chim. Acta*, 68, 801.
- Haasnoot, C.A.G., De Leeuw, F.A.A.M. and Altona, C. (1980) *Tetrahedron*, 36, 2783-2792.
- Haigh, C.W. and Mallion, R.B. (1972) *Org. Magn. Reson.* 4, 203-210.
- Hama, F., Sakata, Y. and Misumi S. (1981) *Tet. Lett.* 22, 1123-1126.
- Harris, R.K. (1983) in "Nuclear Magnetic Resonance Spectroscopy". Pitman, Great Britain, 183-211.
- Hawkes, G.E., Herwig, K. and Roberts, J.D. (1974) *J. Org. Chem.* 39, 1017-1028.
- Hayward, R.J. and Meth-Cohn, O. (1975) *J. Chem. Soc. Perkin Trans. I*, 212-219.
- Huber, W. and Brenner, M. (1953) *Helv. Chim. Acta*, 36, 1109-1115.
- Ito, S., Fujise, Y. and Fukazawa, Y. (1983) in "Cyclophanes". Keehn P.M. and Rosenfeld S.M. eds., Academic Press, N.Y., Vol.2, 485-507.
- Iwakawa, M., Pinto, B.M. and Szarek, W.A. (1978) *Can. J.*

- Chem. 56, 326-335.
- Johnson, C.E. and Bovey, F.A. (1958) J. Chem. Phys. 29,
1012-1014.
- Jordan, F. and Sostman, H.D. (1972) J. Amer. Chem. Soc.
94, 7898.
- Kammula, S.L., Troff, L.D., Jones, M., van Straten, J.W.,
de Wolf, W.H. and Bickelhaupt, F. (1979) J. Amer. Chem.
Soc. 99, 5815.
- Kaneda, T., Otsubo, T., Horita, H. and Misumi, S. (1980)
Bull. Chem. Soc. Jpn. 53, 1015-1018.
- Karger, B.L. et al. (1973) in "An Introduction to
Separation Science". Wiley, N.Y., 272-274.
- Karplus, M. (1959) J. Chem. Phys. 30, 11-15.
- Karplus, M. (1963) J. Amer. Chem. Soc. 85, 2870-2871.
- Kostermans, G.B.M., de Wolf, W.H. and Bickelhaupt, F.
(1987) Tetrahedron, 43, 2955-2966.
- Letsinger, R.L. and Skoog, I. (1955) J. Amer. Chem. Soc.
77, 2491-2494.
- Levy, G.C., Lichter, R.L. and Nelson, G.L. (1980) in
"Carbon-13 NMR Spectroscopy 2nd. ed.". Wiley, N.Y.,
214-220.
- Lister, J.H. (1971) in "Fused Pyrimidines Part II: Purines".
(D.J. Brown ed.), Wiley-Interscience, New York.
- Mancilla, T., Santiesteban, F., Contreras, R. and Kläebe,
A. (1982) Tet. Lett. 23, 1561-1564.

- Mann, B.E. (1977) Progress in NMR Spectroscopy 11, 95-114.
- Manske, R.H. (1943) Org. Synth. Vol. 2, 154-156.
- McConnell, H.M. (1957) J. Chem. Phys. 27, 226-229.
- Meek, D.W. and Springer, C.S. (1966) Inorg. Chem. 5, 445-450.
- Memory, J.D. and Wilson, N.K. (1982) in "NMR of Aromatic Compounds". Wiley, N.Y., 18-33.
- Mitsunobu, O. (1981) Synthesis, 1-28.
- Nozaki, H., Koyama, T. and Mori, T. (1969) Tetrahedron 25, 5357-5364.
- O'Donnell, M.J. and Polt, R.L. (1982) J. Org. Chem. 47, 2663-2666.
- Ogilvie, K.K. and Kroeker, K. (1972) Can. J. Chem. 50, 1211-1215.
- Olah, G.A., Westerman, P.W. and Nishimura, J. (1974) J. Amer. Chem. Soc. 96, 5548.
- Parham, W.E. and Dooley, J.F. (1967) J. Amer. Chem. Soc. 89, 985-988.
- Pelter, A. and Smith, K. (1979) in "Comprehensive Organic Chemistry". Jones, D.N., ed., Pergamon, N.Y., Vol.3, 687-940.
- Pickard, P.L. and Tolbert, T.L. (1973) Org. Synth. Vol. 5, 520-522.
- Pizey, S.S. (1974) in "Synthetic Reagents", Wiley, N.Y., Vol.1, 321-357.

Pople, J.A. (1957) Proc. R. Soc. London, A239, 541-549.

Ribas Prado, F. and Giessner-Prettre, C. (1981) J. Mol. Struct. 76, 81-92.

Robillard, G.T. and Reid, B.R. (1979) in "Biological Applications of Magnetic Resonance". Shulman, R.G., ed., Academic Press, N.Y., 82-86.

Rosenfeld, S.M. and Choe, K.A. (1983) in "Cyclophanes". Keehn, P.M. and Rosenfeld, S.M., eds., Academic Press, N.Y., Vol. 1, 312-325.

Sadtler Standard ^{13}C NMR Spectra (1987) New York, VCH Verlagsgesellschaft.

Saenger, W. (1984) in "Principles of Nucleic Acid Structure". Springer-Verlag, N.Y., 16-28.

Saito, H., Fujise, Y. and Ito, S. (1984) Tet. Lett. 25, 4761-4764.

Sarma, R.H., Lee, C.H., Hruska, F.E. and Wood, D.J. (1973) FEBS Lett. 36, 157.

Smith, B.H. (1964) in "Bridged Aromatic Compounds". Academic Press, N.Y., 24-185.

Smith, E.L. (1927) J. Chem. Soc. 1288.

Smith, M., Rammler, D.H., Goldberg, I.H. and Khorana, H.G. (1962) J. Amer. Chem. Soc. 84, 430.

Still, W.C., Kahn, M. and Mitra, A. (1978) J. Org. Chem. 43, 2923-2925.

Sutherland, I.O. (1971) Ann. Rep. in NMR Spectroscopy, 4,

- 71-235.
- Sutherland, M. and Christensen, B.E. (1957) J. Amer. Chem. Soc. 79, 2251-2252.
- Szammer, J. (1969) Acta Chim. Acad. Scient. Hung. Tomus 61, 417-419.
- Szarek, W.A., Vyas, D.M., Sepulchre, A., Gera, S.D. and Lukacs, G. (1974) Can. J. Chem. 52, 2041-2047.
- Takagi, S. and Hayashi, K. (1959) Chem. Pharm. Bull. 7, 96-98.
- Taylor, R. and Kennard, O. (1982) J. Amer. Chem. Soc. 104, 3209-3212.
- Trost, B.M. and Herdle, W.B. (1976) J. Amer. Chem. Soc. 98, 4080-4086.
- Vaultier, M., Knouzi, N. and Carrié, R. (1983) Tet. Lett. 24, 763-764.
- Waugh, J.S. and Fessenden, R.W. (1957) J. Amer. Chem. Soc. 79, 846-849.
- Wiberg K.B. and O'Donnell, M.J. (1979) J. Amer. Chem. Soc. 101, 6660-6666.
- Wilde, J.A. and Bolton, P.H. (1984) J. Magn. Res. 59, 343-346.
- Wolf, A.D., Kane, V.V., Levin, R.H. and Jones, M. (1973) J. Amer. Chem. Soc. 95, 1680.
- Wolfrum, M.L. and Bhat, H.B. (1967) J. Org. Chem. 32, 1821-1823.

Yoon, N.M. and Cho, B.T. (1982) Tet. Lett. 23, 2475-2478.

Zervas, L. and Theodoropoulos, D.M. (1956) J. Amer. Chem.

Soc. 78, 1359-1363.